Calibration and Validation of a SWAT model for the quantification of water provision ecosystem service for the Conservation Area of Guanacaste

by

Oscar Javier Baron Ruiz

A thesis submitted in partial fulfillment of the requirements for the degree of

Master of Science

Department of Earth and Atmospheric Sciences

University of Alberta

ABSTRACT

Water is considered a cross-cutting resource for all the ecosystem services (ES) types, namely: for the provision of drinking water and food; regulation through flood control; guarantee of a suitable habitat for fauna and flora; and inspiration for many cultures and their intangible heritage around the planet. The evaluation of water ecosystem services has drawn much attention both in the political arena and the scientific community. Still, there is not a consensus in the approach of evaluating them. Recent notions suggest that the study of ES cannot be assessed from a single discourse but through comprehensive frameworks. Therefore, the main objective of this thesis was to evaluate the water provision as an ecosystem service of the Conservation Area of Guanacaste (ACG, for its acronym in Spanish) by adapting an Ecosystem Services (ES)-based approach with four core elements: (1) effects on human well-being, (2) bio-physical underpinning of service delivery, (3) transdisciplinarity, and (4) assessment of services for decision-making. I have deepened in core element two by assessing all the physically-based processes involved in the hydrologic cycle, which generates the quantity of water available for the study region. As a result, here I present the first calibrated and validated Soil and Water Assessment Tool (SWAT) for the entire ACG, including the land use and cover change (LUCC) impact on water availability.

I tested seven different climatic and geospatial information resources to establish the best input data to build the SWAT model. The model showed excellent performance for both the calibration period (r^2 = 0.81, NSE = 0.75, and br^2 = 0.80) and validation period (r^2 = 0.85, NSE = 0.82, and br^2 = 0.85). I have found that the ACG has a high potential for the provision of water as an ecosystem service. I also identified the spatial and temporal patterns and changes in the water availability in this region between 1980 - 2019. I deepened in the vegetation-water dynamic understanding by evaluating the land use cover change (LUCC), finding that the recovery of forests, and decrease in grasslands and agricultural territories have a positive effect on the water availability also associated with exceptional events in Costa Rica's history that put in place the conditions for the recovery of natural resources. I also demonstrated the advantages of using spatially explicit and physically-based models, such as SWAT, to quantify water provision as an ecosystem service. Finally, this work complements the baseline for future applications of ES-based approaches in this region.

Keywords: water, ecosystem services, SWAT model, SWAT-CUP, calibration, validation, Conservation Area of Guanacaste, quantification, water yield, land use cover change.

PREFACE

This thesis is an original work by Oscar Javier Baron-Ruiz. No part of this thesis has been previously published.

DEDICATION

In memory of the Colombian researchers and my mentors Dr. Eng. *Efraín Antonio Domínguez-Calle* (RIP) and Dr. *Javier Alejandro Maldonado-Ocampo* (RIP), may their scientific legacy continue inspiring many scientists in Eco-hydrology.

ACKNOWLEDGEMENTS

I would like to thank my supervisor Dr. Arturo Sánchez-Azofeifa for the honour of being a member of the Centre for Earth Observations Sciences (CEOS). Thank you for believing in my work, and for your continuous support, and patience during this research process.

I extend this acknowledgment to my colleagues at CEOS for all their help and support, especially to Dr. Hamed Sabzchi Dehkharghan for sharing your hydrological expertise in the first stages of this research. Also, thank you to M.Sc. Marissa Castro-Magnani for your willingness to respond from Bolivia to all my inquiries regarding the hydrological processes and input data availability and processing.

A special thanks to the rest of my advisory committee members, Dr. Monireh Faramarzi and Dr. Li Cheng, for your comments and suggestions to improve my research.

I extend my gratitude to Kely Calderón Alfaro and Cristina Araya Villalobos from the National Meteorological Institute of Costa Rica (IMN) and to Irene Alvarado Quesada from the Central Bank of Costa Rica (BCCR), for all the information provided for this investigation.

A sincere thank you to the people I met in the Saint Joseph College (SJC) community, especially the Catholic Students Association (CSA) of the University of Alberta, and the International Friendship Group, where I found a great community of support, friendship, and personal growth throughout this experience as an International Student in Canada.

Most importantly, I express my gratefulness to God, the Blessed Virgin Mary, my parents María Cristina and Marcelo, my brother Rafael Andrés, and to Andrés Merino-Restrepo, without all your unconditional support, help, and encouraging words, I had not been able to complete this program.

Finally, I would like to acknowledge the financial and institutional support of the Foundation for the Future of Colombia (Colfuturo) and the University of Alberta; and the unconditional trust of my aunt Gladys and uncle Alfredo, who believed in me and gave me their support when I decided to undertake this challenge.

TABLE OF CONTENTS

LIST OF FIGURES

LIST OF TABLES

LIST OF APPENDICES

LIST OF SYMBOLS AND ABBREVIATIONS

ACG	Conservation Area of Guanacaste
AAT	All-At-a-Time Sensitivity Analysis
AVHRR	Advanced Very High Resolution Radiometer
BCCR	Central Bank of Costa Rica
CEOS	Centre for Earth Observation Sciences – University of Alberta
CSFR	Climate Forecast System Reanalysis
DSSAT	Decision Support System for Agrotechnology Transfer
DEM	Digital Elevation Model
ES	Ecosystem Services
EPIC	Environmental Policy Integrated Climate
FONAFIFO	National Forest Financing Fund of Costa Rica
HRU	Hydrological Response Unit
HYDGRP	Hydrological Soil Group
ICE	Costa Rican Institute of Electricity
IMN	National Meteorological Institute of Costa Rica
IMN-CEOS	Weather information obtained from IMN and CEOS stations
MINAE	Ministry of Environment and Energy
MERIS	Medium Resolution Imaging Spectrometer
NSE	Nash-Sutcliffe Efficiency
LUCC	Land Use and Cover Change
PROBA-V	Project for On-Board Autonomy-Vegetation

PTF	Pedotransfer Functions
ROTO	Routing Outputs to Outlets
SCS	Soil Conservation Service
SDGs	Sustainable Development Goals
SINAC	National System of Conservation Areas of Costa Rica
SR-EMSS	Santa Rosa National Park and Environmental Monitoring Super Site
SPOT-VGT	Satellite for observation of Earth-Vegetaton
SUFI-2	Sequential Uncertainty FItting ver. 2
SVM	Support Vector Machine
SWAT	Soil and Water Assessment Tool
SWAT-CUP	Soil and Water Assessment Tool-Calibration and Uncertainty Procedures
SWAT-C	Soil and Water Assessment Tool-Carbon
SWAT-LUT	Soil and Water Assessment Tool-Land Update Tool
SWAT-T	Soil and Water Assessment Tool-Tropics
SWRRB	Simulator for Water Resources in Rural Basins
USDA	United States Department of Agriculture

1. Chapter 1: Introduction

Water Ecosystem Services-based approach for the Conservation Area of Guanacaste

Water is recognized as the finite natural resource essential to support the functions of terrestrial ecosystems and provide freshwater for sustaining human life, health, well-being, and survival (Gordon et al., 2015). The provision of water to fulfill human needs has been defined as one of the various ecosystem services (ES) nature provides. ES, or "benefits human populations obtain from ecosystems" (MEA, 2005) , is a concept studied at least for the last six decades through different notions. In the early 60s, the ES were based on economic terms related to the exchange or monetary value obtained by a product or service coming from nature (Martin-Ortega et al., 2015c). In the 80s, the term "finite" appeared in the analysis by understanding that the ES were not unlimited, which could jeopardize the sustainability of human welfare (Martin-Ortega et al., 2015c). The root of this danger was associated with the extinction of different species considered of economic importance. This raised concerns in the scientific community about the need to understand the ecological dynamics of ecosystems and create mechanisms for the quantification of the different services wildlife provides to humanity (Calvo-Rodriguez et al., 2017; Martin-Ortega et al., 2015c). ES-focused research significantly increased during the end of the 20th century and the beginning of the 21st, which gave rise to documents of worldwide relevance, such as *The Millennium Ecosystem Assessment* (MEA), which presented the most general definition of ES, used at the beginning of this introduction; and in turn established the best-known classification of ES in four groups: provisioning, regulating, supporting, and cultural services (Calvo-Rodriguez et al., 2017; Fisher et al., 2009; Martin-Ortega et al., 2015c; MEA, 2005). In this line, water is considered a cross-cutting resource for all ES types, that is: for the provision of drinking water and food; regulation through flood control; suitability of habitat for fauna and flora; and inspiration for many cultures and their intangible heritage around the planet, respectively. Gordon et al. (2015) have defined this unique property as the water cycle's capacity to embrace the ecosystem services paradigm.

The ES concept has drawn much attention both in the political arena and the scientific community. However, as noted above, its accuracy and practicality are still being discussed, essentially for the deviation in the definition of the concept itself (Chaudhary et al., 2015; Lamarque et al., 2011). Therefore, recent notions suggest that the study of ES cannot be approached from a single discourse but through broad and comprehensive frameworks with a set of common guiding core elements. To assess the complex relationship between ecosystems and human welfare, Martin-Ortega et al. (2015a), during their analysis of the global perspective of water ecosystem services, proposed a generic ecosystem services-based approach focused on four defining aspects nested one into another: (1) all elements in ecosystems can have an intrinsic value assigned by humans, and decisions need to be driven by focusing on the status of ecosystems instead of human-centred visions; (2) the understanding, across different spatial and temporal scales, of all the complex biophysical components and interactions that sustain the benefits that humans obtained from ecosystems, in other words, what makes an ecosystem capable of supporting the production and delivery of ES; (3) academic and non-academic approaches (transdisciplinarity) combining natural and social sciences and the knowledge of different stakeholders to gather all the points of view regarding how ecosystems produce human well-being; and (4) a quantitative or qualitative (or both) assessment of the ES, this means to find the values that support the decision-making.

All the previous core elements do not have a 'set in stone' methodology to apply. The comprehensive framework implies site-specific perception and necessities. Therefore, although all core elements must be present in the application of the ES-based approach, depending on the case of study, the representation of those core elements may vary (Martin-Ortega et al., 2015c). For the present study, I applied the ES-based approach into the context of water provision as a basis for the protection of nature and for a better understanding of the natural capital of a region. To operationalize this water ES-based approach, I have chosen to deep in the discussion of the core element 2, the biophysical analysis, mostly by assessing all the physically-based processes involved in the hydrologic cycle, which generate the quantity of water available for a specific area. As Martin-Ortega et al. (2015b) stated, this core element can be assessed through modelling techniques.

Various numerical and process-based hydrological models have been developed to quantify ES at different geographical scales with varying levels of complexity (Francesconi et al., 2016; Martin-Ortega et al., 2015b). As there was a disagreement in the definition of ES that generated broad ES-based approaches, the diversity of existing models has also created a discussion among which is the most suitable model for the ES-quantification purpose. The debate has mainly concentrated on the lack of adequate calibration, validation, and uncertainty assessment of the models used to evaluate ES (Braat and De Groot, 2012; Hamel and Bryant, 2017). However, drawbacks in modelling processes have boosted the development of improved models or the adaptation of advanced tools and data to represent necessary components involved in the characterization of ES (Vigerstol and Aukema, 2011). These improvements helped, to some extent, to shed light on which are the driving forces affecting the ES. Such enhanced models are generally used to support policy analysis for informed decision-making, management and conservation of natural resources at various scales; and, in a broader perspective, to ensure the sustainable use of our planet's resources and subsistence of future generations, as established within global commitments, such as the Sustainable Development Goals (SDGs) set by the United Nations General Assembly (Chaudhary et al., 2015; Fisher et al., 2009; Gordon et al., 2015; MEA, 2005).

Among the different models and techniques developed to study ES, the spatially explicit models have flourished to assess spatial and temporal patterns of the processes related to the detection, delineation, and quantification of ES. They are used to develop frameworks to study the dynamics and functions of ecosystems at high spatial and temporal resolutions (Burkhard et al., 2013; Naidoo et al., 2008). These frameworks support the understanding of ES by which humanity's social, cultural and economic development is possible (MEA, 2005). For example, to evaluate water provision, the Soil and Water Assessment Tool (SWAT) has had several documented applications in the modelling of water ES (Francesconi et al., 2016). SWAT is a computationally efficient and spatially explicit model widely used to predict the impacts of land management practices and climate change in complex watersheds (Arnold et al., 1998; Neitsch et al., 2011; Wang et al., 2019).

In accordance with what has been stated so far, this thesis aims to operationalize the broad framework for evaluating water-ES through creating a SWAT hydrological model. For this, in principle, the nested frame of the four key elements is established as shown in Figure 1 and explained as follows:

(1) The vital value of the ecosystem: the recognition of the existing association between ecosystems and human well-being is represented here in the criteria by which a place is selected as a UNESCO-World Heritage Site for its *Outstanding Universal Value*. The UNESCO defines this value as "cultural and/or natural significance which is so exceptional as to transcend national boundaries and to be of common importance for present and future generations of all humanity" (UNESCO, 2019a). One of those UNESCO sites is the Conservation Area of Guanacaste (ACG), located in Northwest Costa Rica and selected for this study. The ACG harbours a very complex ecological dynamic. Interestingly, it connects in one place coastal ecosystems of the Pacific Ocean with the lowlands of the Caribbean. Within this connectivity different ecosystems of humid and dry tropical forests, savannas, and mangroves coexist; as well as a rich landscape formed by the diversity of terrain with imposing landscapes with volcanoes, coral reefs, cobble beaches, among other unique places whose complex ecological functions offer a great variety of ES for the conservation of biodiversity and human welfare (SINAC, 2010; UNESCO, 2019b). All these characteristics classify this place as a site whose preservation and protection "is of the highest importance to the international community as a whole" (UNESCO, 2019a).

(2) Its bio-physical dynamics: as mentioned above, this core element will be the main focus of this thesis and is developed in **Chapter 2**, whose purpose is the *"Water Yield Quantification and Analysis of Land Cover Change impact in Water Availability for the Conservation Area of Guanacaste, Costa Rica using SWAT."* Here the first calibrated and validated SWAT hydrological model for this conservation area is presented. By means of hydrological modelling tools, the vegetation-soil-terrain dynamics are analyzed and explained through the water yield calculation. The water yield is a variable associated with the provision of this essential service for humanity (Francesconi et al., 2016).

(3) Transdisciplinary approaches: to carry out this study, I relied on all the state-of-the-art infrastructure capacity and the interdisciplinary research team of the Centre for Earth Observation Sciences (CEOS) of the University of Alberta, globally recognized for its comprehensive research in tropical ecosystems. Likewise, this research involved critical stakeholders of the Government of Costa Rica, such as the Central Bank of Costa Rica

(BCCR, for its acronym in Spanish), which supported the hydrological data acquisition. The BCCR expressed interest in the results once the preliminary advances of the model were presented in Spring 2020 (May 6, 2020). It also indicated how promising the model is for this conservation area; and the importance of expanding the hydrological monitoring network in Northwest Costa Rica and developing this type of research for the rest of the country. The National Institute of Meteorology of Costa Rica (IMN, for its acronym in Spanish) is another stakeholder in this research. It was agreed, by written consent, in February 2020 to send a copy of this research to be shared within this entity.

(4) Ecosystem service assessment: the analysis of the provision of water as an ecosystem service arises in this core element, from the inextricable linkage between the land use and the availability of water or, as stated by Martin-Ortega et al. (2015a) in their notion about ES for nature conservation, "every land use decision is a water decision." Therefore, at first glance, I have summarized in Table 1.1 the general effects that the most studied land covers in literature have on water availability in each of the hydrological cycle processes. The land covers were grouped into Agricultural Territories, such as crops and non-native pastures, and Artificial Territories, such as cities, industry, roads, and railways.

The rest of the analysis will be addressed within the Discussion section of Chapter 2 based on the quantification made to the ecosystem service and scientific documentation about the implications of the spatial and temporal variation of the water provision.

Finally, **Chapter 3,** "*Conclusions and future work*," summarizes the major findings regarding water provision estimations and their temporal and spatial variation. Additionally, the potential improvements in hydrological modelling, according to recent technological advances integrated into the SWAT model, and the main challenges in monitoring water as a vital ecosystem service of the ACG are included in this section.

1.1. References

Arnold, J.G., Srinivasan, R., Muttiah, R.S., Williams, J.R., 1998. Large area hydrologic modeling and assessment part I: model development 1. JAWRA J. Am. Water Resour. Assoc. 34, 73–89.

Braat, L.C., De Groot, R., 2012. The ecosystem services agenda: bridging the worlds of natural science and economics, conservation and development, and public and private policy. Ecosyst. Serv. 1, 4–15.

Brooks, K.N., Ffolliott, P.F., Magner, J.A., 2013. Hydrology and the Management of Watersheds. John Wiley & Sons.

Burkhard, B., Crossman, N., Nedkov, S., Petz, K., Alkemade, R., 2013. Mapping and modelling ecosystem services for science, policy and practice. Ecosyst. Serv. 1–3.

Calvo-Rodriguez, S., Sanchez-Azofeifa, A.G., Duran, S.M., Espirito-Santo, M.M., 2017. Assessing ecosystem services in Neotropical dry forests: a systematic review. Environ. Conserv. 44, 34–43. https://doi.org/10.1017/S0376892916000400

Chaudhary, S., McGregor, A., Houston, D., Chettri, N., 2015. The evolution of ecosystem services: A time series and discourse-centered analysis. Environ. Sci. Policy 54, 25–34.

Cheng, C.L., 2007. Evaluating the performances of AnnAGNPS and N-SPECT for tropical conditions.

Fisher, B., Turner, R.K., Morling, P., 2009. Defining and classifying ecosystem services for decision making. Ecol. Econ. 68, 643–653.

Francesconi, W., Srinivasan, R., Pérez-Miñana, E., Willcock, S.P., Quintero, M., 2016. Using the Soil and Water Assessment Tool (SWAT) to model ecosystem services: A systematic review. J. Hydrol. 535, 625–636. https://doi.org/10.1016/j.jhydrol.2016.01.034

Gordon, I.J., Martin-ortega, J., Ferrier, R.C., 2015. Introduction, in: J. Martin-Ortega, R. Ferrier, I. Gordon, S.K. (Ed.), Water Ecosystem Services: A Global Perspective. Cambridge University Press, Cambridge, pp. 1–2. https://doi.org/10.1017/CBO9781316178904.002

Gregersen, H.M., Ffolliott, P.F., Brooks, K.N., 2007. Integrated watershed management: Connecting people to their land and water. CABI.

Hamel, P., Bryant, B.P., 2017. Uncertainty assessment in ecosystem services analyses: Seven challenges and practical responses. Ecosyst. Serv. 24, 1–15.

Lamarque, P., Quetier, F., Lavorel, S., 2011. The diversity of the ecosystem services concept and its implications for their assessment and management. C. R. Biol. 334, 441–449.

Martin-Ortega, J., Ferrier, R.C., Gordon, I.J., 2015a. Water ecosystem services: Moving forward, in: J. Martin-Ortega, R. Ferrier, I. Gordon, S.K. (Ed.), Water Ecosystem Services: A Global Perspective. Cambridge University Press, Cambridge, pp. 170–173. https://doi.org/10.1017/CBO9781316178904.021

Martin-Ortega, J., Ferrier, R.C., Gordon, I.J., Khan, S., 2015b. Water ecosystem services: A global perspective. UNESCO Publishing.

Martin-Ortega, J., Jorda-Capdevila, D., Glenk, K., Holstead, K.L., 2015c. What defines ecosystem services-based approaches?, in: J. Martin-Ortega, R. Ferrier, I. Gordon, & S.K. (Ed.), Water Ecosystem Services: A Global Perspective. Cambridge University Press, Cambridge, pp. 3–14. https://doi.org/10.1017/CBO9781316178904.003

MEA, 2005. Millenium Ecosystem Assessment: ecosystems and human well-being. Island Press, Washington, DC.

Naidoo, R., Balmford, A., Costanza, R., Fisher, B., Green, R.E., Lehner, B., Malcolm, T.R., Ricketts, T.H., 2008. Global mapping of ecosystem services and conservation priorities. Proc. Natl. Acad. Sci. 105, 9495–9500.

Neitsch, S.L., Arnold, J.G., Kiniry, J.R., Williams, J.R., 2011. Soil & Water Assessment Tool Theoretical Documentation Version 2009. Texas Water Resour. Inst. 1–647. https://doi.org/10.1016/j.scitotenv.2015.11.063

Ray, D.K., Nair, U.S., Welch, R.M., Lawton, R.O., 2002. Impact of Deforestation on Cloud Properties and Rainfall Over the Costa Rica-Nicaraguan region, in: AGU Fall Meeting Abstracts. pp. B21B-0724.

SINAC, 2010. Guanacaste Conservation Area (ACG) [WWW Document]. URL http://www.sinac.go.cr/EN-US/ac/acg/Pages/default.aspx

UNESCO, 2019a. Operational Guidelines for the Implementation of the World Heritage Convention. Paris.

UNESCO, 2019b. World Heritage List: Area de Conservación Guanacaste (Costa Rica) [WWW Document].

Vigerstol, K.L., Aukema, J.E., 2011. A comparison of tools for modeling freshwater ecosystem services. J. Environ. Manage. 92, 2403–2409. https://doi.org/10.1016/j.jenvman.2011.06.040

1.2. Figures

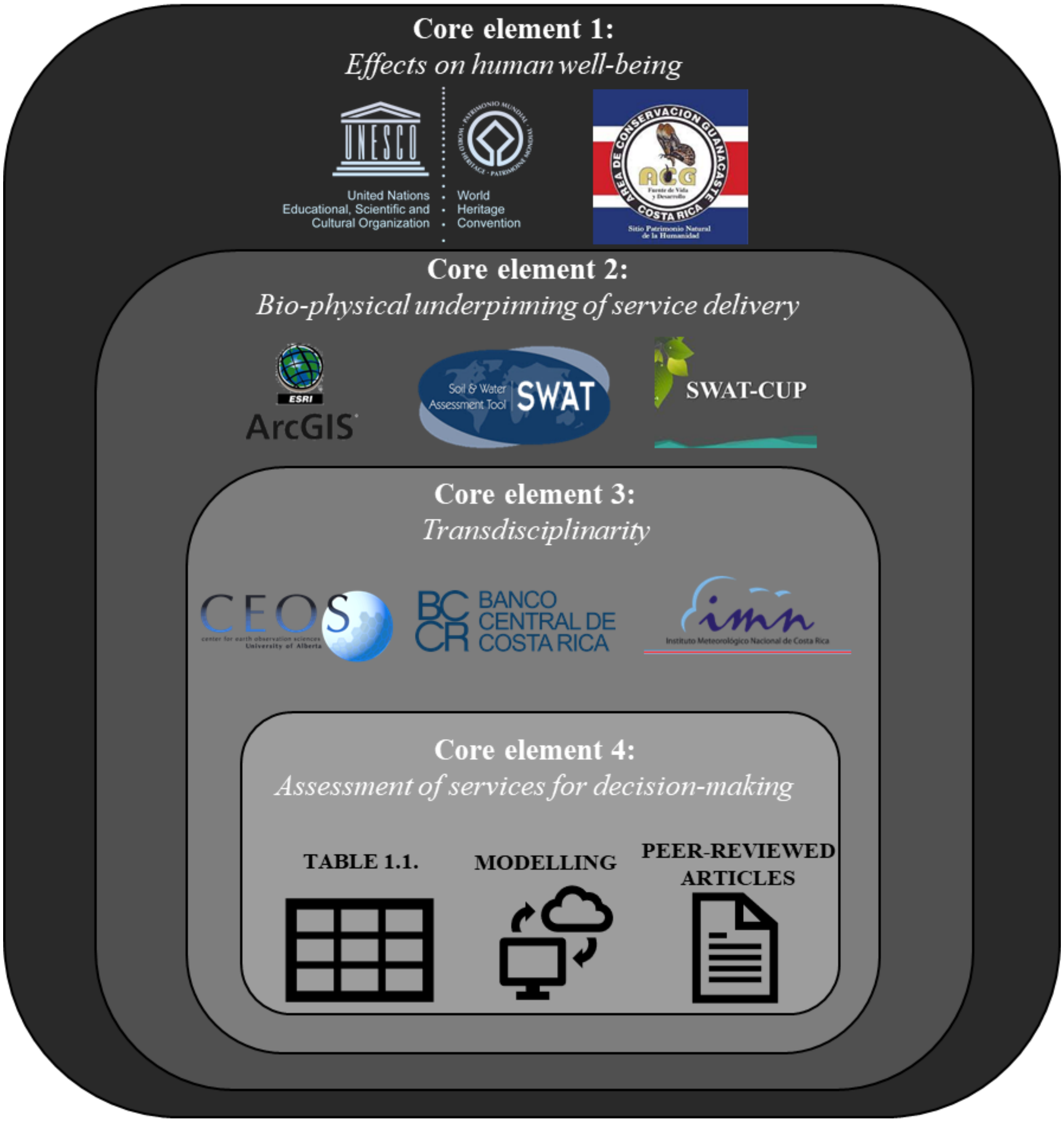

Figure 1.1. Ecosystem Services-based approach for the quantification of water provision in the Conservation Area of Guanacaste (ACG). This is a nested approach of four core elements. The elements represent: (1) The vital value that an ecosystem has for human well-being here represented in the ACG as a World Heritage Site for its Outstanding Universal Value. (2) The bio-physical dynamics in the ACG studied through spatially explicit hydrological modelling. (3) Transdisciplinary approaches. This approach relied on the participation of the Centre for Earth Observations Sciences (CEOS) of the University of Alberta and entities from the Government of Costa Rica, such as the Central Bank of Costa Rica (BCCR), The National Institute of Meteorology of Costa Rica (IMN), among other entities which can benefit from the project. (4) The ecosystem service assessment. It is based on a preliminary analysis (Table 1.1), the quantification made to the ecosystem service, and scientific documentation.

Adapted from Martin-Ortega et al. (2015c)

1.3. Tables

Table 1.1. General Hydrological effects of Land Use and Cover Change

Hydrological Process	Definition of the Hydrological Process	Effects due to Agricultural Territories	Effects due to Artificial Territories	Description of Effects
Precipitation input	The principal amount of water added to the watershed from the atmosphere. It has two forms: rainfall or snowfall.	Decrease or Unchanged	Decrease or Unchanged	Due to the location of the ACG and temperatures above 0 °C during the entire year, the precipitation is only accounted as rainfall. Precipitation rates in Costa Rica are influenced mainly by what is known as the Caribbean and Pacific slopes or mountain systems. For this reason, it could be argued that the removal of vegetation might not impact the precipitation rate directly in this region. However, rainfall is not a unique process in the hydrologic cycle; thus, effects can be exacerbated where forest cover is replaced massively, principally altering the production of clouds.
Interception	Water caught by the different types, extent and condition of the vegetation and plant litter present in the watershed.	Decrease	Decrease	Natural land covers, especially forests, are vital because they intercept water through leaves, stems, bark, and litter; removal of forests reduces this hydrological process dramatically. In the case of crops, water can sometimes fall directly into the soil, increasing the erosion processes. In the case of urbanized regions, impermeability further reduces this process.
Net precipitation	The difference between the water that comes from the atmosphere as precipitation and the water that is evaporated. This is the total input of water from the atmosphere that remains on the land surface.	Increase	Increase	Reduction in water interception generates an increase in net precipitation, meaning that there is more water on the earth's surface. This increment can boost erosion processes and floods because there is no vegetation intercepting the water coming from the atmosphere.
Infiltration capacity	Infiltration is when water enters the soil surface (to start the recharge of groundwaters), and the infiltration capacity is the maximum rate at which water can enter the soil surface. When precipitation rates exceed infiltration capacity, surface runoff occurs. This is observed as	Decrease	Decrease	In general, the deterioration or change of the earth's surface diminishes infiltration capacity. In the case of vegetation, this depends on the type of soil, crop, crop extension, and cropping practices. For the case of artificial territories, this decrease is given by the impervious layers created.

Hydrological Process	Definition of the Hydrological Process	Effects due to Agricultural Territories	Effects due to Artificial Territories	Description of Effects
	ponding of water on the soil.			
Transpiration	The flow of water through the soil-plant-atmosphere interaction. It is one of the most important processes by which water returns to the atmosphere.	Decrease or Unchanged	Decrease	The decrease in transpiration is linked exclusively to the loss of plants; this is noticed in artificial lands where infrastructures replace natural vegetation. In agricultural territories, depending on whether annual or perennial crops and rooting depth differences, transpiration can decrease or remain the same.
Surface runoff	Also known as overland flow. It is the water that flows over the soil layer due to discharges from impervious regions on the landscape or areas where the rainfall rate exceeds the soil's infiltration capacity. It is the water that forms rivers and lakes, and other water bodies.	Increase or Decrease with artificial drainage	Increase	This increase is mainly due to the loss of forests or natural vegetation. Due to the increase in net precipitation and the decrease in the capacity of the ecosystem to intercept, infiltrate and return water to the atmosphere through transpiration. This generates that the excess of available water on the surface increases the runoff. This effect differs between agricultural lands and urbanized areas because in the former, depending on soil and cropping practice (rainfed or irrigated agriculture), it could be reduced if artificial drainage is practiced. In the latter, the impervious layers created always generate an increment in the surface runoff.
Groundwater recharge	It is the process where water typically percolates (drains) downward from the earth's surface to groundwater.	Uncertain	Decrease or Unchanged	This process is directly related to infiltration capacity because once the water is infiltrated into the earth's surface, it begins to percolate through the ground and recharge the groundwater. In the case of agriculture, the change in this process is uncertain because it depends on surface-groundwater linkages. It can generate other impacts, such as the transport of pollutants to the groundwater due to pesticides and nutrient enrichment in soils. Regarding artificial lands, depending on whether or not it is located over groundwater bodies, it can decrease or remain unchanged.

Hydrological Process	Definition of the Hydrological Process	Effects due to Agricultural Territories	Effects due to Artificial Territories	Description of Effects
Peak Stormflow	It is the greatest discharge identified in a certain period of time from rainfall events or following snowmelt runoff, occurring on watersheds	Increase or Variable	Increase	Events of higher peak storm flows can increase due to the increment in surface runoff caused by vegetation removal or impervious layers over the soil.
Baseflow	The flow in groundwater typically feeds a perennial stream, which flows continuously throughout the year. In addition to subsurface drainage from uplands, groundwater flow is responsible for freshwater availability during dry seasons or between precipitation events.	Increase or Unchanged	Decrease or Unchanged	This process varies between agriculture and urbanization. In the former, it can increase or remain the same depending on whether cropping is accompanied by artificial drainage and seasonal changes in crop production. The latter decreases or will be unchanged, depending on the extension of impervious area and surface runoff and groundwater recharge over the landscape.
Annual water yield	The total quantity of water of an area in one year. It depends on streamflow and/or groundwater recharge	Increase or Unchanged	Increase	This process combines the effects of reduced transpiration, interception, and increased surface runoff. The quantity of water can increase per year because there is low vegetation, increasing the risk of floods and erosion in the soils of the watershed.

Sources: Brooks et al. (2013); Cheng (2007); Gregersen et al. (2007); and Ray et al. (2002)

2. Chapter 2: Water Yield Quantification and Analysis of Land Cover Change impact in Water Availability for the Conservation Area of Guanacaste, Costa Rica using SWAT

2.1. Introduction

Hydrological modelling is the instrument selected to develop a water availability assessment for the Conservation Area of Guanacaste (ACG). By means of a simplification of reality, this instrument allows the quantification and evaluation of different physical processes in a drainage area which are influenced by ecological and socio-economic interactions between the upstream and downstream regions. In general, models are an essential decision-making tool between stakeholders and policymakers for planning and land management (Johnston and Smakhtin, 2014; Refsgaard and Abbott, 1990).

The importance of hydrological modelling relies on four aspects: State, Trend, Prediction, and Decision. Firstly, it allows the evaluation of the current state of the hydrological system of a basin and the identification of the factors which alter the current conditions. Secondly, the water resource trend can be assessed by evaluating historical changes, analyzing data from monitoring stations. Thirdly, models help to predict the state of resources according to the impacts generated by different human actions, mainly due to the change in land covers. Finally, models enable the analysis of different decision-making scenarios through changes in the current parameters to consider various management alternatives which demonstrate the optimal strategy and the desired state, in terms of quantity and quality, of water resources.

In summary, among the advantages of hydrological modelling, it allows the understanding of physical phenomena of the basin, the quantification of different variables of interest and the analysis of diverse monitoring datasets. In addition, it facilitates the creation and analysis of scenarios for decision-making and prediction of the quality and quantity of the available resource. However, hydrological models have some limitations because they simplify reality. This simplification entails uncertainty and subjectivity according to the researcher's knowledge and research interests. On the other hand, modelling depends primarily on data. If the data is not of satisfactory quality or there is not much availability, this will alter the modelling reliability.

For hydrological modelling, it is essential to understand the study area to select the most appropriate model, the required quality of the data, and the study scale (Abbaspour et al., 2018, 2015; Arnold et al., 2012b). For the present study in the ACG, I selected a spatially explicit model, the Soil and Water Assessment Tool (SWAT), given its comprehensive and computationally efficient approach based on the analysis of physical properties to explain the vegetation-soil-terrain-water dynamics of complex watersheds (Arnold et al., 1998; Francesconi et al., 2016; Neitsch et al., 2011; Wang et al., 2019). SWAT has had several documented applications in water resources modelling, with the *Water Yield* simulation as the most common output variable for interpreting water provision (Francesconi et al., 2016). Water yield is defined as the net amount of water that leaves the basin and contributes to streamflow during a given time interval (Brooks et al., 2013; Dingman, 2015; Ullrich and Volk, 2009).

In the Neotropics, the SWAT model has been broadly employed to evaluate ecosystem services. I found nearly 200 studies in the Scopus database (www.scopus.com) for the last 20 years. Most studies have been developed in Brazil and Mexico and, to a lesser extent, in Central America, where I did not find any study focused on ecosystem services and SWAT in the continental area. Only one research in the Caribbean zone considered the first SWAT model developed for Cuba to assess the potential effects of climate change in the water produced by Cuba's longest river watershed, the Cauto river (Montecelos-Zamora et al., 2018). In other databases, only one research appeared repeatedly, a M.Sc. thesis from McGill University. This master's project was developed to evaluate the Panama Canal's watershed and its management principally as the main reservoir of water for agricultural activities and hydropower in this region (Oestreicher, 2008). This study is important because it inspired significant SWAT improvements, such as the SWAT-Hydropower Operation Routine developed by Shrestha et al. (2020).

In the rest of the studies analyzed in tropical countries in America, the evaluation of ecosystem services, beyond estimating the quantity of water, have deepened in the assessment of the quality of the water available in ecosystems, primarily in the accumulation of nutrients such as phosphorus and nitrogen and the total solids found in water bodies (Lopes et al., 2020). Overall, the studies are based on applications in agriculture, one of the most important economic activities in this region due to its favourable climatic conditions. Among those applications are the analyzes focused on intensively irrigated areas (Wei et al., 2021) and how climate change can affect water availability for these zones due to persistent periods of droughts (Hoyos et al., 2019).

Climate change studies using SWAT stand out in emblematic ecosystems, for instance, in the transitions between enormous mountain systems like the Andes and plain or flat ecosystems, such as the Amazon. These areas have outstanding ecological, economic, and social values. However, they have been heavily affected by deforestation, extensive cattle ranching, and hydropower generation. These negative impacts have altered the hydrologic dynamic in these regions colonized for extensive human settlements (de Oliveira Serrão et al., 2020; Lopes et al., 2021). Other examples are the coastal habitats in the Pacific and the Caribbean, where the main concern is the degradation of critical environments such as reefs and mangroves (Fernandez-Palomino et al., 2020; Hoyos et al., 2019). To a different extent, there are some applications in the development of policies and programs, such as SWAT for the generation of payments for ecosystem services (PES) programs (Quintero et al., 2009).

SWAT has also been used to assess land use cover change (LUCC) impact on water supply. In this case, SWAT quantifies the change in water balance physically observed in the decrease of streamflow, water management practices, the increment of nutrients and xenobiotics with a toxic concentration of chemicals into the water bodies, among others (Peters and Meybeck, 2000; Rodríguez-Romero et al., 2018). However, SWAT has also allowed the identification of positive changes in water resources caused by better land use management practices, such as reforestation, ecological restoration, and conservation tillage practices. These practices produce a reduction in sediment yield, soil erosion, surface runoff which also reduces the risks of floods, among other benefits (Peters and Meybeck, 2000; Uribe et al., 2018). This last scenario is of interest because this research is based on Costa Rica's critical ecosystems, and this is a country that has dedicated significant efforts to the recovery of altered ecosystems through forest conservation, ecological restoration policies, and the promotion of sustainable tourism (Calvo-Alvarado et al., 2009; Portillo-Quintero and Sánchez-Azofeifa, 2010).

For the different regions in Costa Rica, there are barely any studies published. A report from the NASA DEVELOP National Program shows the initial steps of hydrological modelling based on SWAT in the entire Tempisque River Basin, with the purpose of monitoring droughts and water balance in the Guanacaste Province; calibration was not applied to the model as indicated in the future work section (Durham et al., 2016). Only one scientific article was found, Benavides and Veenstra (2005) developed a SWAT model for the Nosara watershed located in the Southwest of the Guanacaste Province to estimate the concentration of sediments, nitrogen, and phosphorus in the Nosara river that flows into the Pacific Ocean. The parameters used and their range for calibration were not included in the paper. Another document found was an official report related to the development of a SWAT model for the micro-basin Platon-Pacayas located in the Central region of Costa Rica (Arroyo Morales et al., 2010). This study emphasizes the importance of SWAT for the decision-making process; regarding the calibration, it was based on streamflow, nutrients, and sediments; however, the report does not indicate the parameters used. Two theses which specify the calibration process were found, Barquero-Ureña (2015) and Carvajal-Vanegas (2017). The study areas were located within the Tempisque River basin. The first thesis in the Tempisque-Bebedero sub-basin, created a SWAT model, and its calibration was run one variable at a time, beginning with the calibration of the surface flow. Once the established performance thresholds were reached for surface flow, the next variable's calibration (total flow) took place, then for nutrients, and finally sediments; three parameters were identified as the most sensitive parameters (Barquero-Ureña, 2015a). The second thesis was in the Tempisquito river basin (14.29 km^2). The calibration was based on streamflow information, and six sensitive parameters were found (Carvajal-Vanegas, 2017).

Specifically for the entire ACG, there is only one research developed using SWAT, a thesis by Castro-Magnani (2018). The author simulated water yield and emphasized the importance of hydrological process-based models for the estimation of the water provision in ecologically important areas. The author also concluded the necessity of improvements related to the lack of model calibration and validation using field measurements for the reliable application of the hydrological model.

Based on previous information, this chapter's main goal is to present the first calibrated and validated SWAT hydrological model for the ACG for quantifying the water provision ecosystem service. As shown in Figure 1.1, hydrological modelling has been identified as a tool that permits the analysis of the bio-physical underpinning of service delivery, also stated by Martin-Ortega et al. (2015c). By applying calibration and validation to the SWAT model, it is possible to reduce uncertainties in assessing water availability for the ACG, aiming to offer a robust tool for various purposes such as environmental monitoring of water resources and conservation policies. This objective will also include testing different meteorological and hydrological information sources to offer a picture of all the datasets available and their reliability and/or limitations, emphasizing the official datasets existing for the ACG, which the Government entities and stakeholders generally use for the decision-making process.

As the provision of water as an ecosystem service is governed by the inextricable linkage between land use and the water availability (Martin-Ortega et al., 2015a), the impact that land use and cover multitemporal change (LUCC) have on this ES will also be analyzed.

LUCC is recognized as the main anthropogenic cause of the transformation of ecosystems; it is estimated that currently, only 22% of the earth's surface has ecosystems without impacts by human actions (Correa-Ayram et al., 2017; Etter et al., 2011). In the case of the Guanacaste Province, no significant natural vegetation changes have been detected since the late 80’s (Calvo-Alvarado et al., 2009; Castro-Magnani, 2018; SINAC, 2010). But this was not always the situation. During the 60’s and 70’s a dramatic annual deforestation rate of 0.74% was registered, equivalent to 1,441.13 km^2 per year (Calvo-Alvarado et al., 2009). However, the establishment of novel environmental legislation and other socioeconomic factors significantly changed the trends in deforestation, recovering the forest from 26% of coverage in the late 80’s to 47% by the beginning of the 2000s (Calvo-Alvarado et al., 2019, 2009). In general, LUCC is associated with alterations in the hydrologic cycle (Table 1.1), impacting water availability. Therefore, the evaluation of this impact will comprise using the calibrated SWAT model and varying the land cover information from three years 1979, 1997, and 2015, produced by Chen (2020). Furthermore, the LUCC analysis intends to increase the accuracy of the model’s estimations in water availability by representing the dynamic of transformation or recovery of the ecosystem and more realistic watershed conditions.

To recap, the overall objective is to build a calibrated and validated SWAT hydrological model to evaluate the provision of water as an ecosystem service of the Conservation Area of Guanacaste. Additionally, the impact of land use and cover change between 1979, 1997, and 2015 will be addressed. To be best of my knowledge, this is the first calibrated and validated SWAT model, including the land cover variation for this study area.

2.2. Methods

2.2.1. Study Area

The study region is the Conservation Area of Guanacaste (ACG), located in the northwestern part of Costa Rica, between the administrative areas of La Cruz and Liberia in the Province of Guanacaste and Upala in the Province of Alajuela (Castro-Magnani, 2018). It is one of the eleven Conservation Areas of the National System of Conservation Areas (SINAC for its acronym in Spanish) (SINAC, 2010). It is also a natural UNESCO World Heritage Site inscribed in 1999 and extended in 2004 (UNESCO, 2019b). The ACG is described as "the only natural wildland ecosystem likely to survive in northwestern Costa Rica" (Janzen and Hallwachs, 2000). Natural forest is the dominant land cover presented in the ACG, occupying approximately 67% of the total area (Calvo-Alvarado et al., 2009; Castro-Magnani, 2018). Among its hydro-climatological characteristics, the temperature fluctuates between 26.6°C and 27.5°C, precipitation ranges from 1390 mm to 1800 mm, and the dry season, when water becomes a limiting factor, is between December and April. The major basins presented at the ACG are Nicaragua Lake, Santa Elena Bay, Papagayo Gulf, and Tempisque River; the last one is the primary catchment area, draining 10.6% of the national territory (Figure 2.1).

2.2.2. Soil and Water Assessment Tool (SWAT) Model Setup

The Soil and Water Assessment Tool (SWAT) is a physically-based model initially created for agricultural research to predict impacts due to land change, land management, and nutrient loads. Physically-based means that for the model to explain the dynamics and interactions between input and output variables, instead of relying on regression equations, it requires large amounts of specific data related to topography, land use management practices, soil properties, fertilizer inputs, crops or vegetation, and many more weather data inputs (Arnold et al., 2012a; Neitsch et al., 2011).

SWAT development was based on the combination of different models created by the United States Department of Agriculture (USDA). However, the articulation of two models originated the modelling roots of SWAT. The first model is SWRRB (Simulator for Water Resources in Rural Basins), created under the same physically-based approach and enables the simulation of land management practices on water and sediment yields, but only for a maximum of 10 sub-basins per watershed (Neitsch et al., 2011; Williams et al., 1985). The second model is ROTO (Routing Outputs to Outlets), created to link various outputs of different SWRRB models to route the flows through channels and reservoirs, overcoming the 10 sub-basins restriction (Arnold et al., 1995; Neitsch et al., 2011). SWAT overcome both models' limitations allowing simulations in extensive areas. Additionally, during the last three decades, several improvements have been applied in terms of spatial representation; introducing a new unit of study, the Hydrological Response Unit (HRU); water quality including different land management options and crop growth models; meteorological conditions with different snow melt and in-stream procedures; and nutrient cycling and bacteria transportation routines (Krysanova and Arnold, 2008; Neitsch et al., 2011). In terms of technological advancements, SWAT has been adapted to work in Windows Editor, QGIS, and ArcGIS interfaces (Krysanova and Arnold, 2008; Neitsch et al., 2011). In this study, I used the ArcSWAT extension [https://swat.tamu.edu/software/arcswat/] (SWAT, 2018) through the ArcGIS (10.5.1 version) interface for setting up the model for the Conservation Area of Guanacaste (ACG); and selected 1977 - 2019 as the modelling time frame with a warm-up period of three years.

For a better comprehension of the SWAT model set-up, Figure 2.2 illustrates a flow diagram that summarize the main procedures.

2.2.2.1. Driving force in SWAT hydrological modelling: Water Balance

As indicated above, a model such as SWAT is a simplification of reality. The same happens in terms of all the complex and dynamic hydrologic cycle processes that are streamlined in the *Water Balance*. As the name indicates, it is a balance that occurs over a period of time between the inputs and the outputs of water together with the water that is already stored in any watershed (Brooks et al., 2013). The water balance, also known as water budget or hydrological balance is represented in Equation 1 described by Brooks et al. (2013).

$$P + GW_i - Q - ET - GW_0 = \Delta S \qquad (1)$$

$P = Precipitation\ [mm]$

$GW_i = Groundwater\ flow\ into\ the\ watershed\ [mm]$

$Q = Streamflow\ from\ the\ watershed\ [mm]$

$ET = Evapotranspiration\ [mm]$

$GW_0 = Groundwater\ flow\ out\ of\ the\ watershed\ [mm]$

$\Delta S = Change\ in\ the\ amount\ of\ storage\ in\ the\ watershed\ [mm]$

The balance in Equation 1 can be considered as the driving force of all simulations occurring within SWAT. It has been adapted by Neitsch et al. (2011) , as shown in Equation 2.

$$SW_t = SW_0 + \sum_{i=1}^{t}\left(R_{day} - Q_{surf} - E_a - w_{sep} - Q_{gw}\right) \qquad (2)$$

$SW_t = Final\ soil\ water\ content\ [mm]$

$SW_0 = Initial\ soil\ water\ content\ on\ day\ i\ [mm]$

$t = time\ [days]$

$R_{day} = Amount\ of\ precipitation\ on\ day\ i\ [mm]$

$E_a = Amount\ of\ evapotranspiration\ on\ day\ i\ [mm]$

$w_{seep} = Amount\ of\ water\ entering\ the\ vadose\ zone\ from\ the\ soil\ profile\ on\ day\ i\ [mm]$

$Q_{gw} = Return\ flow\ on\ day\ i\ [mm]$

The mechanistic approach of Equation 2 is based on the division of a drainage area into spatially similar regions, the HRUs. This subdivision enables the differentiation of hydrologic variables for various vegetation and soil types (Neitsch et al., 2011). Water balance simulation starts by reading meteorological datasets, initially daily max and min Precipitation and Temperature; and when available Solar Radiation, Wind Speed, and Relative Humidity (this data could also be estimated by SWAT). Then, Soil Temperature is computed together with Snowfall (temperature values < 0°C) and Snowmelt. Precipitation is divided between Rainfall and Snowfall. If the sum of these two variables is higher than 0, Runoff and Infiltration values are computed. Else, Soil water routing, Evapotranspiration, Crop growth, Pond and Wetland balances, and Groundwater flow and height are calculated. All these values are represented at the HRU scale. Neitsch et al. (2011) offer a detailed description of this modelling approach.

The water balance concept has been utilized in the present study for the calculation of the variable of interest, the *Water Yield*. This variable can be calculated by modifying Equation 2 in terms of the water that leaves every spatial unit and enters the main channel as Ayivi and Jha (2018) described, Equation 3.

$$W_{yld} = Q_{surf} + Q_{gw} + Q_{lat} - T_{loss} \quad (3)$$

$W_{yld} = Water\ Yield\ [mm]$

$Q_{surf} = Surface\ runoff\ [mm]$

$Q_{lat} = Lateral\ flow\ contribution\ to\ streamflow\ [mm]$

$Q_{gw} = Groundwater\ contribution\ to\ streamflow\ [mm]$

$T_{loss} = Water\ losses\ from\ tributary\ in\ the\ HRU\ by\ transmission\ through\ the\ bed\ [mm]$

The surface runoff (Q_{surf}) is estimated using the Curve Number (CN) method developed by the Soil Conservation Service (SCS) of the USDA represented in Equation 4 (Ayivi and Jha, 2018; Neitsch et al., 2011).

$$Q_{surf} = \frac{(R_{day}-0.2S)^2}{(R_{day}-0.8S)} \quad (4)$$

$Q_{surf} = The\ accumulated\ runoff\ or\ rainfall\ excess\ [mm]$

$R_{day} = The\ rainfall\ depth\ for\ the\ day\ [mm]$

$S = The\ retention\ parameter\ [mm]$

The type of soil, soil water content, land use, management, and slope influence the retention parameter; hence, it changes spatially as defined in Equation 5 (Ayivi and Jha, 2018; Neitsch et al., 2011).

$$S = 25.4\left(\frac{100}{CN} - 10\right) \quad (5)$$

$S = The\ retention\ parameter\ [mm]$

$CN = Curve\ Number\ for\ the\ day.$

In SWAT, the CN is differentiated by Hydrological Soil Group (HYDGRP), which is a classification of four different groups (A, B, C, and D) based on soil's permeability, land use, and antecedent soil water conditions (Neitsch et al., 2011).

For the ACG, an HYDGRP has been assigned to each of the 12 soil types identified for the area using the Digital Soil Map of Costa Rica (CIA-UCR, 2016). The selection of the HYDGRP per soil type was based on a literature review and is shown in Appendix 1 (Abbaspour and Vaghefi, 2019; Barquero-Ureña, 2015b; Mateo-Sagasta et al., 2017; Ramos, 2016).

The lateral flow (Q_{lat}) is calculated by SWAT as a function of hydraulic conductivity and the each soil layer's permeability capacity at a shallow depth, as shown in Equation 6 (Ayivi and Jha, 2018; Neitsch et al., 2011).

$$Q_{lat} = 0.024\frac{(2\ S\ SC\ \sin\alpha)}{\theta_d\ L} \quad (6)$$

$Q_{lat} = Lateral\ flow\ [mm/day]$

$S = Drainable\ volume\ of\ soil\ water\ per\ unit\ area\ of\ saturated\ thickness\ [mm/day]$

$SC = Saturated\ hydraulic\ conductivity\ [mm/h]$

$L = Flow\ length\ [mm]$

$\alpha = Slope\ of\ the\ land$

$\theta_d = Drainable\ porosity$

The groundwater contribution to the stream (Q_{gw}) is based on base flow estimation according to Equation 7 (Ayivi and Jha, 2018; Neitsch et al., 2011).

$$Q_{gwj} = Q_{gwj-1}\, e^{(-\alpha_{gw}.\Delta t)} + W_{rchrg}\left(1 - e^{(-\alpha_{gw}.\Delta t)}\right) \tag{7}$$

$Q_{gwj} = groundwater\ flow\ into\ the\ main\ channel\ on\ day\ j$

$\alpha_{gw} = base\ flow\ recession\ constant$

$\Delta t = time\ step$

$W_{rchrg} = The\ amount\ of\ recharge\ entering\ the\ aquifers\ [mm/day]$

SWAT separates the simulation of all processes within the water balance into two main phases: the hydrologic cycle's land phase and the water or routing phase. The former controls the amount of aqueous sediment, nutrient, and pesticide loadings that enter the main channel in each sub-basin; while, the latter controls all loadings' movements in the main channel through the channel network and watershed outlet (Neitsch et al., 2011). This research is focused on the amount of water produced in the ACG; therefore, it only concentrates on the results obtained on the land phase of the hydrology, where the value of the water yield is estimated for each sub-basin individually and then routed to obtain the value for the entire drainage area simulated for the study area (Arnold et al., 2012b; Neitsch et al., 2011).

The land phase is spatially represented within SWAT, dividing large watersheds into sub-basins for a more detailed analysis, especially if certain regions within the total watershed have a dominant impact on the hydrological cycle (Neitsch et al., 2011). The sub-basin simulation is useful to differentiate the effect in the hydrological processes of the different land management practices within the watershed. Each sub-basin will contain information of climate, groundwater, the main channel draining the sub-basin, and Hydrologic Response Units (HRUs) that are areas with a unique combination of land cover and management, soil, and slope (Neitsch et al., 2011). In this study, each sub-basin consists of a unique HRU formed by the dominant land cover, soil type, and average slope steepness value.

2.2.2.2. SWAT model Inputs

SWAT needs two types of model inputs, geospatial and time series. Input data quality and availability are critical aspects of hydrological modelling because they are sources of uncertainty (Abbaspour et al., 2015, 2007b). Therefore, the present study explored different sources of information and built several models combining various inputs and compared the results with streamflow observations obtained from La Guardia Station located in the Southwest of the study area on the Tempisque River basin (Figure 2.1). The model with the best initial performance was selected for calibration and further analyses. Inputs of such model and sources of information are detailed in Table 2.1.

Geospatial Data

- ***Topographic Maps***

A Digital Elevation Model (DEM) of 10 m of resolution available in the Costa Rica Atlas of 2014 (Ortiz-Malavasi, 2014) was used to represent the topographic features of the study area. The DEM is the primary source for the drainage area delineation and its later discretization into sub-basins. Additionally, the DEM is used to obtain the slope information for the HRUs definition (Arnold et al., 2012a).

The drainage area, the subbasin delimitation, and the streamflow network were initially modelled with the topographical information. The 'Burn-in' method was used for DEM processing for the streamflow generation, introducing the stream network at 1:200,000 scale available in the

Atlas of Costa Rica 2014 (Ortiz-Malavasi, 2014). 'Burn-in' uses an algorithm that digitalizes, in raster format, the network into the ArcMap interface; then the DEM elevation values overlapping the digital streams are reduced to change slope values. This process allows an enhanced generation and localization of the streams and subsequently an improved basin and sub-basins delimitation (Luo et al., 2011). Appendix 2 shows the improvement in the channel network using the 'Burn in' method.

- ***Land Use and Cover Data***

I selected the land cover maps of the years 1979, 1997, and 2015 produced by Chen (2020). These maps cover the entire Province of Guanacaste; the Districts of Chira, Cobano, Lepanto, Paquera, and Puntarenas of the Puntarenas Province; and the area of the ACG located within the Alajuela Province. Land cover information was created using Landsat images and the supervised classification method known as Support Vector Machine (SVM) (Chen, 2020). The SVM technique is based on machine learning, used in this specific case to recognize spatial patterns through non-linear methods that allow differencing, with a high-level of accuracy, the land cover classes (Vapnik, 2013). According to field verification and comparison with higher resolution data, 1979, 1997, and 2015 maps have an estimated overall accuracy of 87.6%, 86.5% and 90.0%, respectively (Chen, 2020). The spatial resolution of the three land cover maps was indicated in the raster files as 30 m.

In each map, six land cover classes were identified: (1) Forest, including into this category the dry, moist, and wet tropical forests; (2) Grass/Pasture; (3) Agriculture; (4) Mangrove; (5) Urban; and (6) Water. There is missing data in the land cover classification caused by the presence of clouds in Landsat imagery datasets (Chen, 2020). Specifically, in the ACG, the missing data was included as the seventh land cover class named "Cloud" and represented 3.9%, 12.8%, and 26.4% in 1979, 1997, and 2015 maps. Part of the missing data was replaced using the 'Con' Spatial Analyst Tool in ArcMap, which uses conditional expressions and logical operators between two input raster layers to allow changing selected pixels values of an output raster file (ESRI, 2016). 'Con' tool was used to include the 1979 land cover data into the "Cloud" values of the 1997 map, and subsequently, the new resulting 1997 land cover values into the missing data of the 2015 map.

The ‘Con’ process allowed to reduce the “Cloud” data to 3.6% and 2.1% in the 1997 and 2015 maps, respectively (Appendix 3).

As evidenced in Appendix 3, forest cover predominates over time. Therefore, this land cover class has been undissolved between the deciduous forest and the evergreen forest, which are the types of forest characterized in the SWAT 2012 database with different vegetation growth parameters that impact the spatial pattern in the watershed delineation and the simulation of water balance variables. For the forest land cover differentiation, I used the life zones map (Appendix 4) of the year 2008 available in the Atlas 2014 of Costa Rica (Ortiz-Malavasi, 2014).

- ***Soil***

A layer with soil physical and chemical properties information is the second most important geospatial input that SWAT needs. When modelling, this data will determine water movement within the spatial units of HRUs (Abbaspour et al., 2019). In this case, a 2016 updated soil map from the Centre for Agronomic Research (CIA for its acronym in Spanish) of the University of Costa Rica was used (CIA-UCR, 2016). Before introducing the information to SWAT, the shapefile format was transformed to a raster file selecting a pixel of 30 m to have the same spatial resolution as the other spatial inputs. Appendix 1 describes the 12 soil types that are identified for the ACG.

Additionally, a soil table in SWAT database format was created using the soil profiles field database obtained from the CIA. That information contains the physical and chemical properties needed for modelling. Soil parameters are calculated using the Pedotransfer Functions (PTF), a term introduced in 1987 by Bouma and van Lanen to link the information of soil field data or soil survey with soil hydrology, obtaining the soil hydraulic properties based on statistical correlations (Pachepsky and Rawls, 2004). PTF require high amounts of input information that are regularly costly and difficult to measure. Therefore, some studies have developed modern equations that can be applied in a broad range of soil types and moisture regimes, using typically available soil measurements and variables, as shown in Saxton and Rawls (2006). These authors developed a set of water characteristic equations that require information only of common soil texture variables and organic matter; information that is available in the CIA's soil database. To create the SWAT user soil table, I used the Excel template created by Narasimhan and Dhanesh (2012), which calculates all soil parameters based on the PTF proposed by Saxton and Rawls (2006).

Time Series

Typical inputs for the SWAT model include weather information that is divided between mandatory and optional information. The mandatory ones are temperature and precipitation; while solar radiation, wind speed, and relative humidity are optional. These data require a daily resolution. For missing weather values and the generation of the optional input information that is not available, SWAT has a 'Built-in' weather generation model that can be used to define the full-time range values (Arnold et al., 2012a). The weather generation (WGEN) model is based on long-term statistics stored in a WGEN user table in the SWAT database (SWAT2012.mdb). The WGEN user table is area-specific, hence for the ACG, it is created using the information from weather stations and the user-friendly tool developed by Essenfelder (2018) to generate the WGEN statistics and process daily weather data in the format needed to be used in SWAT projects.

- ***Weather Stations***

One of the main purposes of this research is to offer a tool for decision-making in the ACG. For that reason, it was considered crucial to test the official available meteorological and hydrological information that exists for the region, which is the data generally used by the Government entities and stakeholders for the decision-making process. The SWAT model here also aims to show the reliability of the available data and/or limitations.

Information from weather stations was obtained from the National Meteorological Institute (IMN for its acronym in Spanish) in Costa Rica. There are in total five stations distributed as shown in Figure 2.1 and described in Table 2.1 with information for Precipitation, Temperature, Relative Humidity, Solar Radiation, and Wind Speed. In addition, daily precipitation and temperature data from another station located in the Santa Rosa National Park (Western ACG) was included. This station is monitored by the Centre of Earth Observation Sciences (CEOS) of the University of

Alberta. All datasets were organized into a format readable by SWAT. For simulation purposes, a standard time frame for all stations was set, consisting of the period between 1977-01-01 and 2019-12-31; missing values were filled with -99, later replaced by a value generated from the WGEN database.

2.2.3. Model Calibration

The calibration's main purpose is to analyze how well the values simulated by a model fit with the measured values of one or several variables in the study area. The ultimate objective of this analysis is to optimize the difference between simulated and observed values while realistically represents the physical processes of a particular natural system (Abbaspour, 2005; Abbaspour et al., 2018, 2015, 2007b; Arnold et al., 2012b). The calibration process is a subjective process due to the multiple assumptions that must be made for the selection of parameters and the value range that best fits them. This is known in the literature as the *non-uniqueness problem*. It means that the best solution can be reached with multiple combinations of values in the set of parameters (Abbaspour, 2005; Abbaspour et al., 2018).

All the assumptions made in the calibration process of a hydrological model lead to some uncertainties not only for the distributions assigned to the parameters, but also for additional factors such as inadequate definition of the conceptual model, parametrization, selection of the objective function, and selection of the optimization algorithm (Abbaspour et al., 2018). The following section shows how these aspects have been defined in the model built for the Conservation Area of Guanacaste.

SWAT-CUP is the software used for calibration, uncertainty analysis, and validation processes; it stands for SWAT - **C**alibration and **U**ncertainty **P**rocedures. It is recognized for standardizing all the calibration steps and for being computationally and time-efficient. It supports the SUFI2 - The **S**equential **U**ncertainty **FI**tting ver. **2** program, which is the algorithm that accounts for all the uncertainty associated with the parameters ranges used in the calibration and validation procedures (Abbaspour et al., 2007a).

For the SWAT model constructed for the ACG, calibration, uncertainty analysis, and validation were carried out for one hydrological variable, monthly mean streamflow. For the study area was available one station (La Guardia) described in Table 2.1. This station is administered by the Costa Rican Institute of Electricity (ICE for its acronym in Spanish), and it is located in the main river of the watershed, Tempisque River, which drains an area of 955 km^2.

2.2.3.1. The Conceptual Model

The conceptual model seeks to frame all the complexities of the drainage area, including from the permanent and periodic natural water bodies such as wetlands, lakes, lagoons, and ponds, to all the human-made activities for the management of hydrological resources such as dams, irrigation districts, and trans-basin diversion infrastructures.

Regarding the SWAT model developed for the ACG, a drainage area of 2,861.92 km^2 has been characterized. This area comprises the four main basins identified in the official cartographic information of Costa Rica; in the North and Northwest, the Nicaragua Lake watershed; in the East, the Santa Elena Bay basin and the Papagayo Gulf basin; and in the Central and South, the Tempisque River basin. They comprise 41.40%, 5.29%, 4.65%, and 48.66% of the total drainage area, respectively. Within this area, the model estimated the main rivers whose orientation is also characterized in the division of the main basins. This division is produced mainly by the Guanacaste Cordillera represented in the DEM, and where the Orosí, Rincón de la Vieja, and Cacao Volcanoes stand out as the main dividing points of the drainage network of the Nicaragua Lake and Tempisque River basins. The hills of the Santa Elena Peninsula are the primary mountain system that divides the basins from the Papagayo Gulf and Santa Elena Bay watersheds. All this information was contrasted with the base map of high-resolution images available in ArcMap and with the water network characterized in the Atlas of Costa Rica at a scale of 1: 200,000. The model effectively represents the main rivers and its tributaries.

For the identification of additional processes, I proceeded to analyze water bodies available in the Costa Rica Atlas, finding only information of lagoons. Within the drainage area mapped for the ACG, no predominant water bodies were identified; the largest (0.30 km^2) was an intermittent lagoon in the Southeastern part. In total, the water bodies cover 0.06% (1.70 km^2) of the total area. Since there is no information on the water dynamics of these water bodies, they are not considered within this conceptual model. Furthermore, there are no hydroelectric projects or irrigation districts within the conservation area. All the limitations present in the conceptual model, such as lack of information, errors associated with measurements in the input data, or the omission of reservoirs and other infrastructure data, are partially compensated through the calibration process (Arnold et al., 2012b).

The conceptual model also implies the selection of the best input data. Different studies indicate that the existence of a wide variety of geographic and climatic datasets, including different spatial and temporal resolutions, influences the quantification of water resources. It is a good practice the combination of data between the numerous sources of information together with the analysis of the model performance. This practice allows to discriminate and select the best datasets to build a model that represents, with a high level of precision, the hydrological processes of the study area (Abbaspour et al., 2019, 2018, 2015).

I proceeded to analyze different sources of information available to show the stakeholders existing data sources and the effect they have on the construction of the model. This process was also carried out for the selection of the best possible spatial and meteorological inputs. Ten different models are proposed for the selection of the best inputs, namely:

Model 1. In the beginning, I utilized the inputs used by the Castro-Magnani, (2018) study; however, while building this model, it was not possible to use the soil information because the user table in the SWAT database (SWAT2012.mdb) was not being recognized. So, I decided to utilize the FAO soil, which has been widely implemented in the development of different SWAT models (Abbaspour et al., 2019, 2015; Alemayehu et al., 2017; Pagliero et al., 2014).

Model 2. For the second model, the same information used by Castro-Magnani, (2018) was implemented, except for the meteorological information; here, the data from the network of stations of the IMN and from the CEOS monitoring station were employed.

Models 3 and **4**. After the successful construction of the previous models, for models 3 and 4 I decided to analyze the soil information issue mentioned because FAO information has coarse resolution and is limited in terms of description of parameters for local areas, which directly affects the characterization of the spatial patterns in the watershed and consequently the accuracy of the model estimations (Bayabil and Dile, 2020). Therefore, I adjusted the soil information for 2016 from the CIA data (see Section 2.2.2.2). I run again the two previous models that implemented more detailed soil information. After analyzing the performance of the previous four models (Appendix 5), I concluded that the information from the CIA is the best soil input to build the SWAT model. However, there are important differences in magnitude between simulated and observed data.

Models 5 and **6**. Consequently, I evaluated the terrain's effect, introducing a DEM of 10 m to replace the DEM of 30 m used in the previous four models. The differences in magnitude improved noticeably, determining that the DEM of 10 m will be used as the topographic input. Additionally, the IMN-CEOS meteorological information has shown the best performance among the six models evaluated so far; thus, this dataset is selected as the weather input data. The following input to test was the land cover information. The 2015 land use data utilized by Castro-Magnani (2018) offered good performance in the initial models. However, this study also entails the evaluation of the multitemporal LUCC impact on the water resources quantification, hence other periods of land use data are needed.

Models 7, **8**, and **9**. Therefore, I proceeded to analyze different sources of land cover data that offer different periods of information for the same area, starting with the three maps developed by Chen (2020) for the years 1979, 1997, and 2015.

Model 10. I decided to also test Global Land Cover products from the Climate Change Initiative of the European Spatial Agency (ESA) because this data set offers a wide time range (1992-2015) at 300 m of spatial resolution and combines information from different sensors such as MERIS, SPOT-VGT, AVHRR, and PROBA-V (ESA, 2015), for this test only the data from year 1992 was used.

After evaluating the last four models (Appendix 5), it can be concluded that Model 9 presented the best initial performance in the three indices evaluated (r^2, *NSE*, and br^2). This model included the information of the 2015 land cover map from Chen (2020), the IMN-CEOS weather information, the CIA soil data (CIA-UCR, 2016), and the DEM of 10m resolution from the Atlas of Costa Rica (Ortiz-Malavasi, 2014); defining these datasets as the more suitable inputs to build the SWAT model for the ACG and this will be the model to calibrate.

2.2.3.2. Parametrization

Parametrization can be considered the core of the calibration process because calibration mainly relies on adjusting the physically meaningful range of each parameter. The main concern during this phase is the selection of the set of the best parameters according to the variable assessed and method of type of change that can be applied to the parameters, *v*, *a*, or *r*, standing for replace, absolute, and relative change, respectively (Abbaspour, 2007). For this study, I started by looking at the SWAT documentation information, which states that not all inputs and parameters are common for all watersheds; e.g. snowfall parameters do not apply for the ACG, which does not register temperatures bellow 0 °C in the period of study (Arnold et al., 2012a). Therefore, only parameters governing streamflow generation processes were selected, i.e., all parameters related to nutrients loads, water quality, and natural or artificial water bodies (ponds, lakes, wetlands, impoundments, etc.) were excluded. Besides, all the parameters are characterized at the subbasin level because no HRUS were determined within the sub-watersheds; neither infrastructures were identified within the study area, nor natural water bodies such as lakes are representative (< 1%). Thus, this study includes parameters related to general information of the diversity of topographic aspects, overland water flow, vegetation-water interactions, and erosion features within the sub-basin (*.hru*); the physical properties of the soil that govern the movement of water within the soil profiles (*.sol*) and into and out of the aquifers (*.gw*); the parameters related to land and water management practices within the system (*.mgt*); and parameters used to simulate the physical processes affecting the flow of water in the channel network of the watershed (*.rte*) (Arnold et al., 2012a).

The selection of the parameters was also supported by the literature review of scientific articles focused on streamflow calibration. Firstly, with papers widely used as theoretical bases of the calibration process (Abbaspour et al., 2015, 2007b). All studies aimed to develop a SWAT model for the analysis of watershed hydrology and water quality at the basin scale (Abbaspour et al., 2007b) and regional scale (Abbaspour et al., 2015). Secondly, from papers that use water yield as the primary variable of analysis (Ayivi and Jha, 2018). Thirdly, studies based on streamflow modelling but in tropical ecosystems (Alemayehu et al., 2017; Hoyos et al., 2019; Tarigan et al., 2018). Finally, the most important source of information should come from similar studies in the same region of research or the nearby area. Nonetheless, information for Costa Rica in terms of SWAT modelling is barely published as detailed in the Introduction of this chapter.

Among all the studies reviewed, 18 parameters were selected. To assign the initial range for calibration, first, I chose the default values obtained from the ArcSWAT model. 10 out of the 18 parameters presented variation among all the sub-basins, and 8 had constant values throughout the entire drainage area. Thus, the range of the former parameters was assigned according to the minimum and maximum value reported in the input information; and the range of the latter parameters was extracted from the *Absolute_SWAT_values.txt* file. Table 2.2 summarizes the parameters information described in this section.

2.2.3.3. Selection and definition of the objective function

The objective function can be defined as the equation by which the uncertainty caused by the *non-uniqueness problem* of the calibration will be minimized. For calibration, it is possible to select among ten different objective functions (Abbaspour, 2007). The most widely used have been the functions that maximize the coefficient of determination (r^2) and the Nash-Sutcliffe efficiency criterion (*NSE*) (Arnold et al., 2012b; Faramarzi et al., 2015). However, for this study, the objective function is defined as the maximization of the weighted r^2 coefficient (br^2), which comprises r^2 displaying the trend between the observed and simulated data, and b showing the closeness between the observed and simulated data represented by the slope. Therefore, the maximization of this coefficient will seek to diminish the difference between the simulated and the observed data (trend) and to increase the matching in magnitude (Abbaspour, 2007; Faramarzi et al., 2015; Krause et al., 2005). Additionally, br^2 has been proved to be a more efficient index compared to *NSE*, which ranges between -∞ to 1 and only measures the match between simulated outputs and observed data by normalizing the variance of the observed data in a period of time; this process is highly affected by poor simulations, overestimating larger values and neglecting lower values of the time series (Abbaspour, 2007; Faramarzi et al., 2015; Krause et al., 2005). The *NSE* issues are overcome with the br^2 criterion, which has a range between 0 to 1, causing that the over and underestimations are quantified with the dynamics of the time series, removing the effect of poorly simulated stations (Arnold et al., 2012b; Faramarzi et al., 2015; Krause et al., 2005).

The objective function (Equation 8) is defined as shown in Krause et al. (2005):

$$Maximze: \emptyset = \begin{cases} |b| \cdot r^2 \; for \; b \leq 1 \\ |b|^{-1} \cdot r^2 \; for \; b > 1 \end{cases} \tag{8}$$

$r^2 = Coefficient\ of\ determination$

$b = Slope\ of\ the\ regression\ line\ between\ measured\ and\ simulated\ data$

2.2.3.4. Selection of the algorithm of optimization

In this study, I used the Sequential Uncertainty Fitting program (SUFI-2), considered a semi-automated algorithm for calibration, validation, and uncertainty analysis of hydrological models (Abbaspour, 2005; Abbaspour et al., 2007b). Semi-automated means that the parametrization is based on the analyst's knowledge of the physical processes of the modelled watershed and the variability in soil, land use, slope, and the number of sub-basins (Abbaspour, 2007; Arnold et al., 2012b). It is considered one of the most efficient algorithms because "it is capable of analyzing a large number of parameters and measured data from many gauging stations simultaneously" (Faramarzi et al., 2009). SUFI-2 is linked to SWAT through SWAT-CUP software (Abbaspour, 2007).

2.2.3.5. Sensitivity Analysis

Sensitivity analysis is the method which allows the selection of the set of parameters that have the most significant impact on the hydrologic system under analysis (Abbaspour, 2007; Mehan et al., 2017). This technique is essential because the parameters represent physical processes. Therefore, by selecting the most important processes, it is possible to decrease the number of parameters, which allows a more efficient calibration procedure (Abbaspour et al., 2018). For the present study, I selected a *Global Sensitivity Analysis,* also known as *All-parameters-At-a-Time* (AAT), generated from 1000 simulations and 18 parameters. Unlike One-at-a-Time Sensitivity Analysis, AAT has de advantage of the identification of correlations between multiple parameters. The AAT analysis can be used after running the first iteration in SWAT-CUP (Abbaspour, 2007).

The AAT procedure follows a multiple regression system described by Abbaspour (2007) and Abbaspour et al. (2018) as presented in Equation 9 to quantify the sensitivity of each parameter.

$$g = \alpha + \sum_{i=1}^{m} \beta_i b_i \tag{9}$$

$g = Objective\ function\ value. Here\ the\ objective\ fuction\ is\ to\ maximize\ br^2$

$\alpha = Regression\ constant$

$\beta_i = Coefficient\ of\ each\ paramater$

$b_i = Each\ parameter$

Sensitivity (g) represents a value that estimates “the average changes in the objective function resulting from changes in each parameter, while all other parameters are changing” (Abbaspour et al., 2018). Due to the multidimensionality of this analysis, the relative sensitivities are stored in what is known as a Latin hypercube (Abbaspour, 2007; Mehan et al., 2017).

The relative significance of each parameter is calculated by applying a t-test. Each t-stat is obtained by dividing the coefficient of each parameter into its standard error. When comparing all the t-stats in the student's t-distribution, the values located in the tails will then be the most sensitive parameters ($p - value\ < 0.05$) (Abbaspour, 2007; Abbaspour et al., 2018; Mehan et al., 2017).

2.2.3.6. Regionalization of parameters

After the iteration of 1,000 simulations that led to identifying sensitive parameters, I detected some shifts in the peak and base flows (Figure 2.5-Right). The calibration protocols developed by Arnold et al. (2012b) and Abbaspour et al. (2015) show simple parameters' regionalization rules. The regionalization rules help identifying which parameters and values should be decreased or increased to improve the shift between simulated and observed streamflow. These rules need to be used with caution to not overfit the parameters during calibration.

In order to know the combination of parameters that best fit during regionalization, I decided to carry out six data treatments, combining the parameters that I selected for the model and applying the rules proposed by Arnold et al. (2012b) and Abbaspour et al. (2015) over the parameters they identified (regionalized parameters for now on) as those that most influence the response of the simulated peak and base flows. I run 1000 simulations per data treatment, and they are described as follows:

i. Run a new iteration with 18 parameters again using the new parameters' values obtained in the first iteration.

ii. Run a new iteration with 18 parameters again, changing only regionalized parameters according to the decrease or increase rules.

iii. Run a new iteration including the sensitive parameters identified in the first iteration and the regionalized parameters. The parameters' ranges according to the new values obtained in the first iteration.

iv. The same parameters included in data treatment three. But in this case, the regionalized parameters change according to the decrease or increase rules.

v. Run a new iteration only including the sensitive parameters using the new parameters' values obtained in the first iteration.

vi. The same parameters included in data treatment five. But this time, applying the decrease or increase rules only to the regionalized parameters also identified as sensitive.

2.2.4. Uncertainty Analysis

Indeed, all the assumptions which are made during the calibration process produce some uncertainties in the model outputs (Abbaspour et al., 2018). Therefore, the evaluation of uncertainty during the calibration is crucial for getting meaningful modelling results and reliable applications (Abbaspour, 2005). The uncertainty analysis implies mapping all the uncertainties associated with parameter ranges, conceptual model, inputs, analyst's knowledge, etc. that produce different model outputs (Abbaspour et al., 2015; Faramarzi et al., 2009).

These uncertainties can be expressed in the SWAT-CUP 95% prediction uncertainty (95PPU). It is a band that map the propagation of the parameter uncertainties. A wide band indicates a large parameter uncertainty. Particularly, two factors have been developed to evaluate the goodness of calibration/uncertainty performance, the *p-factor* and the *r-factor* (Abbaspour et al., 2015; Abbaspour et al., 2010, 2018; Arnold et al., 2012; Faramarzi et al., 2009). *P-factor* is the percentage of measured data that falls within the 95PPU, meaning the model's capacity to capture uncertainties (Arnold et al., 2012b; Khalid et al., 2016). The measurements which fall within the *p-factor* range are considered well simulated and fall within the acceptable scope of uncertainty in the model (Abbaspour et al., 2018). In turn, *r-factor* represents the uncertainty referred to the width or thickness of the error bracket (95PPU) and is the mean 95PPU divided by the standard deviation of the observed value; in other words, the *r-factor* represents the quality of the calibration (Abbaspour et al., 2018; Arnold et al., 2012b). The acceptable values and ranges of these factors are at the user's discretion. However, ideally, the *p-factor* should be close to one or 100%, meaning that all the measured data is bracketed in the 95PPU band, and from this factor also the model error can be calculated as 1-*p-factor* (Abbaspour et al., 2015, 2007b; Arnold et al., 2012b). Regarding the *r-factor*, values close to zero are desirable; however, for discharge values, between 1 to 1.5 is acceptable for this index, but depending on the quality of the streamflow data, other values apply (Abbaspour et al., 2015, 2007b; Faramarzi et al., 2017; Roth and Lemann, 2016).

2.2.5. Validation

Validation is the process where the calibrated parameter ranges are tested in a new data set of the study area with the purpose of building confidence in the new calibrated model. For this study, the new calibrated parameters are tested in the streamflow data of La Guardia station from the period 2000 – 2009 in one iteration with the same number of simulations (1000) as in the calibration. Later the same measures used for the uncertainty analysis, *p-factor* and *r-factor*, are calculated together with the objective function criterion (br^2). For validation of river discharge, the mean and the variance of the data used for calibration (1980 – 1999) and validation (2000 – 2009) should be similar (Abbaspour et al., 2018).

2.2.6. Ecosystem Service Estimation

This stage presents the water availability estimated as an ecosystem service for humanity by integrating population metrics. I estimated the number of inhabitants in each sub-basin using a spatial analysis in ArcMap extracting the cell's value of the 1-degree resolution Gridded Population of The World in its 4th version (GPWv4) and revision 11, which includes estimates of human population for 2020 (CIESIN, 2018), and adding up the values by sub-basin. The total population for the ACG was projected to be 101,021 inhabitants in 2020. This value was disaggregated for each year, decreasing the population by the Costa Rica's annual rate of population change calculated by the United Nations (UN) [http://data.un.org/]. This estimation does not account for uncertainties as that is not an objective of the present research. However, this approximation of the number of people living within each sub-basin allows calculating the annual water per capita between 1980 and 2019 expressed as $m^3capita^{-1}yr^{-1}$ by dividing the sub-basin's annual water yield into the estimated inhabitants.

2.2.7. Impact of Land Use and Cover Change (LUCC) on the Water Yield availability

The LUCC has been identified as the primary driver of ecosystem transformation impacting many hydrologic processes (Table 1.1). Thus, it is essential to evaluate the dynamic of the land management in the construction of hydrological models such as SWAT (Moriasi et al., 2019; Schilling et al., 2008; Schuol et al., 2008). This study reconfigures the SWAT model constructed for the ACG changing the land cover input to evaluate the effect of the landscape dynamic over the water availability in the ACG.

To evaluate the LUCC impact, I proceeded to create two new SWAT models in ArcSWAT with the same 40 years of historical meteorological data and terrain and soil inputs. But I modified the land cover input by the 1979 and 1997 maps described in section 2.2.2.2. Subsequently, I specified the streamflow data from 1980 to 1989 and 1990 to 1999 as the calibration and validation periods for the 1979 model; and the discharge information from 1990 to 1999 and 2000 to 2009 to calibrate and validate the 1997 model. For the 2015 information, I used the model already built and ran 1000 simulations up to 2019, which is the last year of the input meteorological information, using the *No_observation* option in SWAT-CUP.

2.2.8. Statistical Analyses

The statistical analyses of the modelled hydrologic cycle components relied on the use of descriptive statistics to represent the temporal behaviour of water supply through a box-and-whisker diagram. Also, the Pearson's correlation and determination coefficients allowed to determine the relationship between variables included in a one-to-one analysis to identify model's over and/or underestimations between: (1) all the observed and simulated streamflow; (2) the peak flows; and (3) the base flows.

For the evaluation of the LUCC effect on the provision of water, in addition to the difference calculated from one period to another, I performed a mixed linear model (GLMM), which main assumptions are that observations do not follow a normal distribution and there are random and mixed or nested factors associated. The response variable, the water yield, is not normally distributed. It is assumed that the nested factors are the land covers and the period (decades), and the random factor is the number of sub-basins, which is fixed among all the models.

Graphs were created using the OriginLab software 9.7.0.188 (OriginLab Corp., Northampton, MA, USA) which is a user's friendly tool to plot several statistical charts.

2.3. Results

2.3.1. Hydrological Model

Overall, I developed the first calibrated and validated SWAT model for de Conservation Area of Guanacaste. This process comprised testing different available datasets to select the best spatial and meteorological information for building the SWAT model. The SWAT model created a total drainage area of 2,861.92 km^2 and quantified all the hydrologic cycle processes for 40 years on a monthly scale between 1980 – 2019. The catchment area represents 83% of the total ACG region (3,452.71 km^2). Subsequently, this area was divided into 107 sub-basins, also representing the Hydrological Response Units (HRUs). The SWAT model's performance is shown in Table 2.5 and presented an error of 12% during calibration and 7% in the validation period.

2.3.1.1. Input Data Quality

I performed a preliminary analysis of different climate databases and information sources for the digital elevation model (DEM), land use and cover, and physical and chemical characteristics of the soil. Ten different models were built and compared using measured and simulated discharges for 30 years gauged in the major river basin of the study area, the Tempisque River watershed. Compared results are shown in Appendix 5. All the models simulated the observed data's pattern. However, they presented differences in magnitude, a situation that was expected to improve through calibration.

Considering the bR^2 indicator, the first four models in Appendix 5 showed significant differences in magnitude. I determined up to this point that the best soil input would be that of the

CIA-UCR used by Castro-Magnani (2018). Later, I graphically analyzed the effect of the DEM (Appendix 2). It is observed that the 30m DEM from FONAFIFO (left) is producing a break in the generation of the current network that forms the Tempisque river basin, which is the closest river to La Guardia streamflow station. It generates a too short stream that could cause the discharge underestimations (Models 1-4). Therefore, for the following models (5 and 6), the soil generated by the CIA is used, but in a version updated to 2016 (CIA-UCR, 2016) and the 10 m DEM available in Costa Rica's Atlas. The new DEM generated a significant improvement in the stream network generation, as shown in the central figure of Appendix 2. Nonetheless, there is a spatial offset with the location of La Guardia station, a feature corrected through the “Burn-in” option in SWAT (Appendix 2 – Right). By changing the DEM, the simulations enhanced in magnitude and trend. These models (5 and 6) also revealed that the best meteorological input comes from the IMN and CEOS stations network. The same soil, terrain, and time series inputs were used for the following models (7-10) but varying the land use data. The land cover map from ESA improved the performance in two of the three indicators (r^2 and br^2). Instead, the land cover maps from Chen (2020) showed an excellent fit in all performance indicators. Finally, I could decide that Model 9 was the most appropriate for calibration. The spatial data used is presented in Figure 2.3 and described in Table 2.1, together with the weather information selected.

The other crucial data source is the hydrological information used for calibration and validation procedures. The observed data available comes from La Guardia station. This station has collected 30 years (1980-2009) of monthly streamflow data. I selected the first 20 years as the period for calibration and the last decade as the validation period. For choosing these periods, I followed the recommendation in Abbaspour et al. (2018) that the information should depict similar descriptive statistics, as shown in Figure 2.4.

2.3.1.2. Calibration and Validation

I run in ArcSWAT 43 years (1977-2019) of weather data available to obtain the initial model to calibrate, selecting three years as the warm-up period. For calibration, I run the first iteration with 1,000 simulations for the first 20 years of observed data (Figure 2.4) with the 18 parameters described in Table 2.2. Later I performed the global sensitivity analysis (Figure 2.5 – Left), resulting in seven sensitive parameters (*p-value* < *0.05*) shown in Table 2.4. However, after analyzing the first iteration, a notorious shift in peak and base flows was detected. Therefore, I run the six iterations (data treatments) proposed as the regionalization process. According to the performance shown in Table 2.3, I concluded that the model could not be improved any further with the available input data, confirming that sensitive parameters and new parameters' values found at the beginning would be the second and last iteration also with 1,000 simulations to finally obtain the calibrated result (see data treatment 5 in Table 2.3).

After getting excellent performance coefficients (Table 2.5), I run another 1,000 times the sensitive parameters for the validation period, which also showed excellent performance (Table 2.5). The calibrated and validated streamflow is shown in Figure 2.6, including the 95 PPU band or the 95% confidence interval of the model, representing the range where observed values fit the simulations run during the calibration and validation processes.

Simulated and observed values were correlated through a one-to-one analysis to show the model's over and underestimations. Figure 2.7 displays the result for all streamflow values and the peak and base flows. A theoretical determination coefficient R_T^2 is calculated with respect to what is considered the perfect model; that is, when the simulated values are exactly the same as the observed values.

Lastly, I calculated the Pearson's correlation coefficient between precipitation (PT) and water yield (WY) estimated in each sub-basin for all the 40 years. The multiannual average *r* was 0.8, meaning that the model's main input (PT) has a strong linear relationship with the main output (WY).

2.3.2. Hydrological Characterization of the ACG's drainage area

2.3.2.1. Spatio-temporal

I extracted the multiannual average precipitation and water yield from the calibrated model. Figure 2.8 shows the spatial distribution for both variables. The average precipitation ranges between

1,176 mm and 1,673 mm per year, and the water yield between 687 mm and 1,353 mm per year. In addition, I represented the annual pattern of both variables shown in Figure 2.9 using boxplots that visually show the distribution of the average rainfall and water yield per month through quartiles. The annual average water yield distribution from 1980 to 2019 is also presented in Figure 2.10. Water yield values after 2009 where there is not streamflow data available were calculated using the *No_observation* option in SWAT-CUP.

The water yield has been contextualized within the four major basins presented in the ACG. Figure 2.11 presents the average annual water yield value normalized per area. This normalization helped to differentiate, according to the magnitude, the water availability among basins no matter their size.

2.3.2.2. Ecosystem Service

To address the capacity of the ACG to provide water as an ecosystem service, firstly, the coefficient of variation (CV) between 1980 – 2019 has been spatially represented (Figure 2.12). The CV illustrates the variation and reliability of water resources provision from year to year (Faramarzi et al., 2009). Figure 2.12 points out that the water resources are reliable almost in the entire area as not extremely large CV values were found. The only area of concern is the central west region of the ACG. The CV percentages in this area indicate that it potentially is not reliable enough for the provision of water caused by extreme weather conditions (Faramarzi et al., 2017, 2013, 2009). Additionally, geological features in this area also could be associated with the variation and reliability of water provision. The central region of the ACG is characterized by active volcanoes formations and striking mountains that also altered precipitation regimes (Guzmán-Arias and Calvo-Alvarado, 2013).

I further illustrated in Figure 2.13 the potential water provision at the study area as the average annual m^3 of water per capita available in each sub-basin. Values range between 870 to 453,118 $m^3 capita^{-1} year^{-1}$. South regions appear to have the less water available per person, situation that can be of alert given that this area concentrates most of the population in the ACG (Figure 2.13 – Right). This analysis was also projected across time by re-estimating the average population value per year in each sub-basin. The changes among the fourth decades of study are presented in Figure 2.14. This graph shows that the average water available per capita has slightly decreased. The 2010's revealed the lowest estimations of water in general, with a mean value below the annual average over 40 years. Conversely, as water decreases, the population has shown a constant increase.

2.3.3. Effect of Land Use and Cover Change (LUCC) on water yield variability

The LUCC impact assessment was carried out by analyzing only the land cover classes present in the drainage area (2,861.92 km^2) delimited during the construction of the SWAT model. Figure 2.15 shows the spatial distribution of the land covers within the watershed in 1979, 1997, and 2015; including forest deciduous (FRSD), forest evergreen (FRSE), grass/pastures (PAST), agricultural land (AGRL), mangrove (WETF), urban (URML), and water (WATR). In turn, Table 2.7 shows their area in km2 divided by the main four basins (Nicaragua Lake, Papagayo Gulf, Santa Elena, and Tempisque River).

To build the SWAT model, I selected the dominant land covers within each sub-basin option. Therefore, of the seven land covers present in the input maps (Figure 2.15), four have been determined as the dominant ones in the study area (FRSE, FRSD, PAST, and AGRL). The excluded land covers represent less than or equal to 1% of the drainage area in Table 2.6. Therefore, these land covers excluded from the hydrological modelling will not be considered for subsequent analyzes.

Then, I analyzed the percentage of land cover change between 1979-1997, 1997-2015 and 1979-2015 (Figure 2.16). Table 2.7 represents changes for each of the main watersheds. In general, forests have had a considerable recovery, occupying 50% (1,418.5 km^2) of the drainage area in 1979 and going up to 65% (1,846.8 km^2) in 2015; the most significant recovery is observed in the Papagayo Gulf and Tempisque River basins, with 151% and 33%, respectively. On the other hand, pastures had a 45% decrease between 1979 and 2015, declining more than 30% in all watersheds; the area considered as agricultural land increased by 3% during the entire period with its greatest increment between 1997 and 2015 (10%). This land cover has significantly grown in the

Tempisque River basin, 48% in 36 years. Changes between the 80's and 90's (1979-1997) stood out for presenting the most significant percentages in both, recovery of forest cover (> 20%) and decrease in agricultural territories in 7%, and 33% in grasslands.

The analysis of water yield variability due to the land cover change was carried out through the development of two new calibrated and validated SWAT models (see Section 2.2.7). The graphical results of these models are shown in Figure 2.17. The metrics obtained in the uncertainty analysis (Table 2.8) represent values associated with models with good performance, and that can be considered as reliable for estimating the water yield, in addition to the fact that the inclusion of the new land cover maps offers a better representation of reality concerning the multitemporal land cover change. There is a small increase in the error of the models with respect to the initial model presented in the previous section. This error can be associated with the presence of areas without information (clouds), which are greater in the 1979 and 1997 maps than in 2015, and also to the shorter periods of data for calibration and validation.

Water yield estimations in each land cover were compared during three different periods, using a mixed linear model Figure 2.18 shows that for the values between 1980 - 1989 (Land Cover 1979) and 1990 - 1999 (Land Cover 1997), there is a change in the estimates with respect to the model constructed using only the 2015 land cover data. When analyzing in detail, I established that the change in land cover improved the precision in the water yield estimations because the standard deviation decreased on average by 25.2% and the variance by 39.5%. But most importantly, there is an improvement in the estimation of the average value of the water yield, reflected in a 36.4% decrease in the standard error of the mean.

As seen in the values obtained when changing the land cover (Figure 2.18); on average, water yields during the 80s (Land cover 1979) were higher than in the 90s (Land Cover 1997), and the highest average values are concentrated in the last period analyzed, 2000-2019 (Land cover 2015). Due to the many factors involved in hydrological modelling, I decided to calculate the water yield – precipitation ratio to observe if the mentioned pattern changes and if by eliminating the effect of precipitation, the association between land cover type and water availability can be more clearly seen (Figure 2.19). In general, the pattern is maintained during the three periods, with precipitation relatively constant during the 40 years of analysis for most of the land cover types.

To explain which factors can be associated with the pattern presented in Figure 2.19, Table 2.9 summarizes the main economic, social, and environmental events during the three periods. Overall, the 80s are considered a tipping point for the region of Guanacaste in Costa because the main economic activities and the main drivers of deforestation start to disappear, allowing the ecosystem recovery during the 90s when the annual deforestation had significantly dropped to 0.1% (Calvo-Alvarado et al., 2009). During the last 20 years, even though there was a decrease in the forest recovery rate and an increase in agribusiness, the conservation areas have been maintained (Calvo-Alvarado et al., 2019). This trend (low-increase-high) in natural vegetation distribution in the ACG, at first glance, is benefiting the regeneration of water availability in the region.

I have quantified the change in water yield between decades and compared the average difference between those periods. Table 2.10 and Figure 2.20 represent the proportion of water yield change. Overall, the period between the 80s and 90s experienced average water loss for the whole ACG, approximately 18%, with a significant decrease in the Santa Elena watershed. The 90s seems to be a transition period because, when this period finished, the average water yield tended to significantly increase up to more than 60% at the beginning of the 21st century. This trend continued during the last period but in a smaller proportion except for the Tempisque River watershed that experimented a decrease of 8.0%. During the 40 years of study, the average water yield has increased, with the most significant positive change in the Santa Elena watershed (> 75%); the largest watersheds in the ACG, Nicaragua lake and Tempisque River, had the lowest increase from 1980 to 2019 (<30%). Figure 2.21 displays the spatial distribution of percentages of change in water yield disaggregated per sub-basin across the three temporal changes analyzed 1980s-1990s (a), 1990s-2000s (b), 2000s-2010s (c) and during the 40 years (d). The spatial distribution agrees with the analysis of the average values (Table 2.10) showing that most subbasins experienced a negative change of water yield in the first period of study (a). This situation changed considerably during the following period (b), where water availability increased in all sub-basins, most of them between 30% to 61%. During the last period (c), it was interesting to notice that the trend of small recovery that continued during this period was concentrated in the Northeast part of the ACG. The sub-basins in which water yield decreased are in the Tempisque River basin, while water yield in the Nicaragua Lake basin remained almost the same (+0.98%) during this period. Finally, during the 40 years of study (d), most sub-basins had a positive change in water availability, especially the centre, east, and northeast areas. The lowest proportion of positive change is located in the south that also corresponds with the lowest average water yield (Figure 2.8), and areas with a high percentage of agriculture, grasslands and low forests covers (Figure 2.15).

2.4. Discussion

This chapter sought to delve into the second core element of an ES-based comprehensive approach, through the use of a calibrated and validated SWAT hydrological model to quantify the water provision potential of an area considered ecologically important for humanity; and thus offer data that allows, in a first instance, to support decision-making processes, as proposed in the framework developed by Martin-Ortega et al. (2015c), adapted for this study as shown in Figure 1.1.

First, the calibration, validation, and statistical analysis followed broadly-cited protocols for SWAT modelling (Abbaspour, 2007; Abbaspour et al., 2018, 2015; Arnold et al., 2012b; Moriasi et al., 2007), also it was established the best model inputs after combining seven sources of information. Subsequently, a hydrological characterization of the water availability in the region was carried out together with the ecosystem service quantification, including population estimates from global models. Finally, this research included the impact assessment of the land use and cover change (LUCC), the largest recognized driver that alters global ecosystems, their services and functions, and their resilience against climate change (Calvo-Alvarado et al., 2019; Etter et al., 2011; Ray et al., 2002; Schilling et al., 2008; Stan et al., 2020). This last part involved a twofold analysis. The effect of changing the land cover information during the modelling process; and the impact of the LUCC in the water availability from one period to another.

Overall, SWAT model estimations (*model error = 12%*) suggest that the Conservation Area of Guanacaste (ACG) has a substantial potential for the reliable (*CV = 47.5%*) provision of the water ecosystem service to benefit human populations with an average annual water yield of 1,034.4 mm yr^{-1}; when this value is associated with the total estimated population in 2020 for the ACG (101,027 inhabitants, according to CIESIN (2018)) and its total area (2,861.9 km^2), it is equivalent to 29,301.8 $m^3capita^{-1}yr^{-1}$ water per capita; which is similar to the latest estimation found for Costa Rica, 23,178$m^3capita^{-1}yr^{-1}$ (BCCR, 2017). However, when the average annual water yield is discriminated by population and area in each sub-basin, it is found that the water availability in the ACG ranges from of from 870.82 to 453,118.38 $m^3capita^{-1}yr^{-1}$ and it is spatially distributed as shown in Figure 2.13. All these values also suggest that, on average, the ACG is not facing water stress (<1,700 $m^3capita^{-1}yr^{-1}$) nor water scarcity (<1,000 $m^3capita^{-1}yr^{-1}$) or severe water scarcity (<500 $m^3capita^{-1}yr^{-1}$) (Damkjaer and Taylor, 2017). However, the reliability of water resources might be affected by extreme conditions such as ENSO phenomena and incipient alterations in the conserved area and surrounds driven by big agribusiness (beef and monocultures for biofuel) and future increase in temperature and periods of drought predicted by climate change scenarios for the Guanacaste Province (Calvo-Alvarado et al., 2019; Stan et al., 2020).

This study offers the first calibrated and validated SWAT model for the ACG and complements the baseline for future applications of ES-based approaches in this region.

2.4.1. Hydrological Modelling – Input data

Comparing different inputs of climatic and geospatial information is a good practice in the development of SWAT models (Abbaspour et al., 2018, 2015). I showed the effect of different input datasets for hydrological modelling. According to the analysis (Appendix 5), the best quality input data comes from the information measured and explicitly generated for Costa Rica and not obtained from simulations using global models. Although the meteorological data measured by governmental and academic institutions is temporal and spatially limited, it offers good value for assessing the state of water resources, given that the model shows good performance even before calibration (Table 2.5). Additionally, this analysis showed that climatic datasets from reanalysis products (CSFR) and land cover maps estimated from global models (ESCA-CCI) reveal an initial good performance, suggesting that they could be used in further investigations due to the lack of measured data in the area. This is supported by other studies, which demonstrated that, at least for temperature measurements, products such as CSFR offers good quality and can improve SWAT models when combined with measured data (Faramarzi et al., 2015).

The SWAT model created performs outstandingly over the Conservation Area of Guanacaste (ACG) at the sub-basin scale (Table 2.5). In turn, I could overcome the two major limitations of the model presented by Castro-Magnani (2018), the lack of measured input data and calibration and validation using observed streamflow information.

2.4.2. Calibration, Validation, and Uncertainty analysis

As Figure 2.6, the simulated streamflow is matching the trend of the observed data. The SWAT model exhibited very good performance for both the calibration period (r^2*: 0.78*, *NSE: 0.75*, and br^2*: 0.79*) and the validation period (r^2*: 0.85, NSE: 0.82, and* br^2*: 0.85*). These scores indicate that the model accurately simulated both the magnitude and shape of the streamflow, which is consistent with good performance coefficients' ranges found in other studies to determine that a SWAT model is accurate (Faramarzi et al., 2017; Ritter and Munoz-Carpena, 2013).

There is a high degree of uncertainty when simulating; this lack of confidence is associated with physical processes not represented in the model, input data, and/or geospatial parameters (Abbaspour et al., 2018; Arnold et al., 2012). In this research, the uncertainty is linked to the current streamflow simulation using the SWAT hydrological model. I did not consider the physical processes associated with natural water bodies and infrastructure for this SWAT model because they were not representative of the study region. According to the Atlas of Costa Rica (Ortiz-Malavasi, 2014), the ACG does not have large wetlands or permanent lakes, only an unnamed swamp located in the study zone's southern border whose area occupies less than 1% (8.2 km^2) of the total area. As for the infrastructure, such as dams, there are no regulated rivers within the conservation area, and the closest dams, "El Arenal" (10.47N, 84.99W) and "Miguel Dengo" (10.47N, 85.08W), are located on the Santa Rosa River, which is not sourced inside the study area. Also, I could not have access to irrigation data; this is considered a limitation of this research that should be addressed in further studies since during dry seasons, groundwater usage increases for irrigation of crops, livestock, and human consumption (Janzen and Hallwachs, 2000).

The input information may be another aspect of model uncertainty (Abbaspour et al., 2018). I established the best input data available as stated by the initial performance. However, these datasets can add uncertainty to the model because, as Appendix 5 shows, the spatial information has different scales and temporalities, which can influence the modelled results by not considering recent aspects or impacts that have altered the ecosystem and because the data comes from different entities. Regarding meteorological information from weather stations data, a low number of stations is observed (five) compared to the vast study area analyzed; however, it is highlighted that the stations have measurements for all input parameters, and some stations have measurements of more than 40 years. The monitoring stations' climatic information allowed obtaining a satisfactory simulation regarding the fitting with the observed data (Figure 2.6).

The last sources of the uncertainty analyzed are the geospatial parameters, the most important aspect of the calibration process. They represent meaningful physical processes in the watershed. Its calibration is necessary because of the aggregation of data that has taken place during the modelling process, aiming at accurately fitting parameters to the study area. Eighteen (18) parameters were selected to encompass the most critical processes governing streamflow generation in the ACG. From the global sensitivity analysis (Figure 2.5) and regionalization processes (Table 2.3). I could establish that seven parameters have the biggest effect on the modelling process (Table 2.4). It is noteworthy that 57% of the sensitive parameters are associated with the soil's physical properties governing the movement of water into and out of the aquifers (*.gw*); fact that supports the previous statement of the importance of including groundwater processes and usage (irrigation) to represent water availability in the ACG. Therefore, further research could improve the estimation of water availability, including groundwater flow and aquifer storage measurements and interactions with the surface flow, and the inclusion of improved SWAT modules or more complex models, such as SWAT-MODFLOW (Liu et al., 2020).

After all, results revealed that the model has an excellent performance also supported by the one-to-one analysis (Figure 2.7 - Top) where the correlation between the model's streamflow simulations and the observed data has a coefficient of determination higher than 80%, even when the values are compared with what is considered the perfect model (*simulated=observed*).

Nonetheless, the model simulations have over and underestimations in general. This was differentiated between peak (Figure 2.7 – Bottom-left) and base flows (Figure 2.7 – Bottom-right). Simulated and observed peak flows are less correlated, but the model can still capture them with an acceptable level of accuracy ($R^2 > 0.7$); conversely, base flows are considerably underestimated, which is qualitatively proven by the fact that all the data points are under the perfect model line (*simulated=observed*) and quantitatively given that less than 1% of the variance is explained when compared to the perfect model. This behaviour of the base flows adds to the necessity of improving groundwater processes simulation for this region of study. Regarding water availability components, the average linear relationship between precipitation and water yield was strong ($r = 0.8$), which supports the premise that the model is accurate as are classified hydrological models with $r > 0.7$ (Moriasi et al., 2007).

2.4.3. Hydrological Characterization of the ACG.

2.4.3.1. Hydrologic system patterns

From the SWAT model, I have established the spatial distribution (Figure 2.8) of the main hydrological input (precipitation) and the main output (water yield). As depicted, there is a clear stratification within the ACG for the rainfall and water yield regimes, which appears to follow the division of the main basins displayed in Figure 2.1 delimited by terrain features. Therefore, geological features seem to have a significant effect on the spatial distribution of water. In addition, the vegetation distribution appears to influence the dynamics of the hydrological cycle modelled by SWAT. This is determined from Figure 2.8 and Figure 2.3-Centre, where an overall observation reveals an association between water distribution and land cover patterns. Firstly, agricultural and pasture lands, mainly concentrated in the very south of the ACG (Figure 2.3 – Centre), have the lowest water availability even though the average precipitation is high. Secondly, forested areas, which can be considered as the matrix of the ACG's landscape, occupying 65% of the total area (Appendix 3 – Right), do not have a singular spatial pattern associated with the water distribution (Figure 2.8 – Right); the areas close to the pacific coast seem to have less water in comparison with the sub-basins connected to the central north part of the country.

In terms of seasonality, the multiannual average values presented in Figure 2.9 show that the model captures the seasonal pattern presented in this tropical region for both hydrological variables (precipitation and water yield). Low values during the dry season from December to March and a small summer in July and increases in both variables during the rainy season from May to July and August to December. This pattern also shows that smaller water yield values are observed during rainy months, which may indicate the physically-based capacity of the SWAT model to represent the processes involved in the hydrologic cycle, such as infiltration and groundwater recharge. In other words, this behaviour reveals how precipitation is not entirely converted into water yield; that is, there is a delayed response of water yield to increase. For example, although there are some rainy events during April and July (left), the water yield does not show any significant increment during those months (right), meaning that the water availability depends only on the water stored by the system at that time.

The results in Figure 2.9 are consistent with the temporal response of tropical dry forests assessed by Zou et al. (2020) in the Santa Rosa National Park Environmental Monitoring SuperSite (SRNP-EMS) located east of the ACG. They obtained the same pattern of the monthly precipitation with maximum rainfall values around 1,500 mm per month during the rainy season and almost 0 mm per month in the driest months of the dry season. This pattern is highly correlated with the phenology of the vegetation evaluated through the normalized difference vegetation index (NDVI) and the land surface temperature (LST) derived from remote sensing data, concluding at this point that vegetation changes are strongly correlated to the precipitation pattern but more to the transition wet-dry seasons(Zou et al., 2020).

Additionally, the difference in water quantity in forested areas is influenced by the natural process of water production in Costa Rica drove by what is known as the Caribbean and Pacific slopes, which is a longitudinal division generated by the mountain ranges of Talamanca, Central, and Guanacaste (Guzmán-Arias and Calvo-Alvarado, 2013). This supports the initial assumption that geologic features defined the spatial pattern of water and explains why the sub-basins connected to the Caribbean region of Costa Rica show a larger average quantity of water. The Caribbean region concentrates more humidity due to the orographic pattern of the precipitation directly linked to prominent mountain ranges, what was also initially identified in Table 1.1.

Therefore the eastern subbasins in the ACG received more water in comparison with the Pacific coast, where the humidity decreases due to the clouds retention in the Caribbean region (Guzmán-Arias and Calvo-Alvarado, 2013).

Lastly, the water yield's annual variation during 40 years from 1980 – 2019 is presented in Figure 2.10. In principle, it can be established that there is high variability in the data over the years. The first two decades seem to have similar behaviour with low average water yield values at the beginning, then an increase in the middle (years 1985 and 1996), followed by a decrease, and ending with the highest values of water yield in these decades. However, for the last two decades, there is a different pattern, with a sustained increase in from 2005 to 2011, followed by an extended period of less water yield records with more homogeneous data. This trend in the water availability can be linked with the El Niño-Southern Oscillation (ENSO) phenomenon, which determines the spatial and temporal distribution of the precipitation in Costa Rica, and its periodicity is between 2 to 4 years (Guzmán-Arias and Calvo-Alvarado, 2013; IMN, n.d.). The rainfall anomalies caused by ENSO are related to the differences in the annual water yield availability. For example, strong Niña (1988-1989, 1998-1999, and 2010-2011) and Niño periods (1982-1983, 1997-1998, and 2015-2016) registered in Costa Rica (IMN, n.d.) show high and low values of annual average water yield, respectively (Figure 2.10). When this data is divided into the main four basins and normalized by their areas (Figure 2.11), it is observed that the Tempisque River watershed basin encompasses the lowest water availability per km^2 in the region, followed by the Nicaragua lake, Santa Elena, and the Papagayo gulf as the watershed with highest water yield per km^2. This indicates that the greater average water availability is reduced at the area level since the largest basins have less availability per km^2 than the small basins. This is coupled with sub-basins in the central region of the Tempisque river basin (Figure 2.12) that could be considered the least reliable for the provision of water as per the coefficient of variation of their data (*CV>60%*) (Faramarzi et al., 2017, 2013, 2009). The same happens to a lesser extent (*30%<CV<60%)* towards the northeast zone in the Nicaragua River basin. This low water availability per area in large watersheds also corresponds to sub-basins with the greater transformation of land cover (Figure 2.3-Centre) and with a greater concentration of population (Figure 2.13).

2.4.3.2. Potential of the ACG for the provision of water ecosystem services

To quantify the water provision ecosystem service in the ACG, I started by estimating the water yield that accounts for the water that leaves the basin and contributes to streamflow during a given time interval (Brooks et al., 2013; Dingman, 2015; Ullrich and Volk, 2009). The average annual water yield for the ACG between 1980 – 2019 was 1,034.4 mm. This average was converted into water available per capita using the total estimated population in 2020 for the ACG (101,027 inhabitants, according to CIESIN (2018)) and its total area (2,861.9 km^2); it was equivalent to 29,301.8 $m^3 capita^{-1} yr^{-1}$ water per capita, which is similar to the latest estimation found for Costa Rica, 23,178$m^3 capita^{-1} yr^{-1}$ (BCCR, 2017). In addition, the average water yield value was calculated per sub-basin and converted into water available per capita; it ranged from 870.82 to 453,118.38 $m^3 capita^{-1}$yr-1 (Figure 2.13-Left). The present study used an average value of the population estimated from the gridded product of the SEDAC Centre from NASA as a proxy number of inhabitants in each subbasin (Figure 2.13 – Right).

SWAT model estimations suggest that the ACG has outstanding potential for the provision of water with relatively good reliability (*CV = 47.5%*). This also indicates that, on average, the ACG is not facing water stress (<1,700 $m^3 capita^{-1} yr^{-1}$) nor water scarcity (<1,000 $m^3 capita^{-1} yr^{-1}$) or severe water scarcity (<500 $m^3 capita^{-1} yr^{-1}$) (Damkjaer and Taylor, 2017). However, average water per capita is slightly decreasing across time (Figure 2.14), with the lowest values registered in the last decade that can be related to the previous Niño event in 2015/16 and prolonged dry seasons (Cooley et al., 2019). Conversely, the population steadily increased (1.9% annually), which agrees with the current situation in Guanacaste Province that has become more populated due to the expansion of agricultural and tourist activities (Calvo-Alvarado et al., 2019, 2009). This can be an early warning because the demand is becoming higher than the water offer.

Even though the ACG's water ecosystem service panorama might represent a high abundance of water; in reality, there are several water-associated conflicts affecting people's accessibility to the resource along with recent severe climatic conditions with longer periods of droughts, mainly in the Pacific (Cooley et al., 2019; Kuzdas, 2012). Therefore, the explanation for the crisis in a water-rich zone is that Costa Rica is a country with economic water scarcity, which means that water supply is not an issue, but the lack of sufficient infrastructure for management, including collection, transport, and treatment, produce limited access to freshwater resources (UNESCO, 2019c).

Castro-Magnani (2018) summarized the importance of reliable water provision in the ACG. Firstly, to support the ecosystem functions that maintain the high biological biodiversity and major ecosystem services, especially as this area harbours two of the biggest national parks in Costa Rica, the Santa Rosa and Guanacaste National Parks. Secondly, to guarantee an international benefit as the Nicaragua lake basin in the Northwest part of the ACG is a transboundary catchment area. This implies that the water generated in this area of conservation also contributes to the well-being of Nicaragua's citizens. Thirdly, to sustain all the people and economic activities that rely on water for subsistence and functioning, especially in the south part, the Tempisque River Watershed. In this area, 70.4% of the water concession has been granted to irrigation activities, 28.6% to agroindustry and 1.1% to human consumption. In addition, this basin – Tempisque River – entails a history of high deforestation rates due to cattle ranching and agricultural activities. It also concentrates most of the population and urbanized areas and tourism, where water landscapes are one of the greatest interests for tourists.

2.4.4. Effect of Land Use and Cover Change (LUCC) on water yield variability

The effect of LUCC was first analyzed by examining the change in water yield estimations when the land cover input is varied in the modelling process. It was possible to establish that the precision in the estimation of the average value of water yield was improved with a decrease in the standard deviation of the estimates and the standard error of the mean. Additionally, a pattern is observed between the results of the three models (Figure 2.18). In the 1990s, the lowest average values were recorded for the entire study period. In the last period (2000 - 2019), the highest average values were registered. The effect of precipitation was eliminated by calculating the water yield-precipitation ratio The effect of precipitation was eliminated by calculating the water yield-precipitation ratio (Figure 2.19), noticing that the same pattern is conserved. Therefore, I attempted to relate this pattern to the change in land cover.

Within the LUCC assessment carried out between 1979 - 1997, 1997 - 2015 and 1979 – 2015 (Table 2.7 and Figure 2.16) it is observed that the most important change is the regeneration of the forest cover, largely promoted by the decrease of the area in pastures and in part due to a reduction in the growth of agricultural regions. At the hydrological level, by analyzing the processes of the water cycle explained in Table 1.1, it can be argued that the greater the forest cover, the lesser the water yield availability because there would be an increase in the interception of water by the vegetation covers. However, the increase in water availability also depends on the recovery of critical hydrological processes, such as soil infiltration, infiltration capacity, and the recharge of aquifers. These processes occur mainly due to vegetation covering the soil, in conjunction with other factors such as geology, climate, and the complexity in the structure and functions of the vegetation (Filoso et al., 2017). With the temporal patterns determined, the gradual recovery of the forests in this region has been found to positively impact the availability of water, but it is not the only factor (see also Section 2.4.3.1). Therefore, at this point in the research, the question to be answered is: What has happened in Guanacaste for this pattern in water availability to be generated?

Coincidentally, in Guanacaste, important socioeconomic and environmental changes can be divided between the three periods presented in Figure 2.18 and Figure 2.19. These events are summarized in the Table 2.9. In general, the 1980s can be seen as the end of a forest destruction era in the Pacific North of Costa Rica (Calvo-Alvarado et al., 2019, 2009; Stan and Sanchez-Azofeifa, 2019). The deforestation in Costa Rica registered elevated rates until the 1970s, triggered mainly by laws that encouraged the colonization of these lands to promote (1) the export of wood, (2) the beef industry due to the high price of meat in the international market, (3) and agricultural activities (Calvo-Alvarado et al., 2009; Janzen and Hallwachs, 2000).

By the beginning of the 1980s, most of the wood had been almost completely extracted, but also happened what can be considered the tipping point in the region’s economy, the unprecedented drop in the international price of meat. This caused the beef industry to fall, and the Government of Costa Rica, in turn, eliminated the incentives for this industry (Calvo-Alvarado et al., 2009). The decline of the livestock industry in Costa Rica is considered the historical event that made this Central American country an exceptional case in conserving natural resources

(Calvo-Alvarado et al., 2019). Mainly because between the 80s and 90s, novel laws were implemented at the environmental level that promoted forest recovery and the establishment of large protected areas, such as the Santa Rosa and Guanacaste National Parks located in the ACG. This protection and regeneration of the natural forests led to the inclusion of the ACG as an area of exceptional value for humanity, declared in 1999 by UNESCO (UNESCO, 2019b).

During the last 20 years, the conservation actions reflected a considerable increase in the forest cover calculated for 2012 in 50.74% of the total area of the Province of Guanacaste (Calvo-Alvarado et al., 2019); for the ACG, this coverage occupies more than 60% of the area (Table 2.6). But mainly, the most remarkable social change is the increase in investment in education and public health and the fact that the main economic activity in the region became tourism. Currently, some concerns might affect the conservation use of the land covers in this region, namely: (1) the incipient attempt to make the region's livestock industry grow again because the value of meat at the international level is already at values similar to those of the 70s; (2) the increase of the large-scale agricultural industry for the production of biomass used in the manufacture of biofuels; and (3) an unsustainable tourism sector due to its rapid growth without much control by the authorities (Calvo-Alvarado et al., 2019, 2009; Stan and Sanchez-Azofeifa, 2019).

Regarding the hydrological analysis presented here and according to the socioeconomic and environmental facts presented, I could establish that the 80s represented an initial stage of recovery where there was an average water availability already affected by all the extractive activities of previous times. The 90s characterized a transitional time when the vegetation cover began to regenerate and established the first secondary forests. The forest vegetation in the first stages of succession is highly demanding of water resources and susceptible to climatic changes, as identified for the Province of Guanacaste by Stan et al. (2020), which could explain the low values in water availability during this decade (Figure 2.18 and Figure 2.19). During the beginning of the 21st century, a positive effect of forest regeneration in water yield was observed because during this period, the forest increased 30% (Table 2.6) and the water yield rose more than 60% (Table 2.10). These values of water yield can also be explained by the high resilience and good water use efficiency in tropical forests, especially in dry regions, as described by Stan et al. (2021). Additionally, it has been estimated that the main input of the water cycle (precipitation) in the

Guanacaste Province has remained constant (Figure 2.19) and no dramatic changes are forecasted in future climate change scenarios (Stan et al., 2020). Forest cover regeneration also promotes climate regulation mostly in the rainfall rates related to processes of water exchange between the land and the atmosphere (Ray et al., 2002). However, significant temperature changes are predicted, and it is feared that changes in the frequency of ENSO phenomena could alter climate regulation. Some evidence is seen in the last period of study (Table 2.10), where between 2000s and 2010s there has been a decrease (2.4%) in the water yield, which contrasts with the high increase between the 1990s and 2000s (Figure 2.20). This can be attributed by the recent El Niño event between 2015 and 2016, as well as by prolonged periods of droughts identified in Guanacaste (Cooley et al., 2019).

Finally, Costa Rica's case of conservation of natural resources is considered an exceptional set of circumstances because all the historical and social conditions were in place to promote a more sustainable economy (Calvo-Alvarado et al., 2019). This, in turn, could make this region an exceptional case at a hydrological level too, as discussed in this study. Furthermore, the SWAT hydrological modelling results show that the forest cover recovery is connected to an increase in water yield availability. At the global scale, this statement is supported by a systematic review carried out by Filoso et al. (2017). They found that Central America is the region with the highest number of reports of positive water yield values after an increase in forest cover. Regarding conservation and regeneration policies, it was also stated that if they are implanted too late after a prolonged period of ecosystems' degradation, the hydrological processes will not be recovered, particularly if the soil is too eroded (Filoso et al., 2017). Therefore, the conservation policies in Costa Rica also prevented the high degrees of deforestation from reaching a point of no return for the recovery of hydrological processes as well.

2.5. References

Abbaspour, K. C. (2005). Calibration of hydrologic models: When is a model calibrated? MODSIM 2005 - International Congress on Modelling and Simulation: Advances and Applications for Management and Decision Making, Proceedings, 2449–2455.

Abbaspour, K. C. (2007). User manual for SWAT-CUP, SWAT calibration and uncertainty analysis programs. Dubendorf, Switzerland. Retrieved from https://swat.tamu.edu/media/114860/usermanual_swatcup.pdf

Abbaspour, K. C., & Vaghefi, S. A. (2019). Global FAO/UNESCO Soil Map of the World reformatted with SWAT format. https://doi.org/https://doi.org/10.1594/PANGAEA.901313

Abbaspour, K. C., Yang, J., Maximov, I., Siber, R., Bogner, K., Mieleitner, J., et al. (2007). Modelling hydrology and water quality in the pre-alpine/alpine Thur watershed using SWAT. Journal of Hydrology, 333(2–4), 413–430.

Abbaspour, K. C., Vejdani, M., Haghighat, S., & Yang, J. (2007). SWAT-CUP calibration and uncertainty programs for SWAT. In MODSIM 2007 international congress on modelling and simulation, modelling and simulation society of Australia and New Zealand (pp. 1596–1602).

Abbaspour, K. C., Faramarzi, M., & Rouholahnejad, E. (2010). Hydrological modeling of Alberta using SWAT model. AWAG, Swiss Federal Institute of Aquatic Scienec and Technology, 83.

Abbaspour, K. C., Rouholahnejad, E., Vaghefi, S., Srinivasan, R., & Klöve, B. (2015). Modelling hydrology and water quality of the European Continent at a subbasin scale: calibration of a high-resolution large-scale SWAT model. J. Hydrol, 524, 733–752.

Abbaspour, K. C., Vaghefi, S. A., & Srinivasan, R. (2018). A guideline for successful calibration and uncertainty analysis for soil and water assessment: A review of papers from the 2016 International SWAT Conference. Multidisciplinary Digital Publishing Institute.

Abbaspour, K. C., Vaghefi, S. A., Yang, H., & Srinivasan, R. (2019). Global soil, landuse, evapotranspiration, historical and future weather databases for SWAT Applications. Scientific Data, 6(1), 1–11.

Alemayehu, T., Van Griensven, A., Woldegiorgis, B. T., & Bauwens, W. (2017). An improved SWAT vegetation growth module and its evaluation for four tropical ecosystems. Hydrology and Earth System Sciences, 21(9), 4449.

Arnold, J. G., Williams, J. R., & Maidment, D. R. (1995). Continuous-time water and sediment-routing model for large basins. Journal of Hydraulic Engineering, 121(2), 171–183.

Arnold, J. G., Srinivasan, R., Muttiah, R. S., & Williams, J. R. (1998). Large area hydrologic modeling and assessment part I: model development 1. JAWRA Journal of the American Water Resources Association, 34(1), 73–89.

Arnold, J. G., Kiniry, J. R., Srinivasan, R., Williams, J. R., Haney, E. B., & Neitsch, S. L. (2012). Input/Output Documentation Soil & Water Assessment Tool. Retrieved from https://swat.tamu.edu/media/69296/swat-io-documentation-2012.pdf

Arnold, J. G., Moriasi, D. N., Gassman, P. W., Abbaspour, K. C., White, M. J., Srinivasan, R., et al. (2012). SWAT: Model use, calibration, and validation. Transactions of the ASABE, 55(4), 1491–1508.

Arroyo Morales, L., Heidinger, H., & Araya Morales, E. J. (2010). Modelo Hidrológico SWAT como Herramienta para Procesos de Toma de Desición. San Jose: Proyecto Microriego Plantón-Pacayas.

Ayivi, F., & Jha, M. K. (2018). Estimation of water balance and water yield in the Reedy Fork-Buffalo Creek Watershed in North Carolina using SWAT. International Soil and Water Conservation Research, 6(3), 203–213.

Barquero-Ureña, A. (2015a). Modelación hidrológica en las cuencas San Jerónimo-Piedras, Río Blanco y Tenorio usando SWAT.

Barquero-Ureña, A. (2015b). Modelación hidrológica en las cuencas San Jerónimo-Piedras, Río Blanco y Tenorio usando SWAT [Hydrological modeling in the San Jerónimo-Piedras, White River, and Tenorio basins using SWAT]. Retrieved from http://www.kerwa.ucr.ac.cr/handle/10669/75480

Bayabil, H. K., & Dile, Y. T. (2020). Improving hydrologic simulations of a small watershed through soil data integration. Water (Switzerland), 12(10). https://doi.org/10.3390/w12102763

BCCR. (2017). Cuentas AGUA 2012-2015, 15. Retrieved from https://activos.bccr.fi.cr/sitios/bccr/cuentasambientales/DocCuentaAgua/Cuenta_agua_2012_2015.pdf

Benavides, F., & Veenstra, J. N. (2005). The impact of tropical deforestation on river chemical pollution. In Proceedings of the International Conference on Environmental Science and Technology (Vol. 1, pp. 173–178).

Brooks, K. N., Ffolliott, P. F., & Magner, J. A. (2013). Hydrology and the Management of Watersheds. John Wiley & Sons.

Calvo-Alvarado, J., McLennan, B., Sánchez-Azofeifa, A., & Garvin, T. (2009). Deforestation and forest restoration in Guanacaste, Costa Rica: Putting conservation policies in context. Forest Ecology and Management, 258(6), 931–940. https://doi.org/10.1016/j.foreco.2008.10.035

Calvo-Alvarado, J., Jiménez, V., Calvo-Obando, A., & Castillo, M. (2019). Current perspectives on forest recovery trends in Guanacaste, Costa Rica. International Forestry Review, 21(4), 425–431.

Carvajal-Vanegas, D. (2017). Dinámica hídrica bajo condiciones climáticas cambiantes en la subcuenca del Río Tempisquito, cuenca del Tempisque, Guanacaste, Costa Rica.

Castro-Magnani, M. (2018). Evaluating ecosystem services in Tropical Dry Forests, 127. Retrieved from https://era.library.ualberta.ca/items/eb06a5e3-73ba-4630-9b73-8070e6d58473/view/27178acf-2168-4f2d-b573-1bc9d5caab68/Castro-Magnani_Marissa_201804_MSc.pdf

Chen, J. (2020). Spatial Dynamic Modeling of Tropical Forest Change.

CIA-UCR. (2016). Digital Soil Map of Costa Rica. Retrieved from http://www.cia.ucr.ac.cr/?page_id=139

CIESIN. (2018). Gridded Population of the World, Version 4 (GPWv4): Population Count. New York. Retrieved from https://sedac.ciesin.columbia.edu/data/set/gpw-v4-population-count-rev11

Cooley, S. S., Williams, C. A., Fisher, J. B., Halverson, G. H., Perret, J., & Lee, C. M. (2019). Assessing regional drought impacts on vegetation and evapotranspiration: a case study in Guanacaste, Costa Rica. Ecological Applications, 29(2), e01834.

Correa-Ayram, C. A., Mendoza, M. E., Etter, A., & Pérez Salicrup, D. R. (2017). Anthropogenic impact on habitat connectivity: A multidimensional human footprint index evaluated in a highly biodiverse landscape of Mexico. Ecological Indicators, 72(January), 895–909. https://doi.org/10.1016/j.ecolind.2016.09.007

Damkjaer, S., & Taylor, R. (2017). The measurement of water scarcity: Defining a meaningful indicator. Ambio, 46(5), 513–531.

Dingman, S. L. (2015). Physical hydrology (Third). Waveland press.

Durham, R., Rivera-Araya, M. J., Madison, D., Quesada, L., Vanegas, N., & Cui, D. (2016). DEVELOP Technical Report. Costa Rica Water Resources. Monitoring Drought and Water Balance in the Guanacaste Province to Enhance Decision Making and Response Planning Costa Rica., (August). Retrieved from https://bit.ly/32rXN7K

ESA. (2015). Land Cover CCI-Product User Guide Version 2.0. Retrieved from http://maps.elie.ucl.ac.be/CCI/viewer/download/ESACCI-LC-Ph2-PUGv2_2.0.pdf

ESRI. (2016). Conditional Toolset. Retrieved from https://desktop.arcgis.com/en/arcmap/10.3/tools/spatial-analyst-toolbox/con-.htm

Essenfelder, A. H. (2018). SWAT Weather Database: A Quick Guide. https://doi.org/doi: 10.13140/RG.2.1.4329.1927

Etter, A., McAlpine, C. A., Seabrook, L., & Wilson, K. A. (2011). Incorporating temporality and biophysical vulnerability to quantify the human spatial footprint on ecosystems. Biological Conservation. https://doi.org/10.1016/j.biocon.2011.02.004

Faramarzi, M., Abbaspour, K. C., Schulin, R., & Yang, H. (2009). Modelling blue and green water resources availability in Iran. Hydrological Processes: An International Journal, 23(3), 486–501.

Faramarzi, M., Abbaspour, K. C., Vaghefi, S. A., Farzaneh, M. R., Zehnder, A. J. B., Srinivasan, R., & Yang, H. (2013). Modeling impacts of climate change on freshwater availability in Africa. Journal of Hydrology, 480, 85–101.

Faramarzi, M., Srinivasan, R., Iravani, M., Bladon, K. D., Abbaspour, K. C., Zehnder, A. J. B., & Goss, G. G. (2015). Setting up a hydrological model of Alberta: Data discrimination analyses prior to calibration. Environmental Modelling & Software, 74, 48–65.

Faramarzi, M., Abbaspour, K. C., Lu, W., Fennell, J., Zehnder, A. J. B., & Goss, G. G. (2017). Uncertainty based assessment of dynamic freshwater scarcity in semi-arid watersheds of Alberta, Canada. Journal of Hydrology: Regional Studies, 9, 48–68.

Fernandez-Palomino, C. A., Hattermann, F. F., Krysanova, V., Vega-Jácome, F., & Bronstert, A. (2020). Towards a more consistent eco-hydrological modelling through multi-objective calibration: a case study in the Andean Vilcanota River basin, Peru. Hydrological Sciences Journal, 1–16.

Filoso, S., Bezerra, M. O., Weiss, K. C. B., & Palmer, M. A. (2017). Impacts of forest restoration on water yield: A systematic review. PLoS ONE, 12(8), 1–26. https://doi.org/10.1371/journal.pone.0183210

Francesconi, W., Srinivasan, R., Pérez-Miñana, E., Willcock, S. P., & Quintero, M. (2016). Using the Soil and Water Assessment Tool (SWAT) to model ecosystem services: A systematic review. Journal of Hydrology, 535, 625–636. https://doi.org/10.1016/j.jhydrol.2016.01.034

Guzmán-Arias, I., & Calvo-Alvarado, J. C. (2013). Planning and development of Costa Rica water resources: current status and perspectives. Revista Tecnología En Marcha, 26(4), 52. https://doi.org/10.18845/tm.v26i4.1583

Hoyos, N., Correa-Metrio, A., Jepsen, S. M., Wemple, B., Valencia, S., Marsik, M., et al. (2019). Modeling streamflow response to persistent drought in a coastal tropical mountainous watershed, Sierra Nevada De Santa Marta, Colombia. Water, 11(1), 94.

IMN. (n.d.). ENSO. Retrieved April 14, 2021, from https://www.imn.ac.cr/en/54

Janzen, D. H., & Hallwachs, W. (2000). Costa Rica's Area de Conservación Guanacaste: a long march to survival through non-damaging biodevelopment. Biodiversity, 1(2), 7–20.

Johnston, R., & Smakhtin, V. (2014). Hydrological modeling of large river basins: how much is enough? Water Resources Management, 28(10), 2695–2730.

Khalid, K., Ali, M. F., Rahman, N. F. A., Mispan, M. R., Haron, S. H., Othman, Z., & Bachok, M. F. (2016). Sensitivity analysis in watershed model using SUFI-2 algorithm. Procedia Eng, 162, 441–447.

Krause, P., Boyle, D. P., & Bäse, F. (2005). Comparison of different efficiency criteria for hydrological model assessment.

Krysanova, V., & Arnold, J. G. (2008). Advances in ecohydrological modelling with SWAT—a review. Hydrological Sciences Journal, 53(5), 939–947.

Kuzdas, C. (2012). Unpacking water conflict in Unpacking water conflict in Guanacaste, Costa Rica.

Liu, W., Park, S., Bailey, R. T., Molina-Navarro, E., Andersen, H. E., Thodsen, H., et al. (2020). Quantifying the streamflow response to groundwater abstractions for irrigation or drinking water at catchment scale using SWAT and SWAT–MODFLOW. Environmental Sciences Europe, 32(1), 1–25.

Lopes, T. R., Folegatti, M. V., Duarte, S. N., Zolin, C. A., Junior, L. S. F., Moura, L. B., et al. (2020). Hydrological modeling for the Piracicaba River basin to support water management and ecosystem services. Journal of South American Earth Sciences, 103, 102752.

Lopes, T. R., Zolin, C. A., Mingoti, R., Vendrusculo, L. G., de Almeida, F. T., de Souza, A. P., et al. (2021). Hydrological regime, water availability and land use/land cover change impact on the water balance in a large agriculture basin in the Southern Brazilian Amazon. Journal of South American Earth Sciences, 108, 103224.

Luo, Y., Su, B., Yuan, J., Li, H., & Zhang, Q. (2011). GIS techniques for watershed delineation of SWAT model in plain polders. Procedia Environmental Sciences, 10(PART C), 2050–2057. https://doi.org/10.1016/j.proenv.2011.09.321

Martin-Ortega, J., Ferrier, R. C., & Gordon, I. J. (2015). Water ecosystem services: Moving forward. In S. K. J. Martin-Ortega, R. Ferrier, I. Gordon (Ed.), Water Ecosystem Services: A Global Perspective (pp. 170–173). Cambridge: Cambridge University Press. https://doi.org/10.1017/CBO9781316178904.021

Martin-Ortega, J., Jorda-Capdevila, D., Glenk, K., & Holstead, K. L. (2015). What defines ecosystem services-based approaches? In & S. K. J. Martin-Ortega, R. Ferrier, I. Gordon (Ed.), Water Ecosystem Services: A Global Perspective (pp. 3–14). Cambridge: Cambridge University Press. https://doi.org/10.1017/CBO9781316178904.003

Mateo-Sagasta, J., Zadeh, S. M., Turral, H., & Burke, J. (2017). Water pollution from agriculture: a global review. Executive summary. Rome, Italy: FAO Colombo, Sri Lanka: International Water Management ….

Mehan, S., Neupane, R. P., & Kumar, S. (2017). Coupling of SUFI 2 and SWAT for Improving the Simulation of Streamflow in an Agricultural Watershed of South Dakota. Hydrol. Curr. Res, 8(3).

Montecelos-Zamora, Y., Cavazos, T., Kretzschmar, T., Vivoni, E. R., Corzo, G., & Molina-Navarro, E. (2018). Hydrological modeling of climate change impacts in a tropical river basin: A case study of the Cauto river, Cuba. Water, 10(9), 1135.

Moriasi, D.N., Arnold, J. G., Van Liew, M. W., Bingner, R. L., Harmel, R. D., & Veith, T. L. (2007). Model evaluation guidelines for systematic quantification of accuracy in watershed simulations. Transactions of the ASABE, 50(3), 885–900.

Moriasi, Daniel N, Pai, N., Steiner, J. L., Gowda, P. H., Winchell, M., Rathjens, H., et al. (2019). SWAT-LUT: A desktop graphical user interface for updating land use in SWAT. JAWRA Journal of the American Water Resources Association, 55(5), 1102–1115.

Narasimhan, B., & Dhanesh, Y. (2012). SWAT user soil table template. Retrieved from shorturl.at/hmFRX

Neitsch, S. L., Arnold, J. G., Kiniry, J. R., & Williams, J. R. (2011). Soil & Water Assessment Tool Theoretical Documentation Version 2009. Texas Water Resources Institute, 1–647. https://doi.org/10.1016/j.scitotenv.2015.11.063

Oestreicher, J. (2008). Application of the Soil Water Assessment Tool in a Tropical Agricultural Catchment of the Panama Canal Watershed: Implications for its use in watershed management activities. McGill University.

de Oliveira Serrão, E. A., Silva, M. T., Ferreira, T. R., da Silva, V. de P. R., de Sousa, F. de S., de Lima, A. M. M., et al. (2020). Land use change scenarios and their effects on hydropower energy in the Amazon. Science of The Total Environment, 744, 140981.

Ortiz-Malavasi, E. (2014). Atlas de Costa Rica 2014. Retrieved from https://repositoriotec.tec.ac.cr/handle/2238/6749

Pachepsky, Y., & Rawls, W. J. (2004). Development of pedotransfer functions in soil hydrology. Elsevier.

Pagliero, L., Bouraoui, F., Willems, P., & Diels, J. (2014). Large-Scale Hydrological Simulations Using the Soil Water Assessment Tool, Protocol Development, and Application in the Danube Basin. Journal of Environmental Quality, 43(1), 145–154.

Peters, N. E., & Meybeck, M. (2000). Water quality degradation effects on freshwater availability: impacts of human activities. Water International, 25(2), 185–193.

Portillo-Quintero, C. A., & Sánchez-Azofeifa, G. A. (2010). Extent and conservation of tropical dry forests in the Americas. Biological Conservation, 143(1), 144–155.

Quintero, M., Wunder, S., & Estrada, R. D. (2009). For services rendered? Modeling hydrology and livelihoods in Andean payments for environmental services schemes. Forest Ecology and Management, 258(9), 1871–1880.

Ramos, J. H. (2016). Análisis Hidrológico de la Cuenca del río Sensunapán, como alternativa para el fortalecimiento de la Gestion de Riesgos y Reducción de la Vulnerabilidad, en el Departamento de Sonsonate, El Salvador [Hydrological Analysis of the Sensunapán River Basin, as. El Salvador University. Retrieved from http://ri.ues.edu.sv/id/eprint/10245/

Ray, D. K., Nair, U. S., Welch, R. M., & Lawton, R. O. (2002). Impact of Deforestation on Cloud Properties and Rainfall Over the Costa Rica-Nicaraguan region. In AGU Fall Meeting Abstracts (Vol. 2002, pp. B21B-0724).

Refsgaard, J. C., & Abbott, M. B. (1990). The role of distributed hydrological modelling in water resources management. In Distributed hydrological modelling (pp. 1–16). Springer.

Ritter, A., & Munoz-Carpena, R. (2013). Performance evaluation of hydrological models: Statistical significance for reducing subjectivity in goodness-of-fit assessments. Journal of Hydrology, 480, 33–45.

Rodríguez-Romero, A. J., Rico-Sánchez, A. E., Mendoza-Martínez, E., Gómez-Ruiz, A., Sedeño-Díaz, J. E., & López-López, E. (2018). Impact of changes of land use on water quality, from tropical forest to anthropogenic occupation: a multivariate approach. Water, 10(11), 1518.

Roth, V., & Lemann, T. (2016). Comparing CFSR and conventional weather data for discharge and soil loss modelling with SWAT in small catchments in the Ethiopian Highlands. Hydrology and Earth System Sciences, 20(2), 921–934.

Saxton, K. E., & Rawls, W. J. (2006). Soil water characteristic estimates by texture and organic matter for hydrologic solutions. Soil Science Society of America Journal, 70(5), 1569–1578.

Schilling, K. E., Jha, M. K., Zhang, Y., Gassman, P. W., & Wolter, C. F. (2008). Impact of land use and land cover change on the water balance of a large agricultural watershed: Historical effects and future directions. Water Resources Research, 44(7).

Schuol, J., Abbaspour, K. C., Yang, H., Srinivasan, R., & Zehnder, A. J. B. (2008). Modeling blue and green water availability in Africa. Water Resources Research, 44(7).

Shrestha, J. P., Pahlow, M., & Cochrane, T. A. (2020). Development of a SWAT hydropower operation routine and its application to assessing hydrological alterations in the mekong. Water (Switzerland), 12(8). https://doi.org/10.3390/W12082193

SINAC. (2010). Guanacaste Conservation Area (ACG). Retrieved from http://www.sinac.go.cr/EN-US/ac/acg/Pages/default.aspx

Stan, K., & Sanchez-Azofeifa, A. (2019). Deforestation and secondary growth in Costa Rica along the path of development. Regional Environmental Change, 19(2), 587–597.

Stan, K., Sanchez-Azofeifa, A., Calvo-Rodriguez, S., Castro-Magnani, M., Chen, J., Ludwig, R., & Zou, L. (2020). Climate change scenarios and projected impacts for forest productivity in Guanacaste Province (Costa Rica): lessons for tropical forest regions. Regional Environmental Change, 20(1), 1–13.

Stan, K. D., Sanchez-Azofeifa, A., Duran, S. M., Guzman, J. A., Hesketh, M., Portillo-Quintero, C., et al. (2021). Tropical Dry Forest resilience and Water Use Efficiency: an analysis of productivity under climate change. Environmental Research Letters. https://doi.org/https://doi.org/10.1088/1748-9326/abf6f3

SWAT. (2018). ArcSWAT. Retrieved from https://swat.tamu.edu/software/arcswat/

Tang, F. F., Xu, H. S., & Xu, Z. X. (2012). Model calibration and uncertainty analysis for runoff in the Chao River Basin using sequential uncertainty fitting. Procedia Environmental Sciences, 13, 1760–1770.

Tarigan, S., Wiegand, K., Sunarti, & Slamet, B. (2018). Minimum forest cover required for sustainable water flow regulation of a watershed: A case study in Jambi Province, Indonesia. Hydrology and Earth System Sciences, 22(1), 581–594. https://doi.org/10.5194/hess-22-581-2018

Ullrich, A., & Volk, M. (2009). Application of the Soil and Water Assessment Tool (SWAT) to predict the impact of alternative management practices on water quality and quantity. Agricultural Water Management, 96(8), 1207–1217.

UNESCO. (2019a). World Heritage List: Area de Conservación Guanacaste (Costa Rica).

UNESCO. (2019b). WWAP The United Nations World Water Development Report 2019. Leaving No One Behind. Retrieved from https://www.unwater.org/publications/world-water-development-report-2019/

Uribe, N., Corzo, G., Quintero, M., van Griensven, A., & Solomatine, D. (2018). Impact of conservation tillage on nitrogen and phosphorus runoff losses in a potato crop system in Fuquene watershed, Colombia. Agricultural Water Management, 209, 62–72.

Vapnik, V. (2013). The nature of statistical learning theory. Springer science & business media.

Wang, Y., Jiang, R., Xie, J., Zhao, Y., Yan, D., & Yang, S. (2019). Soil and water assessment tool (SWAT) model: A systemic review. Journal of Coastal Research, 93(SI), 22–30.

Wei, X., Garcia-Chevesich, P., Alejo, F., García, V., Martínez, G., Daneshvar, F., et al. (2021). Hydrologic Analysis of an Intensively Irrigated Area in Southern Peru Using a Crop-Field Scale Framework. Water, 13(3), 318.

Williams, J. R., Nicks, A. D., & Arnold, J. G. (1985). Simulator for water resources in rural basins. Journal of Hydraulic Engineering, 111(6), 970–986.

Zou, L., Cao, S., Zhao, A., & Sanchez-Azofeifa, A. (2020). Assessing the Temporal Response of Tropical Dry Forests to Meteorological Drought. Remote Sensing, 12(14), 2341.

2.6. Figures

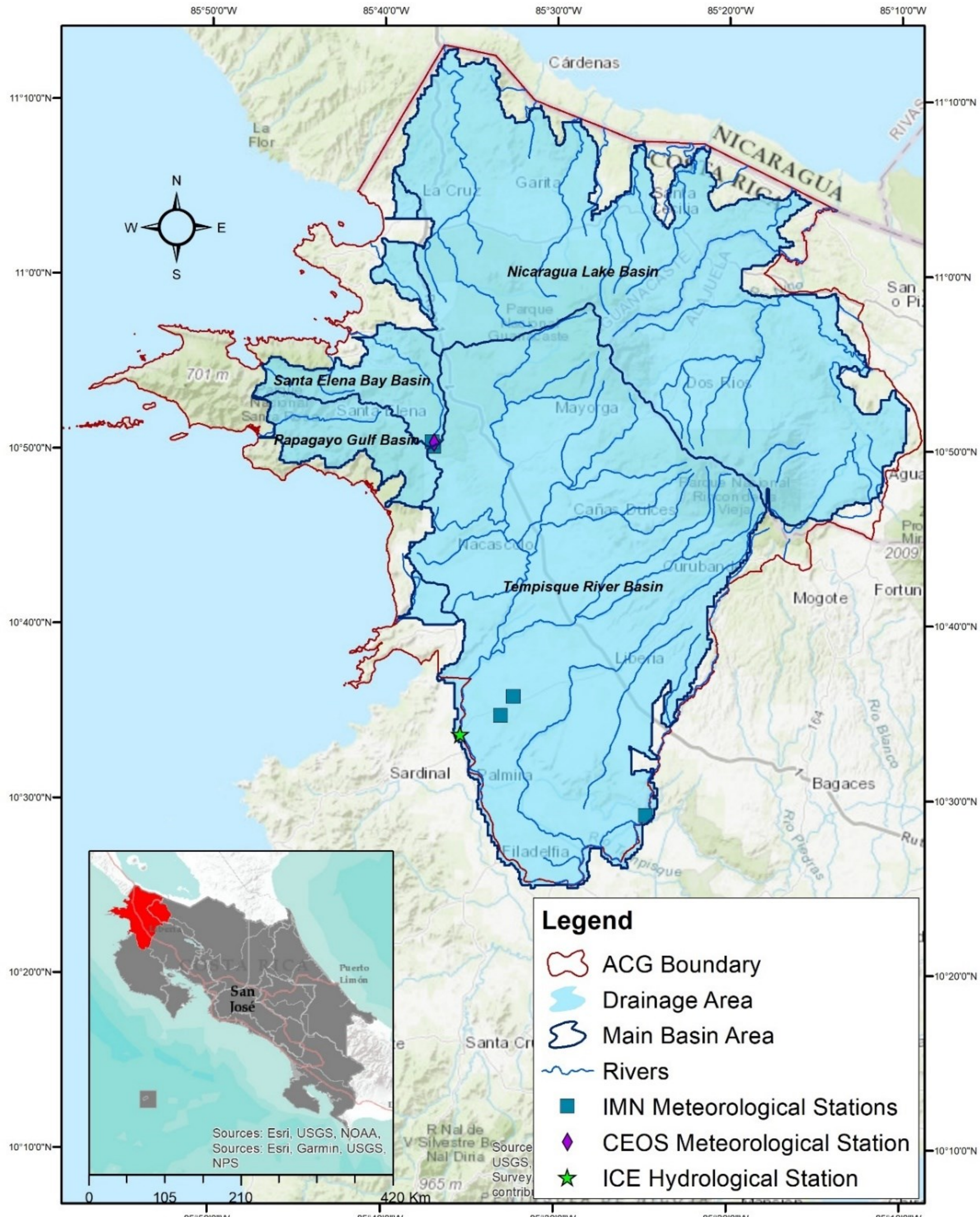

Figure 2.1. Location of the Study Area at the Conservation Area of Guanacaste (ACG, for its acronym in Spanish) in Northwest part of Costa Rica, incorporating the total drainage area obtained through the SWAT model, the major basins boundaries and the rivers from the Atlas of Costa Rica 2014, and the location of the meteorological and hydrological stations which gauges were used as input data for hydrological modelling.

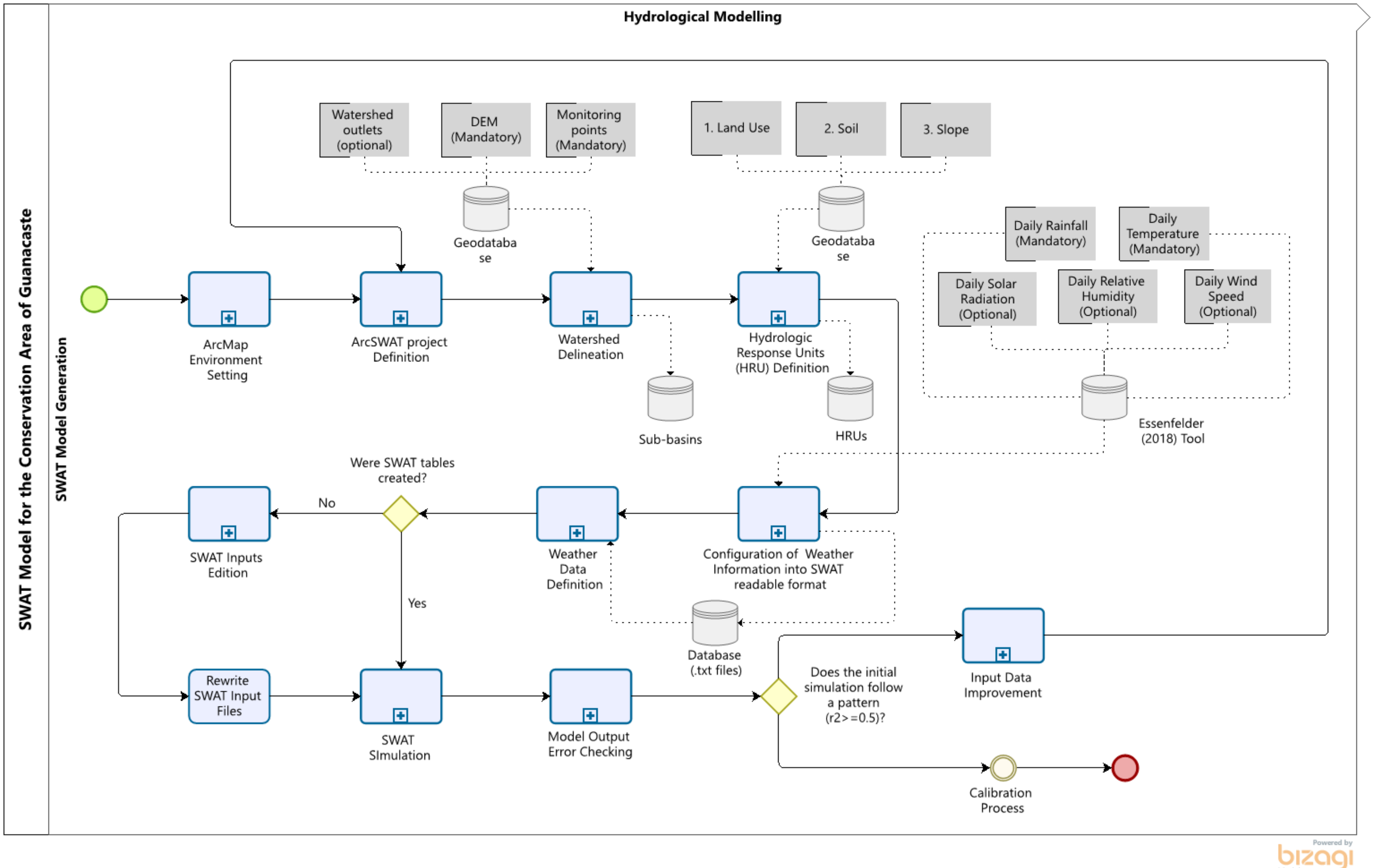

Figure 2.2. Flow Diagram of the Hydrological Model Set-up (SWAT Model Generation in ArcSWAT).

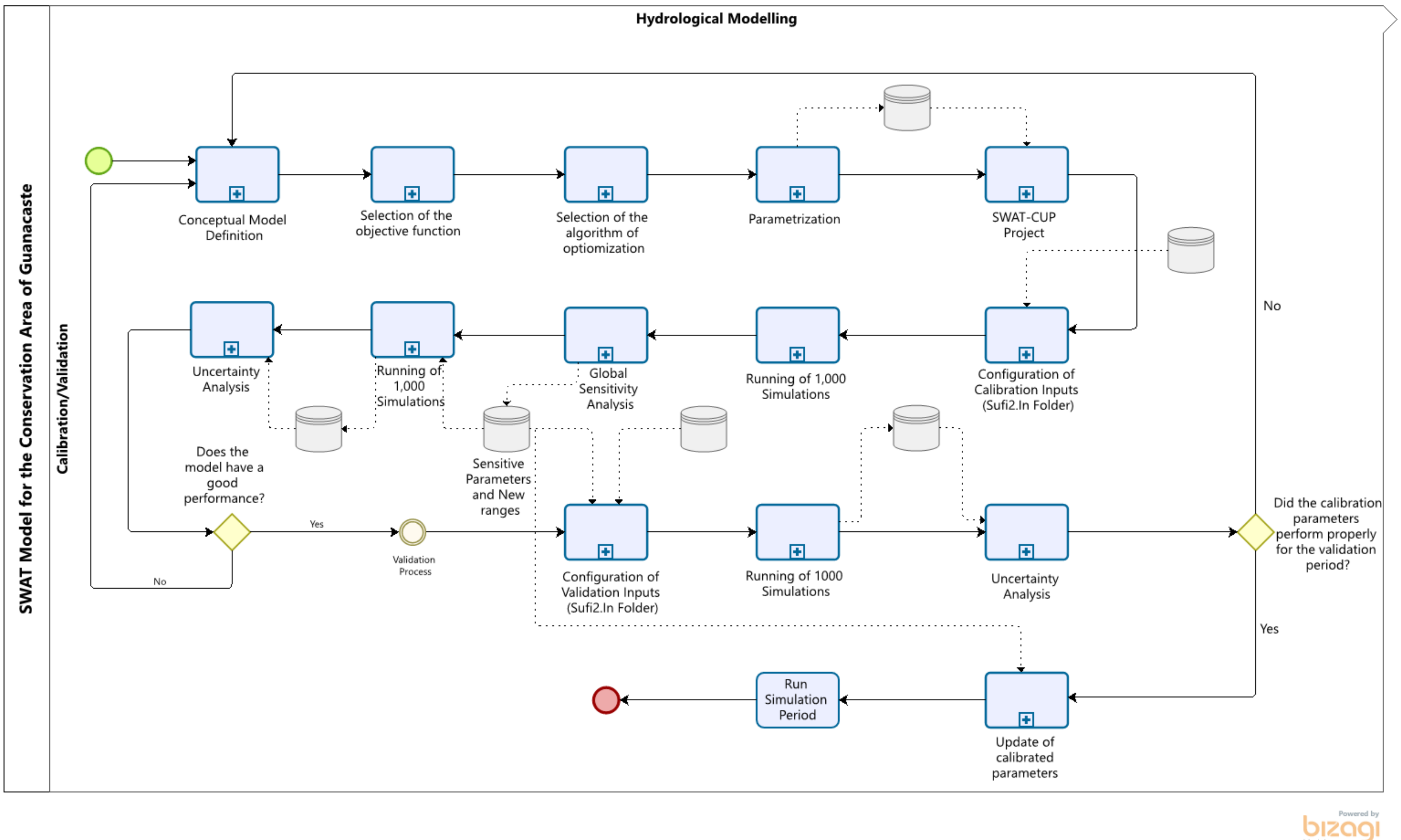

Figure 2.2 [Cont.]. Flow Diagram of the Hydrological Model Set-up (Calibration and Validation of the SWAT Model).

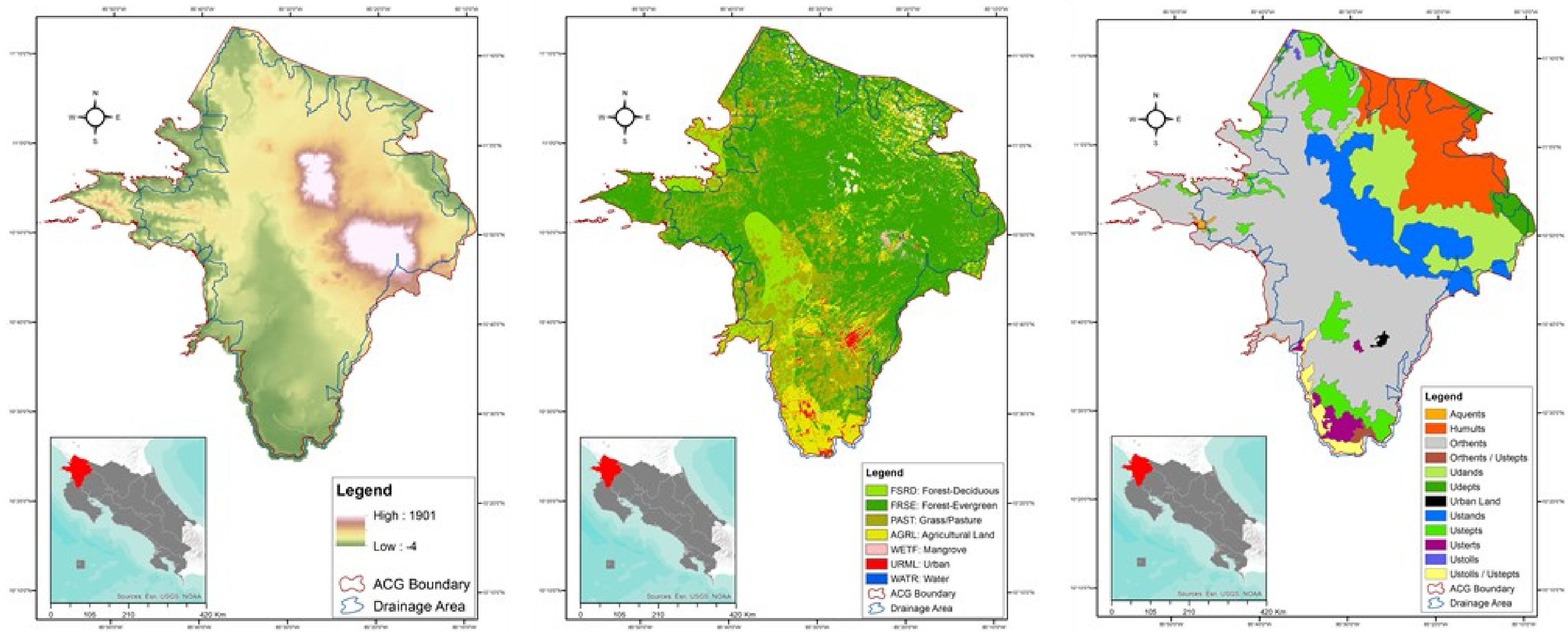

Figure 2.3. Spatial input data for the SWAT Model selected for calibration. The Digital Elevation Model of 10 m (*Left*), the 2015 Land Cover Map with seven categories (*Centre*), and the 2016 Soil Layer (*Right*) with 12 types of soil. All inputs' characteristics are described in Table 2.1.

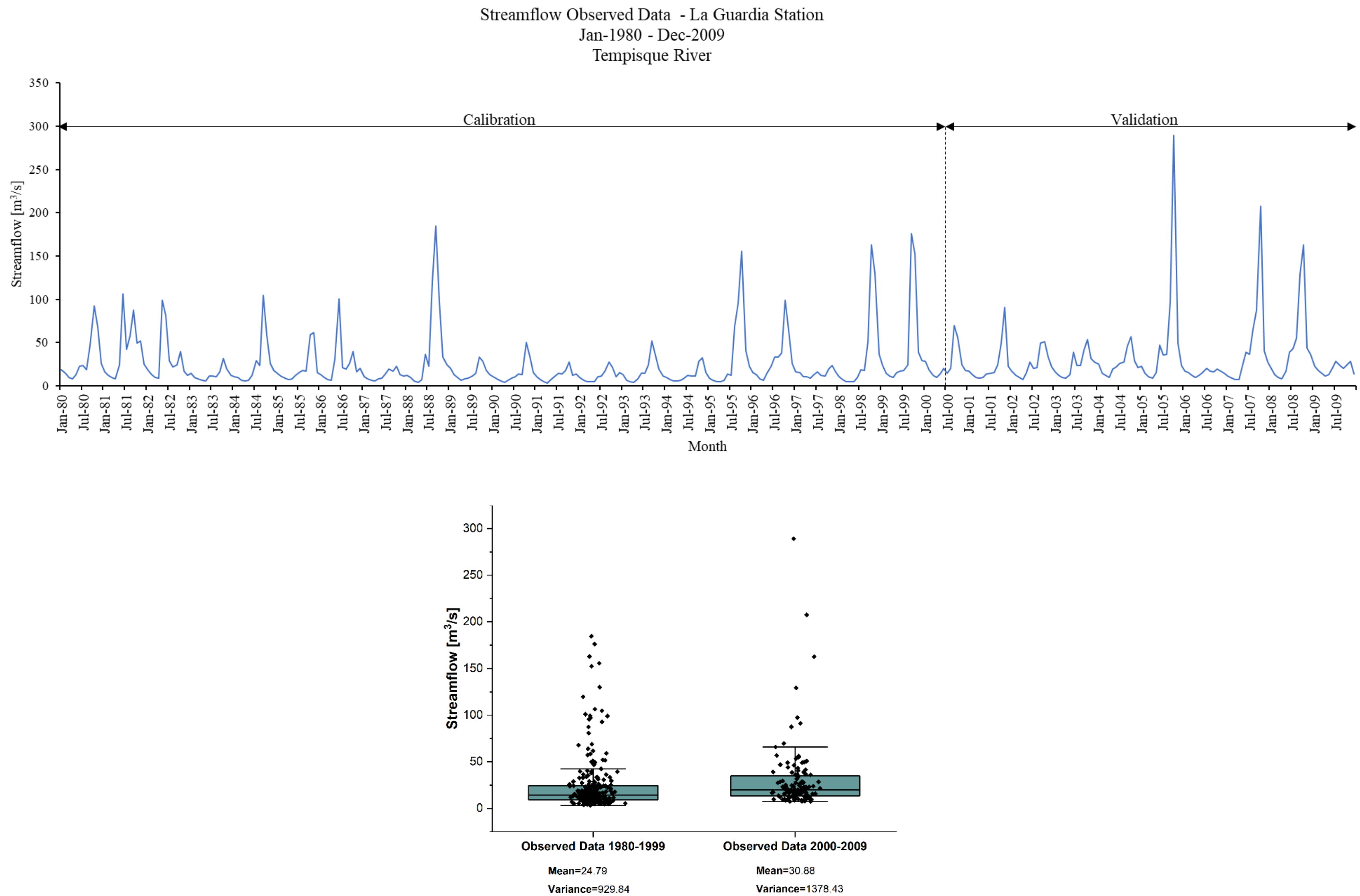

Figure 2.4. 30 years of monthly Streamflow Observed Data available for calibration and validation (*Top*). Periods for calibration and validation have been represented as boxplots (*Bottom*) to show similarities in descriptive statistics as a required condition for selecting hydrological information for calibration and validation procedures, as indicated by Abbaspour et al. (2018).

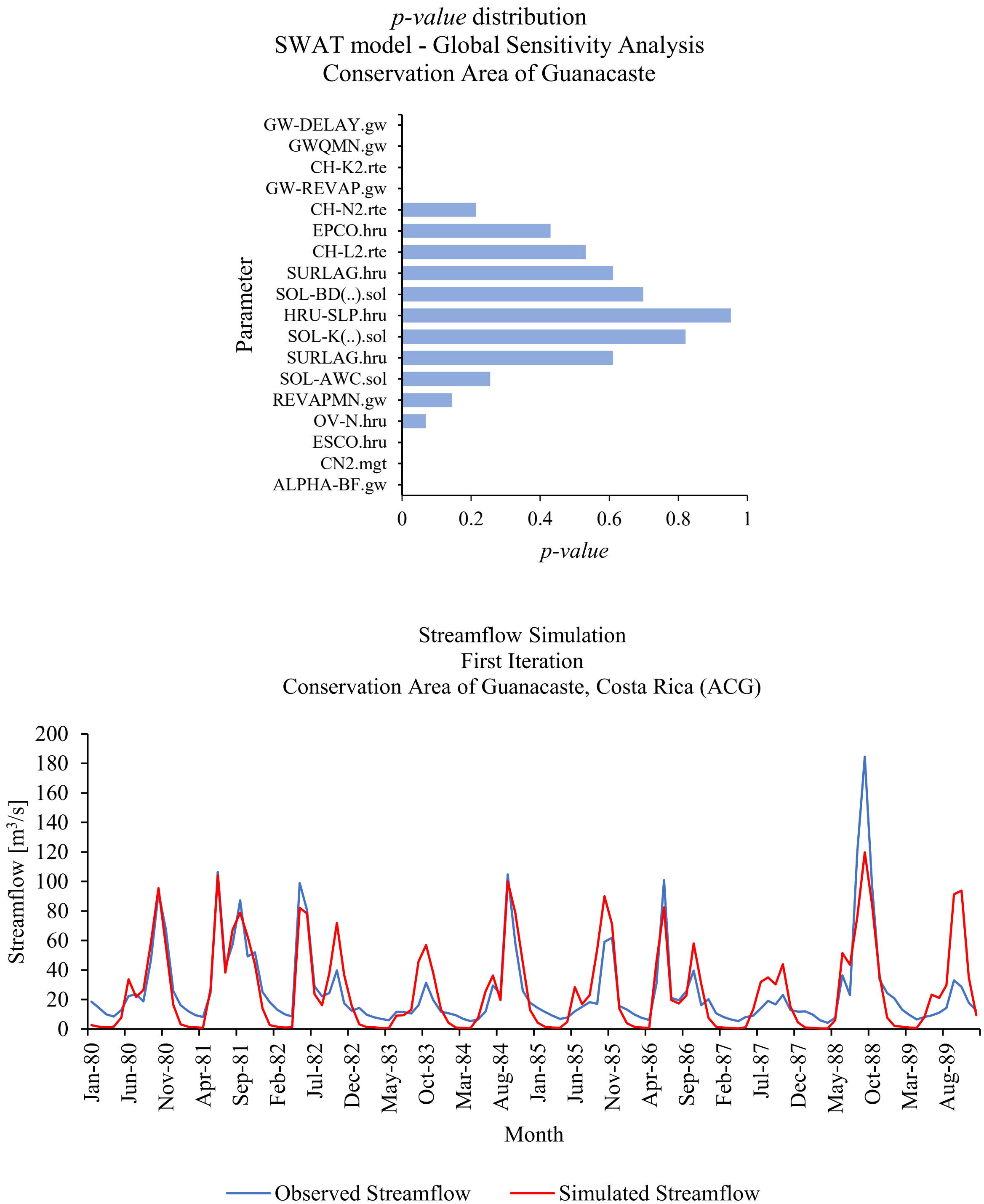

Figure 2.5. *Top:* Normal distribution of p-values obtained during the global sensitivity analysis. The seven parameters in the top (GW-DELAY, GWQMN, CH-K2, and GW-REVAP) and bottom tails (ESCO, CN2, and ALPHA-BF) are the sensitive parameters (p-value < 0.05). *Bottom:* Partial result (10 years) of the best simulation obtained from the first iteration of 1,000 simulations.

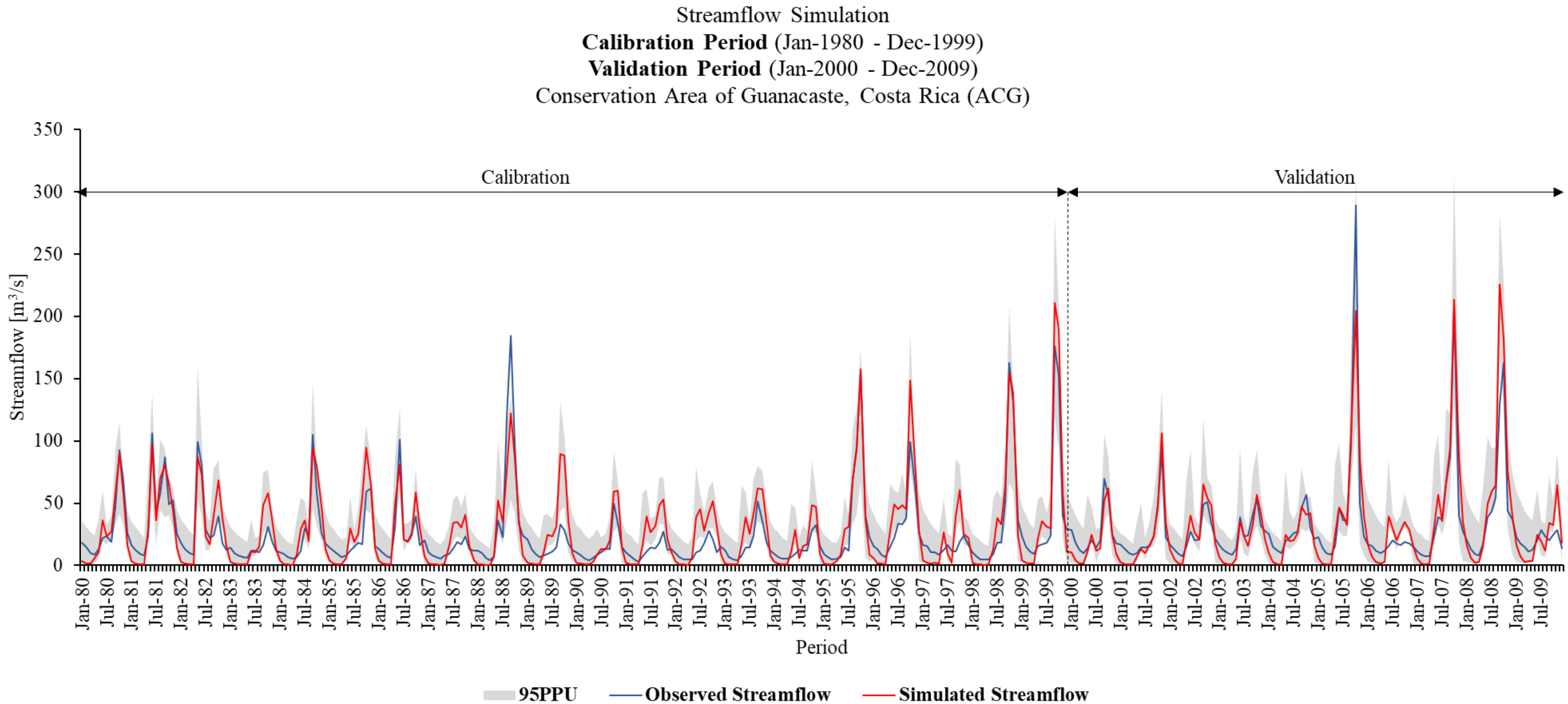

Figure 2.6. Best simulated SWAT monthly discharge (red) compared to measured monthly discharge (blue) from La Guardia Station. Simulation of 20 years of streamflow data from 1980 – 1999 for calibration and 10 years from 2000 – 2009 for validation. The grey area represents the 95% interval (95 PPU, percent prediction uncertainty) or the range where observed values fit the simulations run during the calibration and validation processes.

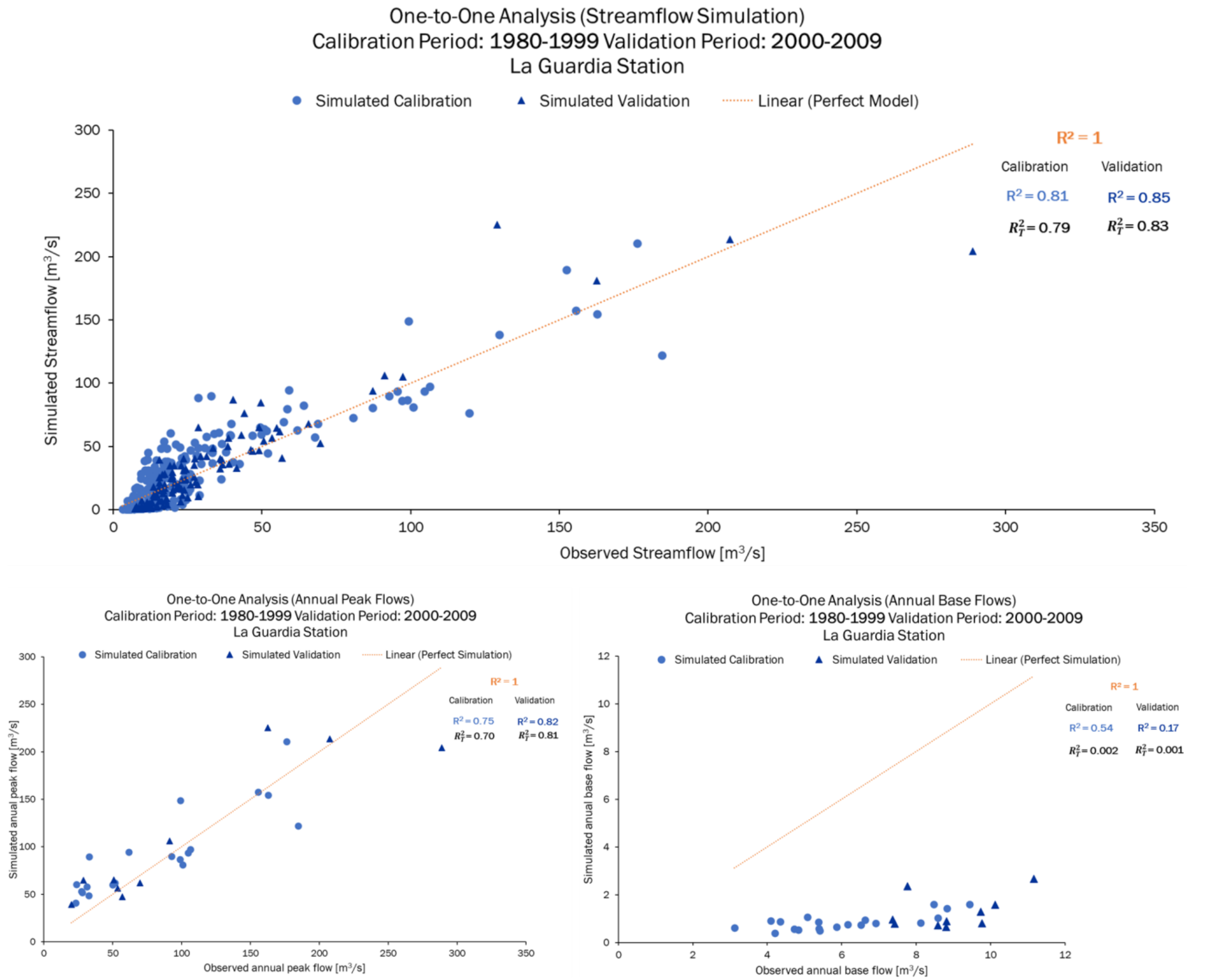

Figure 2.7. One-to-one analysis. Observed and simulated streamflow values (blue) are compared with respect to what is considered the perfect model (orange). This analysis is discriminated between all values (Top), peak flows (Bottom-left), and base flows (Bottom-right). Finally, a theoretical coefficient of determination R_T^2 is calculated to evaluate the proportion of the variance of the calibrated and validated results that is explained by the perfect model. This theoretical coefficient is determined by analyzing the distance between the simulated values and the perfect value or where the observation is equal to the simulation.

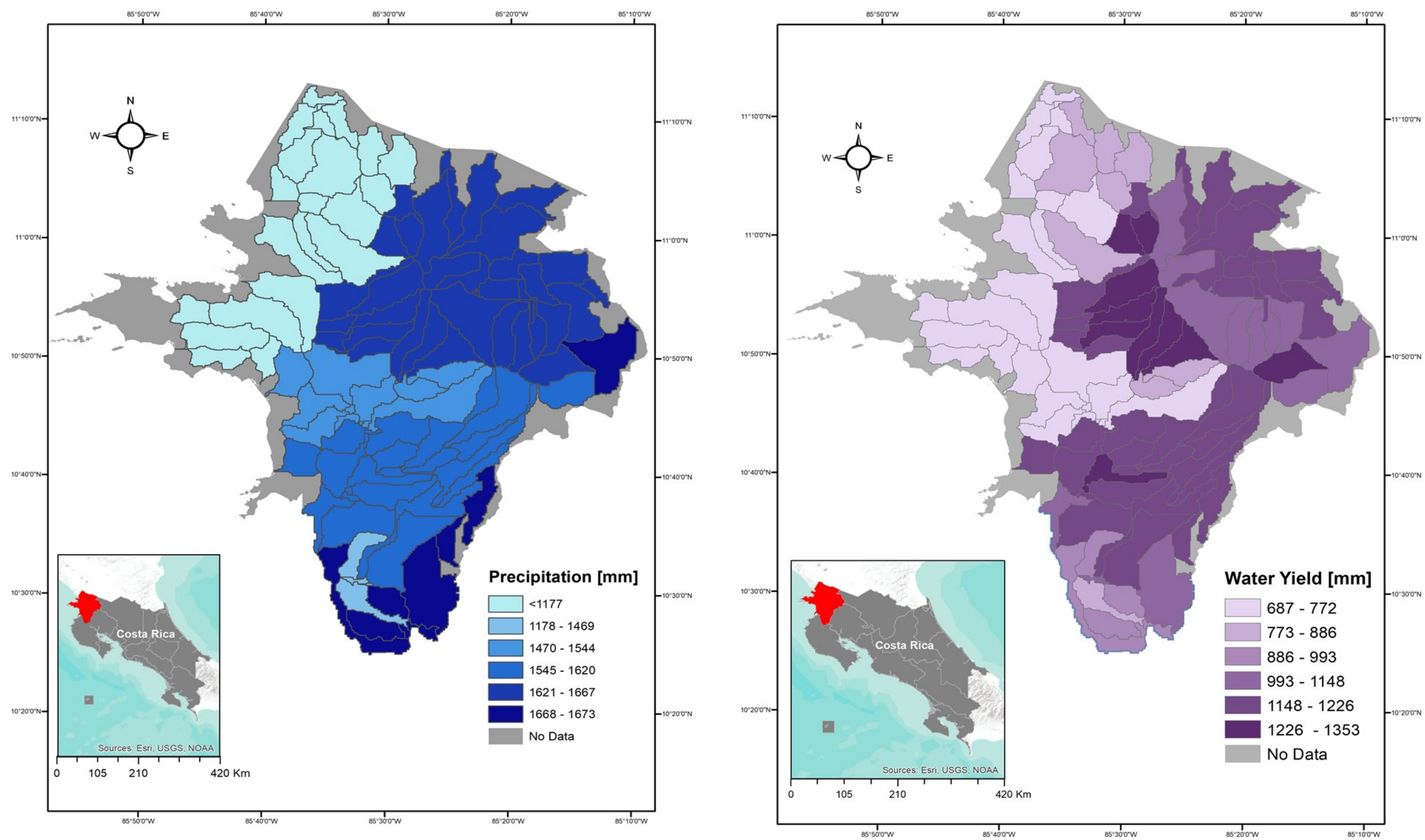

Figure 2.8. Spatial representation of precipitation (Left) and water yield (Right) simulated. The information is presented at the sub-basin scale.

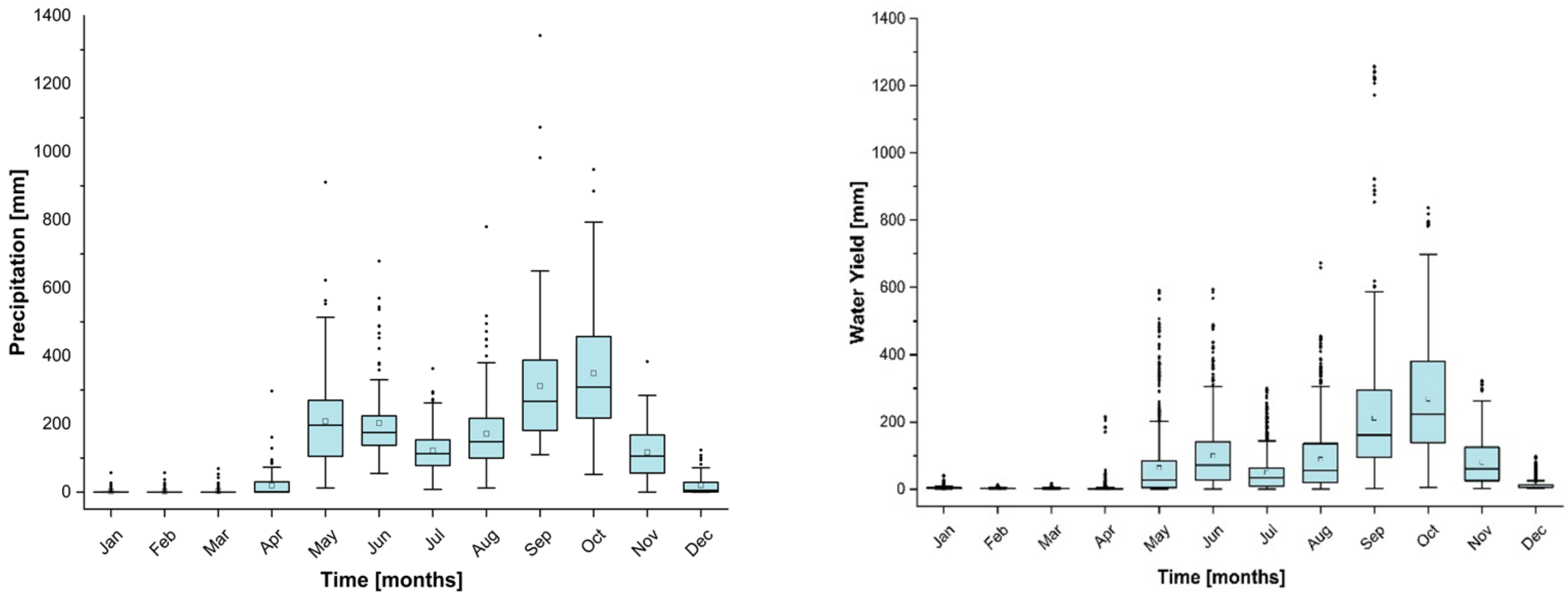

Figure 2.9. Total monthly simulated rainfall (Left) and simulated water yield (Right) distribution as box plots. The plots represent the annual pattern of both hydrological variables, low values during the dry season from December to March and a small summer in July, and increases in both variables during the rainy season from May to July and August to December.

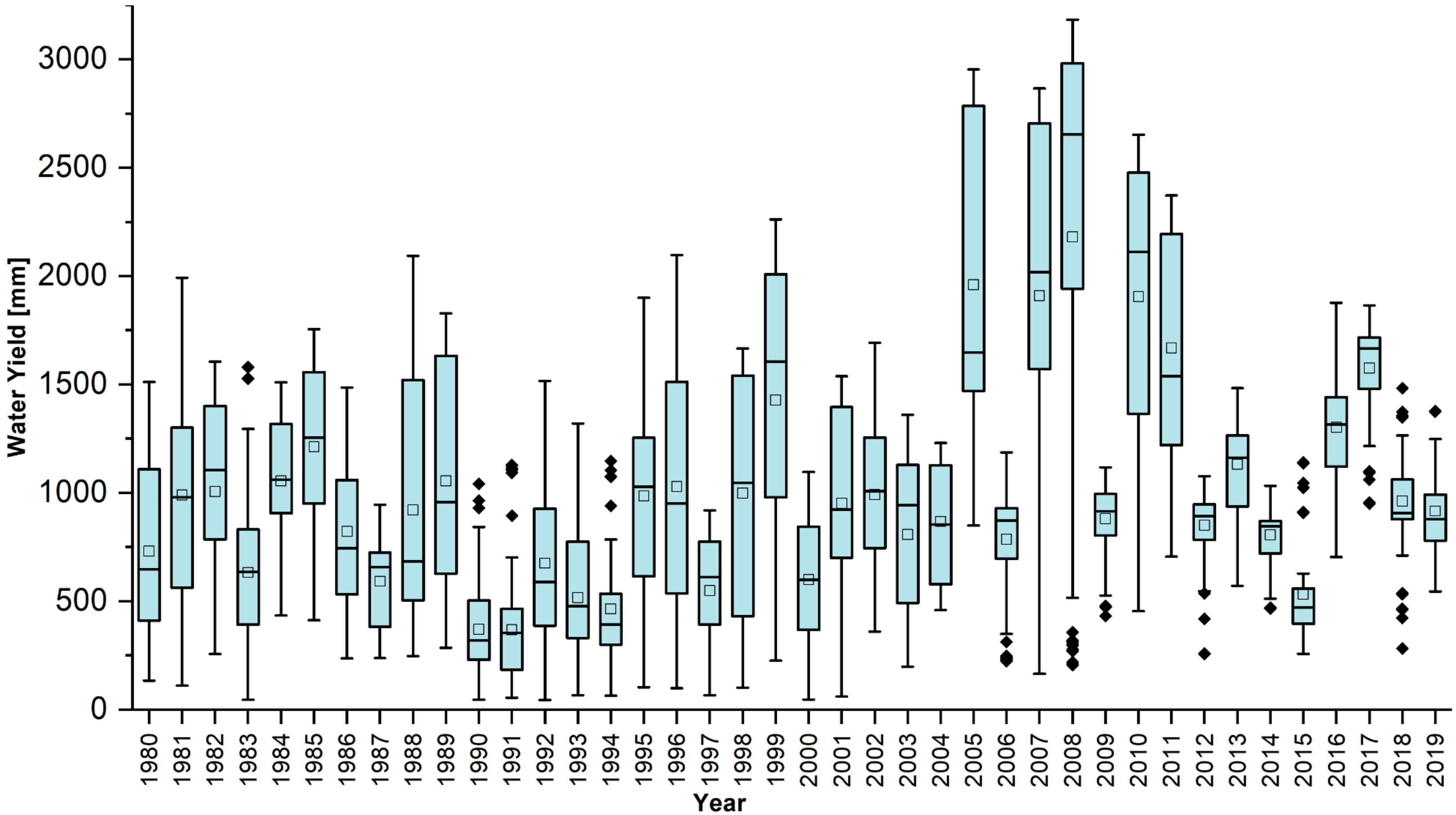

Figure 2.10. Inter-annual variation of the average water yield in the ACG from 1980 – 2019. Box-plots' width represents the spatial variation of water yield among all 107 sub-basins that can be associated with geological features, seasonal meteorological conditions, and extreme conditions such as ENSO phenomena.

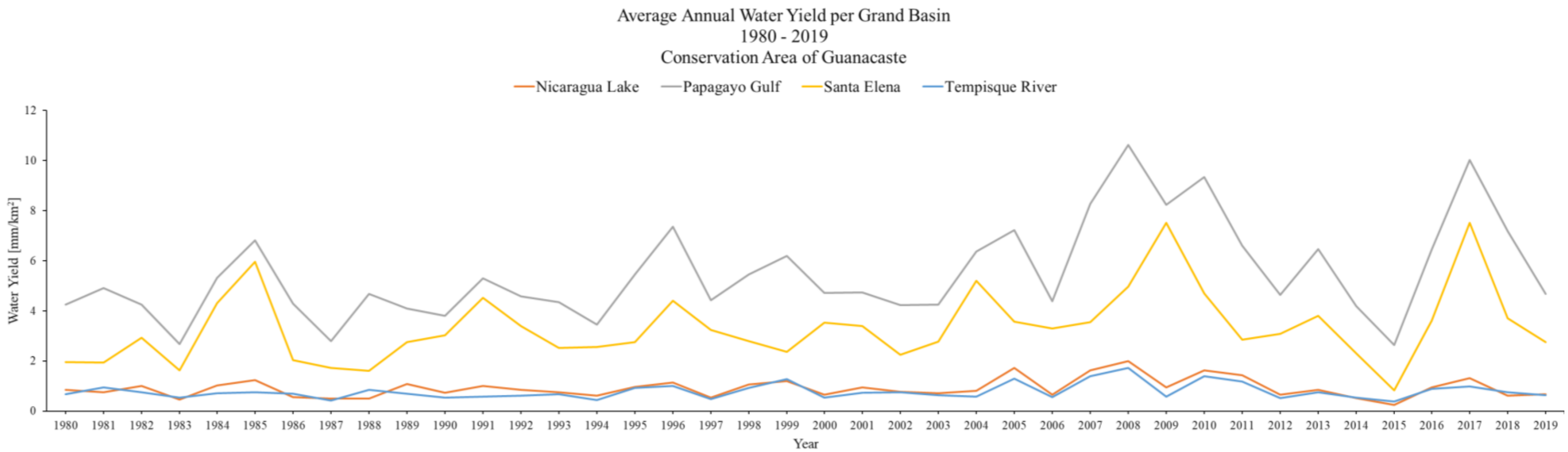

Figure 2.11 Average Annual Water Yield in the four main basins of the ACG from 1980-2019. Water Yield values have been normalized per basin area [mm/km^2].

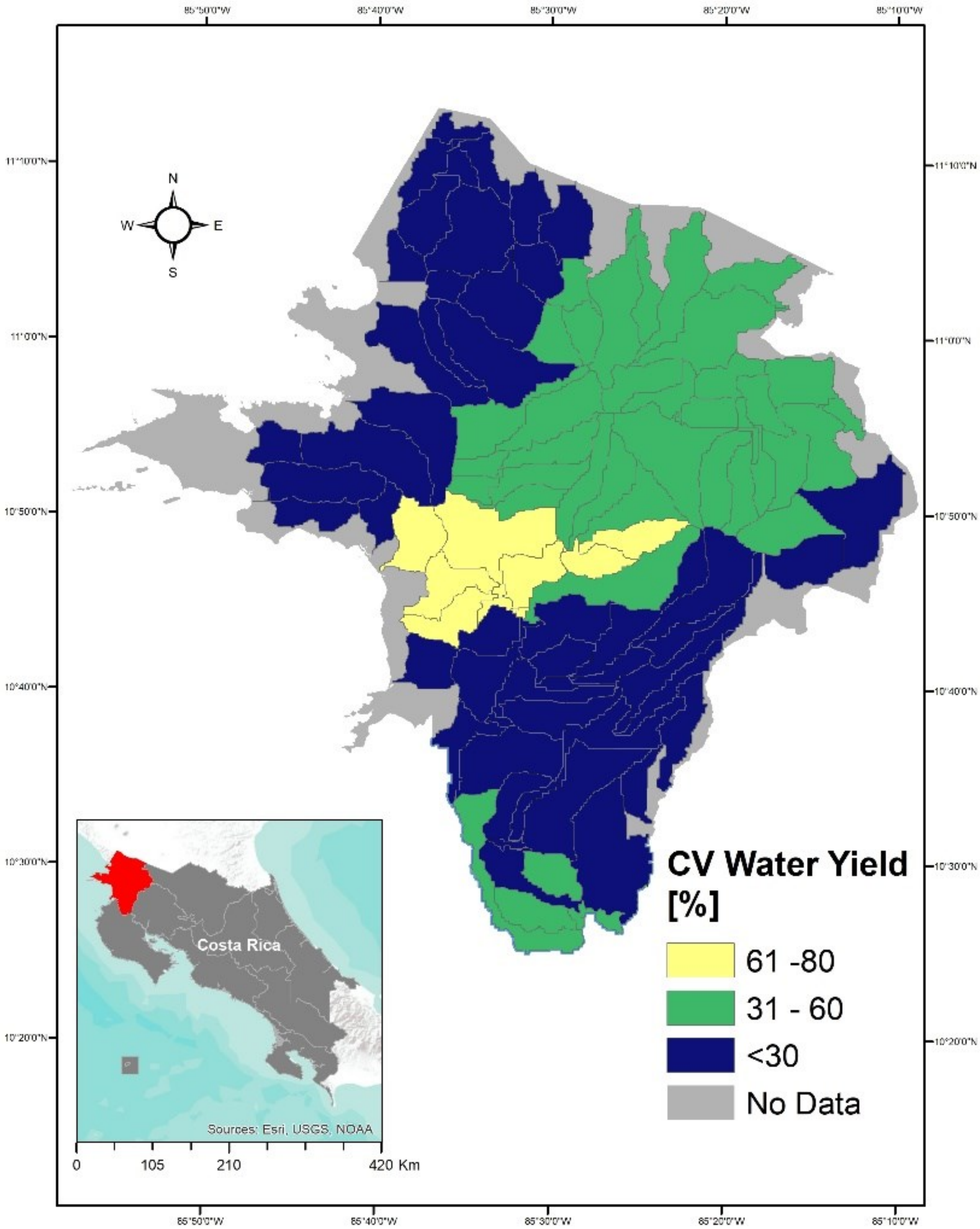

Figure 2.12. Coefficient of Variation of the average annual water yield. Larger values (>60%) indicate that the water availability is not reliable from one period to another.

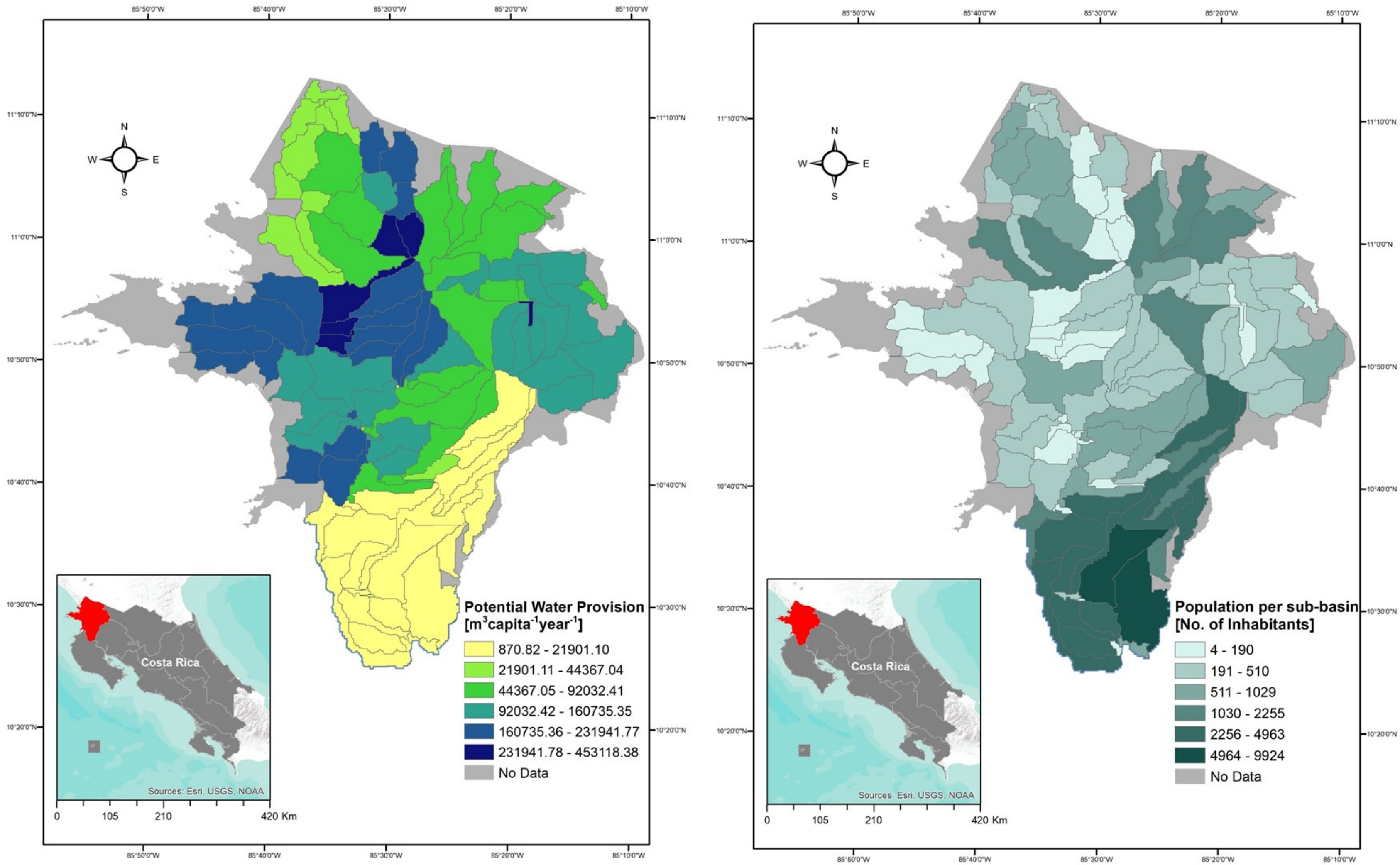

Figure 2.13. Potential Water Provision (left) and average population estimated per sub-basin during 1980 - 2019 (right).

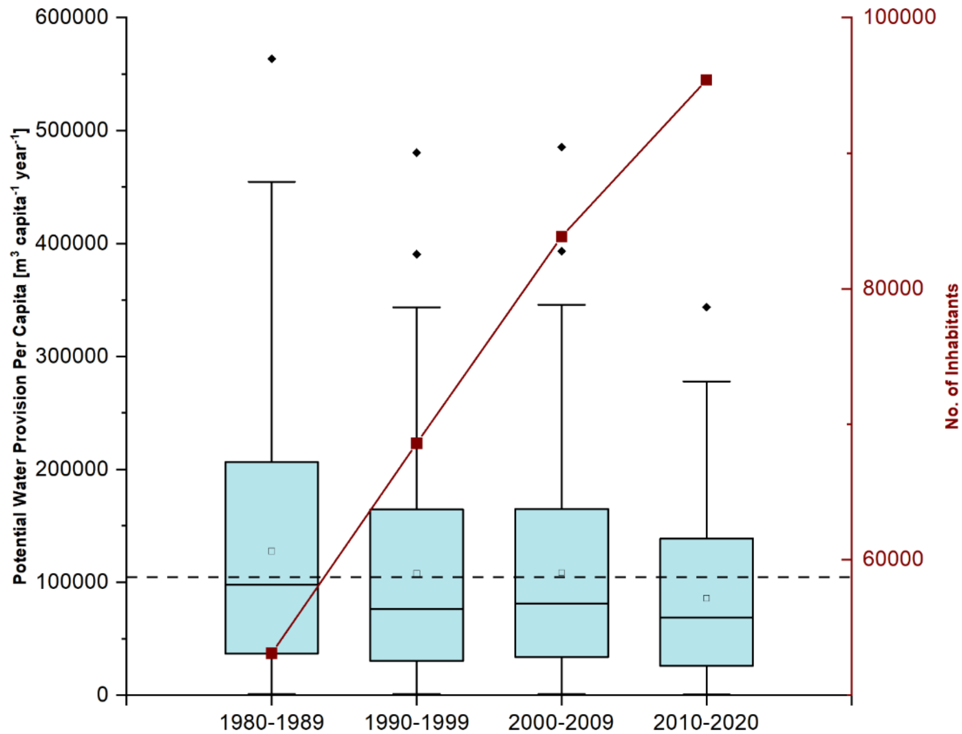

Figure 2.14. Potential Water Provision per capita in each decade of study (boxplots). The dash line represents the multiannual average of water per capita, and the increasing dark red line corresponds to the average population (secondary axis).

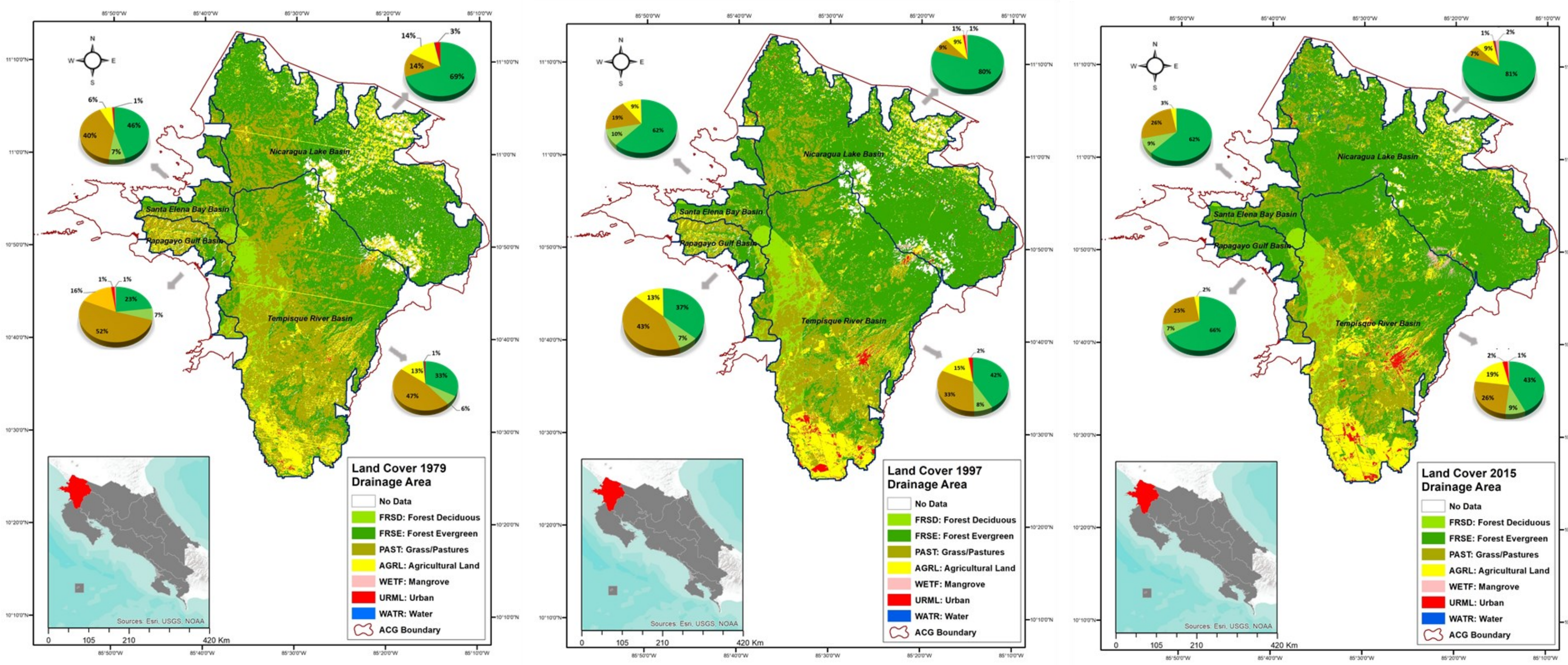

Figure 2.15. Land Covers maps developed by Chen (2020), represented within the drainage area modelled by SWAT for the ACG. Years 1979 (Left), 1997 (Centre), and 2015 (Right). Pie charts show the land cover percentage in each watershed.

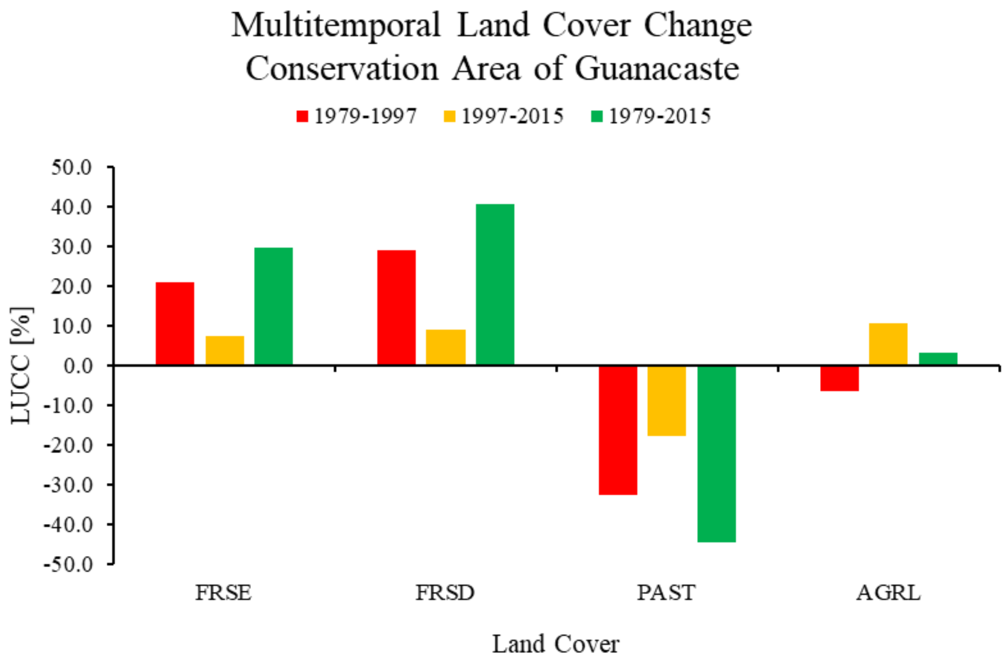

Figure 2.16. Multitemporal Land Cover Change between 1979-1997, 1997-2015, and 1979-2015. FRSE: Forest Evergreen; AGRL: Agriculture; PAST: Pasture; and FRSD: Deciduous Forest.

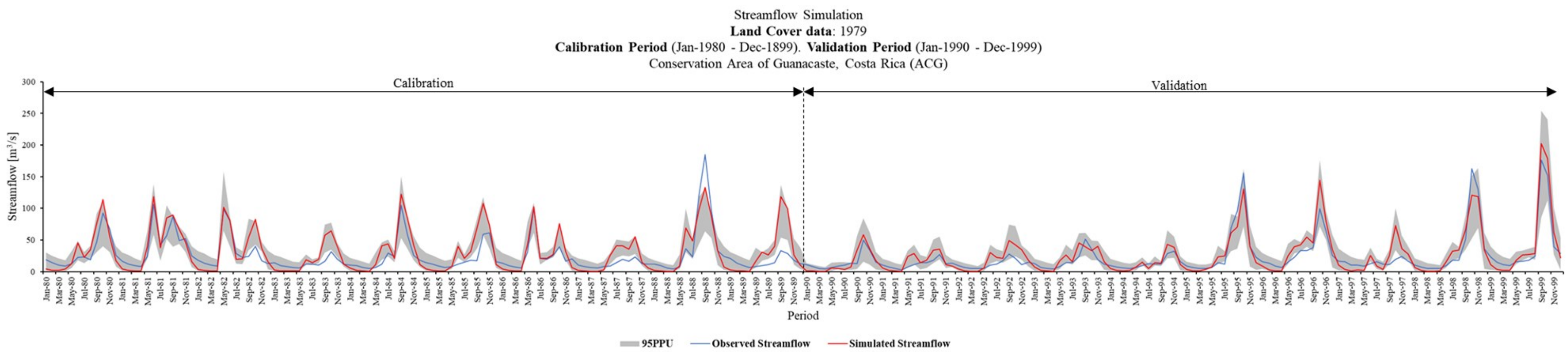

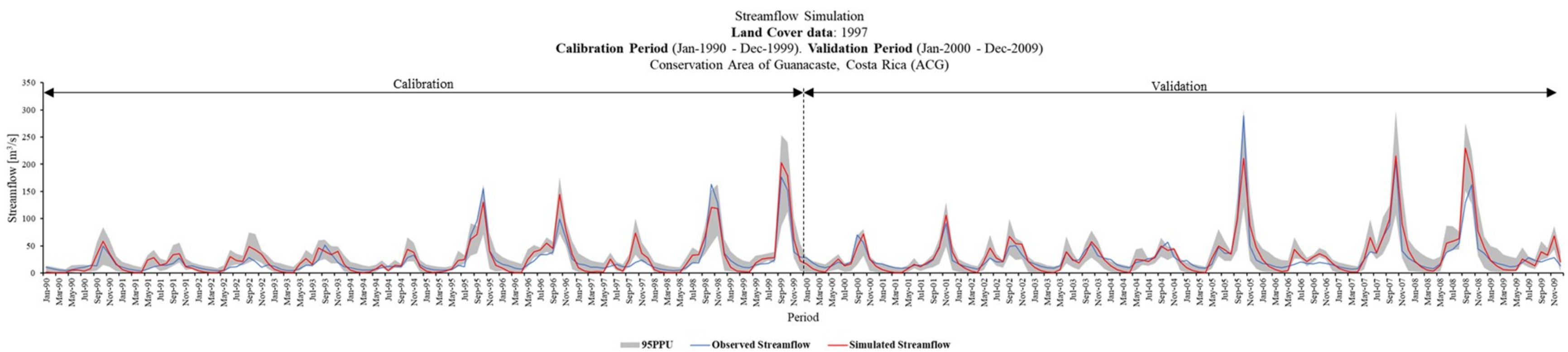

Figure 2.17. Modelled SWAT monthly discharge (red) compared to measured monthly discharge (blue) from La Guardia Station. For these models, the land cover input data was modified by the 1979 (Top) and 1997 (Bottom) maps developed by Chen (2020). The periods of calibration and validation were 1980 – 1989 and 1990 – 1999 for the 1979 model; and 1990 – 1999 and 2000 – 2009 for the 1997 model, respectively. The grey area represents the 95% interval (95 PPU, percent prediction uncertainty) or the range where observed values fit the simulations run during the calibration and validation processes.

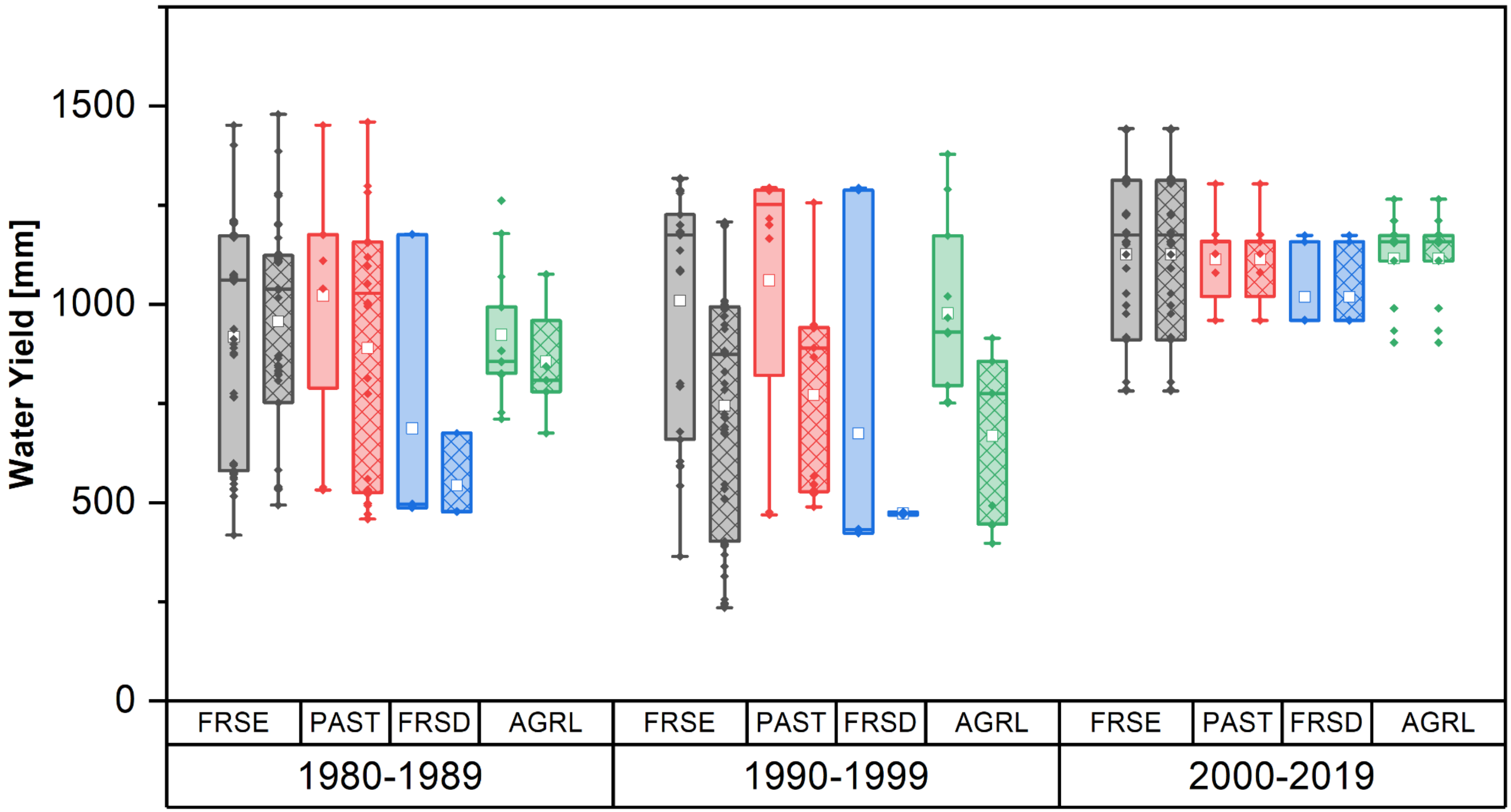

Figure 2.18. Water Yield Simulation results Pre and Post Land Cover Change: Comparison of Generalized Linear Mixed Models (GLMM) between SWAT average water yield estimations introducing only the 2015 land cover during model building (plain colour boxplots) and changing the land cover information with 1979 map for the 1980 – 1989 estimations and with 1997 map for the water yield quantified between 1990 – 1999 (boxplots with criss-cross lines). Values between 2000 – 2019 are the same because they were calculated with the 2015 land cover map and estimations were projected until 2019 using the No_Observations option in SWAT-CUP. The GLMM relates the combined effect of the LUCC and the period of evaluation with the multiannual average water yield produced in all the sub-basins (107) identified in the ACG. FRSE: Forest Evergreen; AGRL: Agriculture; PAST: Pasture; and FRSD: Deciduous Forest.

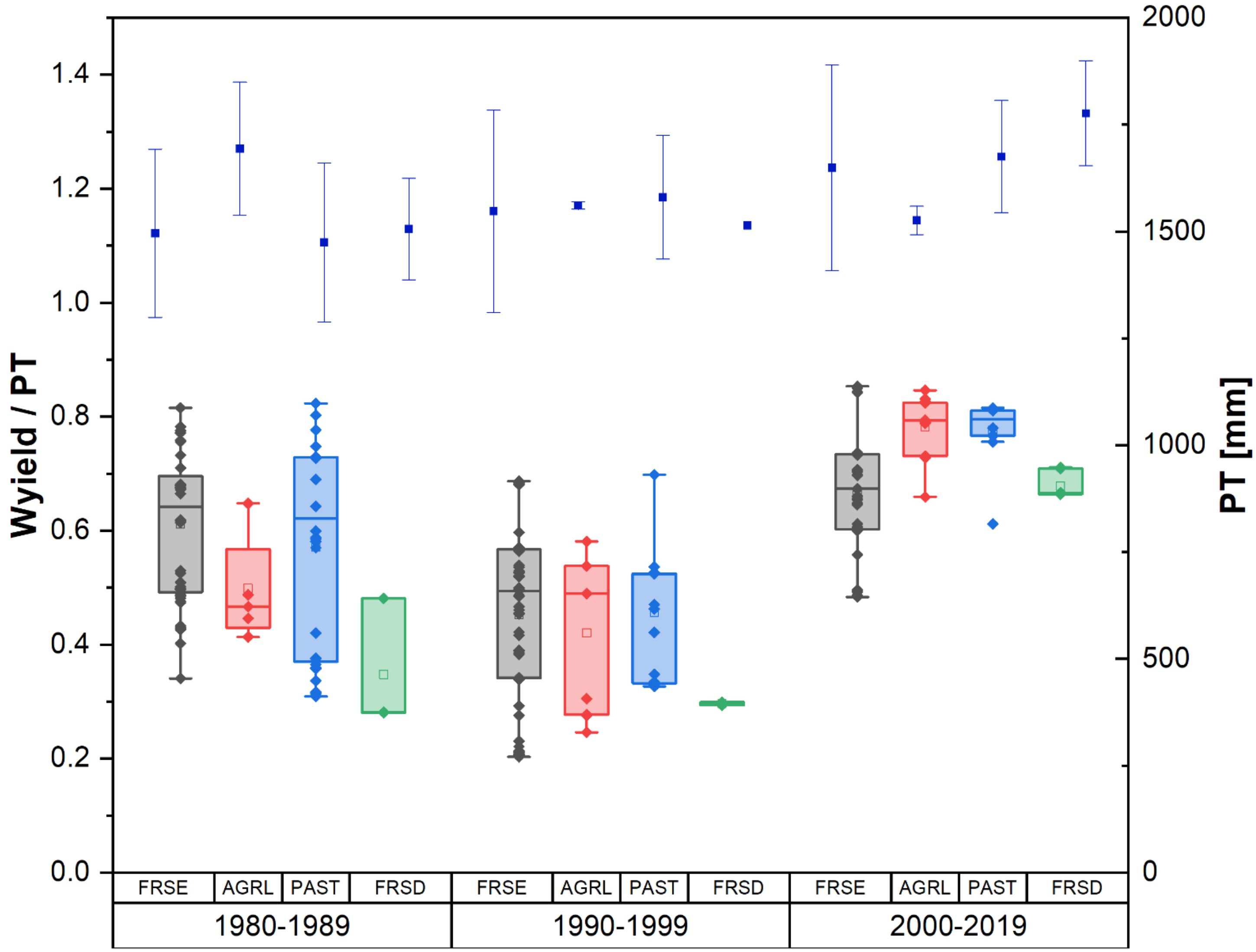

Figure 2.19. Generalized Linear Mixed Models (GLMM) associating the combined effect of the LUCC and the period of evaluation with the multiannual average water yield – precipitation ratio in all the sub-basins (107) identified in the ACG. FRSE: Forest Evergreen; AGRL: Agriculture; PAST: Pasture; and FRSD: Deciduous Forest. Dots on the top represent the average multiannual precipitation (secondary axis).

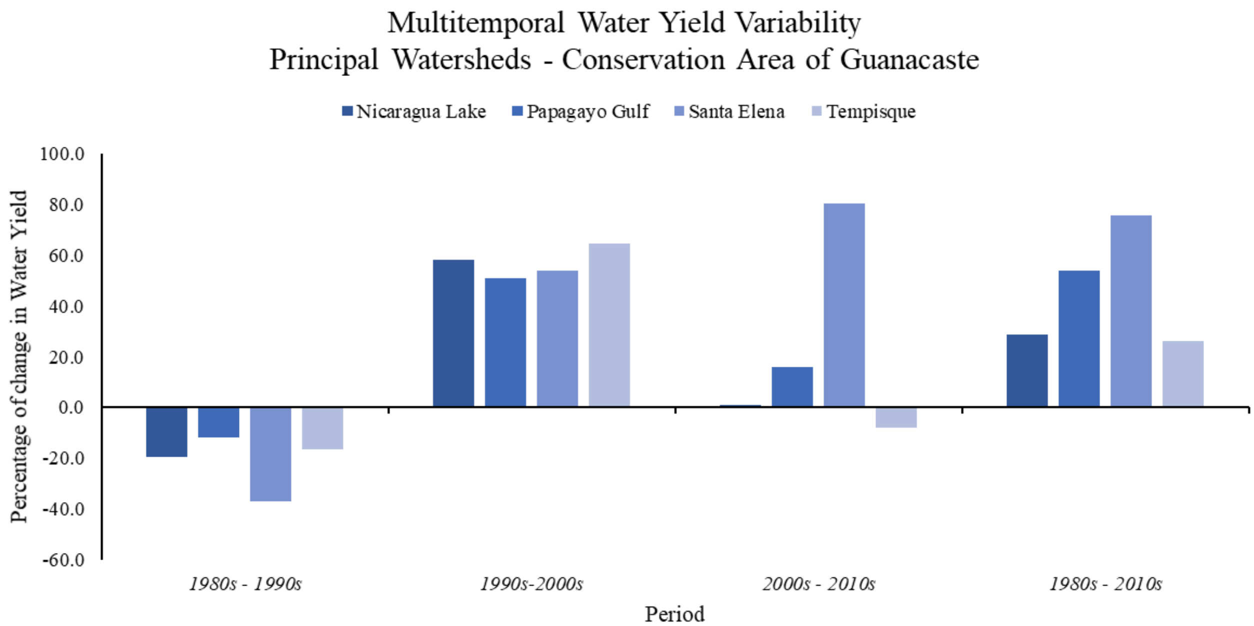

Figure 2.20. Decadal Water Yield Variability in the main four watersheds of the ACG between the 1980s and 2010s.

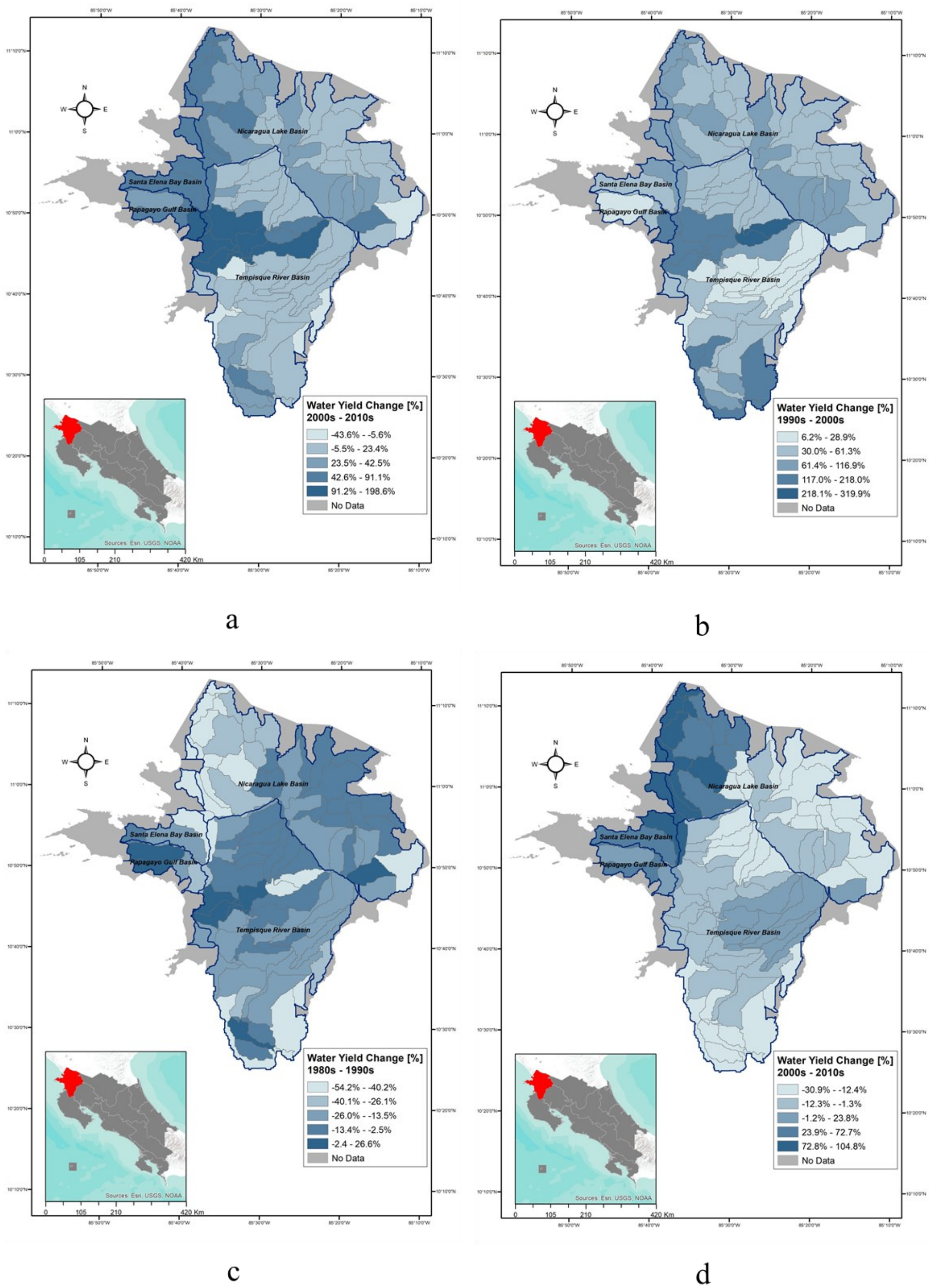

Figure 2.21. Spatial distribution of percentages of change in water yield disaggregated per sub-basin across the three temporal changes analyzed 1980s-1990s (a), 1990s-2000s (b), 2000s-2010s (c) and during the 40 years (d) of study (1980s-2010s)

2.7. Tables

Table 2.1. Time Series and Geospatial datasets available for the construction and calibration of the SWAT model for the quantification of water supply in the Conservation Area of Guanacaste.

SWAT Input Data	**Digital Elevation Model (DEM)**	**Spatial Resolution**	10 m
		Source	Atlas of Costa Rica
		Year	2014
	Land Use and Cover Map	**Number of Classes**	6
		Year	2015
		Spatial Resolution	30 m
		Source	(Chen, 2020)
	Soil	**Number of Soil Types**	39 in total (12 for the ACG)
		Scale	1: 200.000
		Year	2016
		Source	Centre for Agronomic Research (CIA for its acronym in Spanish) of the University of Costa Rica

		Station Name	**Lat.**	**Long.**	**Elevation (m.a.s.l)**	**Reported Period**				
						Precipitation	**Temperature**	**Wind Speed**	**Relative Humidity**	**Solar Radiation**
SWAT Input Data	**Weather Data National Meteorological Institute of Costa Rica (IMN)**	72106-Santa Rosa National Park	10.84	-85.62	315	1971-04 2015-07	1971-05 1983-12	1985-06 1987-03	No Data	No Data
		72163-Santa Rosa CC	10.84	-85.62	315	2012-04 2019-12	2012-04 2019-12	2012-03 2019-12	2012-03 2019-12	2012-03 2019-12
		74008-Pelon de Bajira	10.49	-85.41	40	1968-06 2019-06	1978-08 1984-07	1983-03 1984-11	No Data	No Data
		74020-Llano Grande, Liberia	10.60	-85.54	80	1957-01 2017-06	1973-01 2017-07	1974-05 2004-12	1976-04 2011-10	No Data
		74051-Liberia Airport	10.59	-85.55	89	1998-11 2019-12	1998-11 2019-12	1998-11 2019-12	1998-11 2019-12	1998-11 2019-12
	Weather Data Centre for Earth Observation Sciences (CEOS)	99999-CEOS	10.84	-85.62	302.9	1994-11 2019-12	2011-05 2018-12	No Data	No Data	No Data

Calibration Validation Input Data	Streamflow Data Costa Rican Institute of Electricity (ICE)	19-01-La Guardia	10.55	-85.58	110	**Reported Period of Streamflow**
						1979-09 – 2010-07

Table 2.2. Summary of the parameters used for calibration of the SWAT model built for the ACG.

No	Parameter	Name	Unit	File	Calibration Method	Min Initial	Max Initial
1	CN2	Initial SCS runoff curve number for moisture condition II	Dimensionless	.mgt	r	-0.15	0.15
2	CH_K2	Effective hydraulic conductivity in main channel alluvium	mm/hr	.rte	v	-0.01	500
3	CH_N2	Manning's roughness coefficient "n" for the main channel	Dimensionless		v	-0.01	0.3
4	CH_L2	Lemgth of main channel	km		v	0.085	29.557
5	GW_DELAY	Growndwater delay time	days	.gw	v	0	500
6	ALPHA_BF	Baseflow Alpha Factor or Baseflow recession constant	1/days		v	0	1
7	GWQMN	Threshold depth of water in the shallow aquifer required for return flow to occur	mm H2O		v	0	5000
8	GW_REVAP	Groundwater "revap" coefficient	Dimensionless		v	0.02	0.2
9	REVAPMN	Threshold depth of water in the shallow aquifer for revap to occur	mm H2O		v	0	500
10	SOL_AWC	Available water capacity of the first soil layer	mm H2O/mm soil	.sol	r	-0.15	0.15
11	SOL_BD	Moist bulk density	Mg/m^3 or g/cm^3		r	-0.15	0.15
12	SOL_K	Saturated hydraulic conductivity	mm/hr		r	-0.15	0.15
13	OV_N	Manning's roughness coefficient "n" for overland flow		.hru	r	-0.15	0.15
14	ESCO	Soil evaporation compensation factor	Dimensionless		v	0	1
15	EPCO	Plant uptake compensation factor	Dimensionless		v	0	1
16	SURLAG	Sueface runoff lag coefficient	Dimensionless		v	0.05	24
17	HRU_SLP	Average slope steepness	m/m		v	0.008	0.256
18	SLSUBBSN	Average slope length	m		v	9.15	121.95

Table 2.3. Regionalization data treatments. Data treatment 5 is highlighted as the iteration with the best performance**.**

Data Treatment	*p-factor*	*r-factor*	r^2	*NS*	br^2
1	0.84	1.19	0.78	0.7	0.77
2	0.72	1.12	0.76	0.58	0.75
3	0.81	1.1	0.76	0.67	0.75
4	0.71	1.01	0.78	0.63	0.76
5	0.88	1.08	0.81	0.75	0.80
6	0.72	1.01	0.78	0.65	0.77

Table 2.4. Sensitive parameters for the generation of simulated streamflow in the ACG.

No.	Parameter	File	Calibration Method	Calibrated range		Fitted Value	P-value
				Min	Max		
1	CN2	.mgt	r	-0.19	0.04	-0.01	0.000
2	CH_K2	.rte	v	133.35	400.14	291.96	0.000
3	GW_DELAY	.gw	v	-224.15	258.65	36.32	0.000
4	ALPHA_BF	.gw	v	0.40	1.21	0.88	0.000
5	GWQMN	.gw	v	-1476.43	2841.43	2834.95	0.000
6	GW_REVAP	.gw	r	-0.03	0.20	0.19	0.000
7	ESCO	.hru	v	-0.46	0.51	0.23	0.001

Table 2.5. SWAT model performance for the calibration and validation periods.

Coefficient	Pre-Calibration	Calibration	Validation
p-factor	-	0.88	0.93
r-factor	-	1.08	1.18
r^2	0.74	0.81	0.85
NSE	0.58	0.75	0.82
br^2	0.67	0.80	0.85
Model error *(1 - p-factor)x100%*	-	12%	7%

Table 2.6. Land cover areas in the drainage zone modelled by SWAT for the ACG divided by the four main watersheds and years 1979, 1997, and 2015.

Land Cover [SWAT code]	Year	Area [km^2]				Total [km^2]	% in Total Drinage area [2,861.92 km^2]
		Nicaragua Lake Basin	Papagayo Gulf Basin	Santa Elena Bay Basin	Tempisque River Basin		
FRSE: Forest Evergreen	1979	767.5	29.5	67.9	454.4	**1,319.3**	**46%**
	1997	888.0	46.5	91.0	567.2	**1,592.7**	**56%**
	2015	933.9	87.2	92.5	593.6	**1,707.2**	**60%**
FRSD: Deciduous Forest	1979	0.0	8.7	10.5	80.0	**99.3**	**3%**
	1997	0.0	8.9	14.7	104.4	**128.1**	**4%**
	2015	0.0	8.8	13.8	117.0	**139.6**	**5%**
PAST: Pastures/Grassland	1979	158.7	67.0	60.0	638.8	**924.5**	**32%**
	1997	97.8	54.4	27.7	443.0	**622.9**	**22%**
	2015	85.9	32.2	38.8	354.5	**511.4**	**18%**
AGRL: Agriculture	1979	151.6	20.2	9.2	178.8	**359.9**	**13%**
	1997	95.3	16.2	13.8	211.1	**336.3**	**12%**
	2015	99.2	3.1	4.2	264.7	**371.2**	**13%**
URML: Urban	1979	3.7	2.0	0.5	8.6	**14.8**	**1%**
	1997	10.5	0.1	0.4	28.7	**39.7**	**1%**
	2015	8.2	0.1	0.2	34.4	**42.9**	**1%**
WATR: Water	1979	0.01	0.0	0.0	0.01	**0.0**	**0%**
	1997	0.1	0.0	0.0	0.1	**0.2**	**0%**
	2015	4.6	0.0	0.0	0.5	**5.1**	**0%**
WETF: Mangrove	1979	30.9	0.9	1.5	8.4	**41.7**	**1%**
	1997	14.6	0.2	0.1	1.7	**16.6**	**1%**
	2015	20.0	0.1	0.1	12.2	**32.4**	**1%**

Table 2.7. Multitemporal percentage of land cover change divided by the four main basins. Positives values correspond to a gain in the land cover from one year to another, and negative values represent percentage of loss. For forest covers, a colour scale indicates zones of significant forest recovery (greenish) or an area with a low percentage of recovery or loss of this natural vegetation (reddish). An opposite pattern for agriculture and grasslands is chosen. In this case, negative values are linked to the green colours, meaning a decrease in those land covers, and values associated with the red colours pallet imply an increment from one year to another as a sign of ecosystem transformation.

Land Cover [SWAT code]	Period of Change	Percentage of change				Total Change [%]
		Nicaragua Lake Basin	Papagayo Gulf Basin	Santa Elena Bay Basin	Tempisque River Basin	
FRSE: Forest Evergreen	1979-1997	16%	58%	34%	25%	21%
	1997-2015	5%	88%	2%	5%	7%
	1979-2015	22%	196%	36%	31%	29%
FRSD: Deciduous Forest	1979-1997	0%	2%	40%	30%	29%
	1997-2015	0%	-2%	-6%	12%	9%
	1979-2015	0%	1%	32%	46%	41%
PAST: Pastures/Grassland	1979-1997	-38%	-19%	-54%	-31%	-33%
	1997-2015	-12%	-41%	40%	-20%	-18%
	1979-2015	-46%	-52%	-35%	-45%	-45%
AGRL: Agriculture	1979-1997	-37%	-20%	49%	18%	-7%
	1997-2015	4%	-81%	-70%	25%	10%
	1979-2015	-35%	-85%	-55%	48%	3%

Table 2.8. SWAT model performance using the 1979 and 1997 land cover maps.

Coefficient	Land Use: 1979		Land Use: 1997	
	Calibration	Validation	Calibration	Validation
p-factor	0.81	0.89	0.89	0.89
r-factor	1.04	0.91	0.91	0.95
r^2	0.70	0.86	0.86	0.83
NSE	0.63	0.83	0.83	0.79
br^2	0.69	0.86	0.86	0.83
Model error *(1 - p-factor)x100%*	19%	11%	11%	11%

Table 2.9. Main socioeconomic and environmental events in Guanacaste during the 40 years of study (1980 - 2019).

<table>
<tr><th>COMPONENT</th><th>1980-1989</th><th>1990-1999</th><th>2000-2019</th></tr>
<tr><td rowspan="2">Economic</td><td>Increase in the colonization from the central region citizens.

Some of the largest transformed areas were in the north of the ACG, they were large farms established since the XVII century by Spanish colonizers.</td><td>The services sector, primarily tourism, has started to become the main source of income for many families in Guanacaste.</td><td rowspan="2">There is a pressure from a population sector to reactivate the beef industry through a national cattle farming reactivation program.

Tourism and real state sectors have increased 40% between 2005 and 2012.

New agribusiness to produce biofuel.

Central American-Dominican Republic Free Trade Agreement (CAFTA)</td></tr>
<tr><td colspan="2">In this period, there is a change of perspective in the economic development of Guanacaste through the decrease of beef production caused by the collapse of the international meat market. Additionally, the Government of Costa Rica withdrew the financial support to this industry during the 1980s.</td></tr>
<tr><td>Social</td><td colspan="2">Sustained growth of population and urbanized areas, predominantly in the south of the ACG close to Province's capital, Liberia.

The employment rate in the agricultural sector decreased dramatically, only 9% of the labour force was concentrated in this sector by the end of the 90s.

Rising investment in public education and health. The high level of education was another main factor that promotes the change in socioeconomic activities focused on the services sector.</td><td>Tourism is established as the main source for the economy with almost 24% of the hotels in Costa Rica located in Guanacaste, turning this area into the second most visited after the capital region.

Despite the increase in the international price of beef at the beginning of the 2010s, this has not driven an increment in cattle raising activity. Farmers have continued to respect forest laws.</td></tr>
<tr><td>Environmental</td><td>Introduction of conservation policies and the acceptance of the concept of sustainable development by Costa Rica's Government.</td><td>Inscription in 1999 of the Conservation Area of Guanacaste (ACG) into the UNESCO World Heritage Sites List.

Creation of the National System of Conservation (SINAC)

Establishment of the Forest law of 1996 for the restriction of timber extraction.

New program of Payments for Environmental Services PSA to promote</td><td>In 2004 the ACG – World Heritage Site was extended 15,000 hectares of private property.

Expansion of irrigation lands in the lowlands of Guanacaste

Monoculture farming in hilly terrain threatens forest cover sustainability, especially those in recovered areas (secondary forests).

By 2012 it was registered that the forest land cover</td></tr>
</table>

COMPONENT	1980-1989	1990-1999	2000-2019
		reforestation in private land.	continued to increase, occupying 50.74% of Guanacaste. However, the forest regrowth rate has decreased.
	9.6% of the total territory in Guanacaste has been designated as a protected zone administered by the National Park System. The two largest protected areas are in the ACG region, the Santa Rosa (495 km^2) and the Guanacaste (324 km^2) National Parks.		

Sources: Calvo-Alvarado et al. (2009, 2019); Stan & Sanchez-Azofeifa (2019); UNESCO (2019)

Table 2.10. Decadal change in mm and % of water availability between the different decades of the study period (1980 – 2019) divided by the four main watersheds in the ACG. Positives values correspond to increase in water yield from one period to another and negative values represent loss of water. The colour scale indicates zones of significant increase (greenish) or decrease (reddish) in the average water yield.

Average decadal change of Water Yield								
Watershed	**1980s - 1990s**		**1990s-2000s**		**2000s - 2010s**		**1980s - 2010s**	
	mm	**%**	**mm**	**%**	**mm**	**%**	**mm**	**%**
Nicaragua Lake	-173.49	-19.38	419.14	58.09	11.23	0.98	256.88	28.70
Papagayo Gulf	-74.62	-11.99	278.89	50.94	130.04	15.74	334.32	53.74
Santa Elena	-172.94	-36.83	160.54	54.13	367.77	80.45	355.38	75.69
Tempisque River	-162.35	-16.73	522.50	64.67	-107.07	-8.05	253.07	26.08
Grand Total	-163.01	-18.08	454.60	61.53	-28.47	-2.39	263.11	29.18

3. Chapter 3: Conclusions and Future Work

The main objective of this thesis was to assess the water provision as an ecosystem service of the Conservation Area of Guanacaste (ACG). To do so, I have adapted an Ecosystem Services (ES)-based approach comprised of four core elements, (1) effects on human well-being, (2) bio-physical underpinning of service delivery, (3) transdisciplinarity, and (4) assessment of services for decision-making. In addition, I have deepened in core element two by assessing all the physically-based processes involved in the hydrologic cycle, which generate the quantity of water available for the region of study. As a result, I present the first calibrated and validated Soil and Water Assessment Tool (SWAT) for the entire ACG, including the land use and cover change (LUCC) impact on water availability.

3.1. Synthesis of significant contributions

The results of Chapter 2 **“Water Yield Quantification and Analysis of Land Cover Change impact in Water Availability for the Conservation Area of Guanacaste, Costa Rica using SWAT”** have demonstrated the relevance of hydrological modelling for studies related to ecosystem services because it allows the understanding of physical phenomena of the basin, the quantification of different variables of interest and the analysis of diverse monitoring datasets; but most importantly, it facilitates the creation and analysis of scenarios for decision-making and prediction of the quality and quantity of the available resource. The SWAT hydrological model has been barely used in Costa Rica; thus, this work complements the baseline for future applications of ES-based approaches in this region.

By building the SWAT model, I have filled a knowledge gap regarding the lack of calibration and model testing in the ACG, but also used, for the first time, the measured data from the meteorological and hydrological stations available for this region in this type of models. In principle, I tested different resources, resulting in selecting the data provided by governmental and academic institutions instead of reanalysis and remote-sensing products. However, this result looks to draw attention to increasing the monitoring stations in the area, both meteorological and hydrological. Some assumptions had to be made due to the high number of missing values and the lack of coverage, especially in the sub-basins bordering Nicaragua, the south areas with a high concentration of human settlements and agricultural activities, and the sub-watersheds connecting the Caribbean region. For an area of international importance as the ACG, increasing meteorological and hydrological monitoring should be considered in the foreseeable future, in addition to updated land cover information maps.

With an excellent SWAT model performance (error of 12% during calibration and 7% in the validation period), I have found that the ACG has a high potential for the provision of water as an ecosystem service with high reliability (CV < 50%). Nevertheless, the spatial distribution of the water availability is associated with some geographical factors that cause the spatial variation in the water yield regimes. For instance, the region with a high population and agricultural activity concentration has the lowest water yield magnitudes even though the average precipitation appears high. The same occurs when water yield is represented as water per capita. This pattern revealed the spatial explicitness of the water provision (Filoso et al., 2017). The annual seasonality was also captured together with the delayed response of water yield to increase after rainfall events due to all the physical processes of the hydrologic cycle that take place, such as infiltration and groundwater recharge (Brooks et al., 2013). By capturing the spatial and temporal patterns of the water yield, I demonstrated the advantages of using spatially explicit and physically-based models for the quantification of water provision as an ecosystem service and to support decision-making processes(Chaudhary et al., 2015; Fisher et al., 2009; Gordon et al., 2015).

As the water yield generation depends on many factors and natural dynamics, I deepened in the effect of the land use cover change (LUCC), finding that the recovery of forest, decrease in grasslands, and a low number of agricultural areas have a positive effect in water availability. I also found that this gradual forest recovery is associated with historical events coincidentally related to the values found during the study period (1980 - 2019). Costa Rica’s situation is considered as an unique set of circumstances not only in the success of implementing conservation and sustainable development policies, as stated by Calvo-Alvarado et al. (2019), but also in turning this country, or at least the ACG at the moment with this research, into an exceptional case at the hydrological level, as it has been identified in a first-level for the Central American region (Filoso et al., 2017).

Finally, although some limitations were found, and some other aspects are required to fully implement an ES-based approach for the ACG, this thesis has proved the reliability of the SWAT model to quantify water ecosystem services and to detect the effect of different factors affecting the dynamics of water availability, such as the LUCC. This hydrological modelling can be replicated in other areas of Costa Rica, something that government's stakeholders, such as the Central Bank of Costa Rica (BCCR, for its acronym in Spanish) and the National Institute of Meteorology (IMN, for its acronym in Spanish) found already promising to implement for the rest of the country or future studies in the ACG as already planned by the Centre of Earth Atmospheric Sciences (CEOS) of the University of Alberta, where this information will remain.

3.2. Future works and challenges

The main challenge identified is the full implementation of comprehensive frameworks, such as the proposed by Martin-Ortega et al. (2015c) that helps to understand the linkages between ecological processes and human welfare. This thesis only addressed one of the core elements of the ES-based approach. Thus, more robust models that include socioeconomic information together with more detailed meteorological, hydrological, and land use data are needed to monitor this region that harbours extremely important ecosystems for humankind.

To help addressing the previous challenge. I have found important advancements that could help for future studies:

(1) Different tool extensions have been constructed to enhance SWAT estimations. According to the high-level and robust data that CEOS is collecting and developing through terrestrial laser scanning and high-resolution remote sensors to monitor and characterize the tropical dry forest of the Santa Rosa National Park; I have found two tools that could help to improve hydrological modelling. The first one is SWAT-T, developed by Alemayehu et al. (2017). This module enhances the vegetation growth cycles when SWAT is applied in tropical ecosystems, hence the name of SWAT-T. The main source of information needed is Leaf Area Index (LAI) to compute potential plant

transpiration (PPT). LAI is a variable that is constantly monitored in different studies conducted at CEOS.

The second tool is SWAT-C or SWAT-Carbon, developed by Zhang et al. (2013). This module was primarily created to enhance the estimations of water quality by incorporating into SWAT other modules from global models, such as EPIC, CENTURY, and DSSAT, to assess the potential for Carbon sequestration/emission effects from a variety of land management practices. This module offers better estimations of land-atmosphere carbon exchange and evapotranspiration. The primary source of information is Eddy-Covariance (EC) daily water and C exchange. These variables are collected in the EC flux tower located in the Santa Rosa National Park and Environmental Monitoring SuperSite (SR-EMSS) administered by CEOS.

(2) There are more efficient procedures to analyze the LUCC effect. In this study, I used the SWAT-**L**and **U**pdate **T**ool (SWAT-LUT) developed by Moriasi et al. (2019) that processes multitemporal land covers data to reconfigure the SWAT model and evaluate the effect of the landscape dynamics over hydrologic variables estimations. The tool presented glitches in the georeferentiation. Directed communication with the developers revealed that the module presents difficulties in areas outside of the United States. A new version of the model was sent from the USDA in Texas, which is georeferenced for the ACG. However, this new version generated regions without information in the spatial outputs. Faced with this problem, developers could not offer a solution in the short term. Therefore, three different models were carried out to analyze the LUCC. However, it is recommended that future research looks for an enhanced version of SWAT-LUT or generate a collaboration to develop a new version for tropical ecosystems.

Another limitation is associated with the assumptions made to run the model. In principle, I decided to calibrate the entire region using a single streamflow station. Although this station captures the information from the largest basin in the whole study area (Tempisque River), it does not receive the flows from the other three basins in the ACG. This decision was made because there are no more gauging stations within this region. The advantage of the region is its high state of conservation that promotes the climatic and hydrological stability of the area, which in part made it possible to obtain a model with good performance. However, this limitation increases the uncertainty of the simulations, and it is recommended to address this problem. Further improvements on the model could include calibration using other parameters such as evapotranspiration through data from the Eddy-Covariance tower installed in the Santa Rosa National Park; information from reanalysis products; or calibration and validation of the SWAT model by using the approach of regionalization with physical similarity, in other words, obtaining the calibration and validation data through a donor basin that can be considered physically similar, a process explained by Mengistu et al. (2019).

Groundwater processes characterization needs to be improved, principally due to the lack of information. This is one of the main sources of water for agriculture activities in the area of study and initiatives that look to expand the irrigation lands in Guanacaste could jeopardize the sustainability of this resource (Calvo-Alvarado et al., 2019). In this context, the use of wells is a water management technique that could not be included in the research. Extraction of groundwater through artisan and drilled wells is a common practice in the Guanacaste region. Unfortunately, there is limited control by the MINAE (Ministry of Environment and Energy) of water extractions and unregulated wells construction, and monitoring data is unavailable (Morataya-Montenegro and Bautista-Solís, 2020).

Finally, it is suggested to look analyze the impact of the external regions. For instance, the transboundary effects coming from Nicaragua, south-Pacific and central-Caribbean sub-basins.

3.3. References

Alemayehu, T., Van Griensven, A., Woldegiorgis, B. T., & Bauwens, W. (2017). An improved SWAT vegetation growth module and its evaluation for four tropical ecosystems. Hydrology and Earth System Sciences, 21(9), 4449.

Brooks, K. N., Ffolliott, P. F., & Magner, J. A. (2013). Hydrology and the Management of Watersheds. John Wiley & Sons.

Calvo-Alvarado, J., Jiménez, V., Calvo-Obando, A., & Castillo, M. (2019). Current perspectives on forest recovery trends in Guanacaste, Costa Rica. International Forestry Review, 21(4), 425–431.

Chaudhary, S., McGregor, A., Houston, D., & Chettri, N. (2015). The evolution of ecosystem services: A time series and discourse-centered analysis. Environmental Science & Policy, 54, 25–34.

Filoso, S., Bezerra, M. O., Weiss, K. C. B., & Palmer, M. A. (2017). Impacts of forest restoration on water yield: A systematic review. PLoS ONE, 12(8), 1–26. https://doi.org/10.1371/journal.pone.0183210

Fisher, B., Turner, R. K., & Morling, P. (2009). Defining and classifying ecosystem services for decision making. Ecological Economics, 68(3), 643–653.

Gordon, I. J., Martin-ortega, J., & Ferrier, R. C. (2015). Introduction. In S. K. J. Martin-Ortega, R. Ferrier, I. Gordon (Ed.), Water Ecosystem Services: A Global Perspective (pp. 1–2). Cambridge: Cambridge University Press. https://doi.org/10.1017/CBO9781316178904.002

Martin-Ortega, J., Jorda-Capdevila, D., Glenk, K., & Holstead, K. L. (2015). What defines ecosystem services-based approaches? In & S. K. J. Martin-Ortega, R. Ferrier, I. Gordon (Ed.), Water Ecosystem Services: A Global Perspective (pp. 3–14). Cambridge: Cambridge University Press. https://doi.org/10.1017/CBO9781316178904.003

Mengistu, A. G., van Rensburg, L. D., & Woyessa, Y. E. (2019). Techniques for calibration and validation of SWAT model in data scarce arid and semi-arid catchments in South Africa. Journal of Hydrology: Regional Studies, 25(July), 100621. https://doi.org/10.1016/j.ejrh.2019.100621

Morataya-Montenegro, R., & Bautista-Solís, P. (2020). Water Governance and Adaptation to Drought in Guanacaste, Costa Rica. In Integrated Water Resource Management (pp. 85–99). Springer.

Moriasi, D. N., Pai, N., Steiner, J. L., Gowda, P. H., Winchell, M., Rathjens, H., et al. (2019). SWAT-LUT: A desktop graphical user interface for updating land use in SWAT. JAWRA Journal of the American Water Resources Association, 55(5), 1102–1115.

Zhang, X., Izaurralde, R. C., Arnold, J. G., Williams, J. R., & Srinivasan, R. (2013). Modifying the soil and water assessment tool to simulate cropland carbon flux: model development and initial evaluation. Science of the Total Environment, 463, 810–822.

BIBLIOGRAPHY

CHAPTER 1: INTRODUCTION

Arnold, J.G., Srinivasan, R., Muttiah, R.S., Williams, J.R., 1998. Large area hydrologic modeling and assessment part I: model development 1. JAWRA J. Am. Water Resour. Assoc. 34, 73–89.

Braat, L.C., De Groot, R., 2012. The ecosystem services agenda: bridging the worlds of natural science and economics, conservation and development, and public and private policy. Ecosyst. Serv. 1, 4–15.

Brooks, K.N., Ffolliott, P.F., Magner, J.A., 2013. Hydrology and the Management of Watersheds. John Wiley & Sons.

Burkhard, B., Crossman, N., Nedkov, S., Petz, K., Alkemade, R., 2013. Mapping and modelling ecosystem services for science, policy and practice. Ecosyst. Serv. 1–3.

Calvo-Rodriguez, S., Sanchez-Azofeifa, A.G., Duran, S.M., Espirito-Santo, M.M., 2017. Assessing ecosystem services in Neotropical dry forests: a systematic review. Environ. Conserv. 44, 34–43. https://doi.org/10.1017/S0376892916000400

Chaudhary, S., McGregor, A., Houston, D., Chettri, N., 2015. The evolution of ecosystem services: A time series and discourse-centered analysis. Environ. Sci. Policy 54, 25–34.

Cheng, C.L., 2007. Evaluating the performances of AnnAGNPS and N-SPECT for tropical conditions.

Fisher, B., Turner, R.K., Morling, P., 2009. Defining and classifying ecosystem services for decision making. Ecol. Econ. 68, 643–653.

Francesconi, W., Srinivasan, R., Pérez-Miñana, E., Willcock, S.P., Quintero, M., 2016. Using the Soil and Water Assessment Tool (SWAT) to model ecosystem services: A systematic review. J. Hydrol. 535, 625–636. https://doi.org/10.1016/j.jhydrol.2016.01.034

Gordon, I.J., Martin-ortega, J., Ferrier, R.C., 2015. Introduction, in: J. Martin-Ortega, R. Ferrier, I. Gordon, S.K. (Ed.), Water Ecosystem Services: A Global Perspective. Cambridge University Press, Cambridge, pp. 1–2. https://doi.org/10.1017/CBO9781316178904.002

Gregersen, H.M., Ffolliott, P.F., Brooks, K.N., 2007. Integrated watershed management: Connecting people to their land and water. CABI.

Hamel, P., Bryant, B.P., 2017. Uncertainty assessment in ecosystem services analyses: Seven challenges and practical responses. Ecosyst. Serv. 24, 1–15.

Lamarque, P., Quetier, F., Lavorel, S., 2011. The diversity of the ecosystem services concept and its implications for their assessment and management. C. R. Biol. 334, 441–449.

Martin-Ortega, J., Ferrier, R.C., Gordon, I.J., 2015a. Water ecosystem services: Moving forward, in: J. Martin-Ortega, R. Ferrier, I. Gordon, S.K. (Ed.), Water Ecosystem Services: A Global Perspective. Cambridge University Press, Cambridge, pp. 170–173. https://doi.org/10.1017/CBO9781316178904.021

Martin-Ortega, J., Ferrier, R.C., Gordon, I.J., Khan, S., 2015b. Water ecosystem services: A global perspective. UNESCO Publishing.

Martin-Ortega, J., Jorda-Capdevila, D., Glenk, K., Holstead, K.L., 2015c. What defines ecosystem services-based approaches?, in: J. Martin-Ortega, R. Ferrier, I. Gordon, & S.K. (Ed.), Water Ecosystem Services: A Global Perspective. Cambridge University Press, Cambridge, pp. 3–14. https://doi.org/10.1017/CBO9781316178904.003

MEA, 2005. Millenium Ecosystem Assessment: ecosystems and human well-being. Island Press, Washington, DC.

Naidoo, R., Balmford, A., Costanza, R., Fisher, B., Green, R.E., Lehner, B., Malcolm, T.R., Ricketts, T.H., 2008. Global mapping of ecosystem services and conservation priorities. Proc. Natl. Acad. Sci. 105, 9495–9500.

Neitsch, S.L., Arnold, J.G., Kiniry, J.R., Williams, J.R., 2011. Soil & Water Assessment Tool Theoretical Documentation Version 2009. Texas Water Resour. Inst. 1–647. https://doi.org/10.1016/j.scitotenv.2015.11.063

Ray, D.K., Nair, U.S., Welch, R.M., Lawton, R.O., 2002. Impact of Deforestation on Cloud Properties and Rainfall Over the Costa Rica-Nicaraguan region, in: AGU Fall Meeting Abstracts. pp. B21B-0724.

SINAC, 2010. Guanacaste Conservation Area (ACG) [WWW Document]. URL http://www.sinac.go.cr/EN-US/ac/acg/Pages/default.aspx

UNESCO, 2019a. Operational Guidelines for the Implementation of the World Heritage Convention. Paris.

UNESCO, 2019b. World Heritage List: Area de Conservación Guanacaste (Costa Rica) [WWW Document].

Vigerstol, K.L., Aukema, J.E., 2011. A comparison of tools for modeling freshwater ecosystem services. J. Environ. Manage. 92, 2403–2409. https://doi.org/10.1016/j.jenvman.2011.06.040

CHAPTER 2: WATER YIELD QUANTIFICATION AND ANALYSIS OF LAND COVER CHANGE IMPACT IN WATER AVAILABILITY FOR THE CONSERVATION AREA OF GUANACASTE, COSTA RICA USING SWAT

Abbaspour, K. C. (2005). Calibration of hydrologic models: When is a model calibrated? MODSIM 2005 - International Congress on Modelling and Simulation: Advances and Applications for Management and Decision Making, Proceedings, 2449–2455.

Abbaspour, K. C. (2007). User manual for SWAT-CUP, SWAT calibration and uncertainty analysis programs. Dubendorf, Switzerland. Retrieved from https://swat.tamu.edu/media/114860/usermanual_swatcup.pdf

Abbaspour, K. C., & Vaghefi, S. A. (2019). Global FAO/UNESCO Soil Map of the World reformatted with SWAT format. https://doi.org/https://doi.org/10.1594/PANGAEA.901313

Abbaspour, K. C., Yang, J., Maximov, I., Siber, R., Bogner, K., Mieleitner, J., et al. (2007). Modelling hydrology and water quality in the pre-alpine/alpine Thur watershed using SWAT. Journal of Hydrology, 333(2–4), 413–430.

Abbaspour, K. C., Vejdani, M., Haghighat, S., & Yang, J. (2007). SWAT-CUP calibration and uncertainty programs for SWAT. In MODSIM 2007 international congress on modelling and simulation, modelling and simulation society of Australia and New Zealand (pp. 1596–1602).

Abbaspour, K. C., Faramarzi, M., & Rouholahnejad, E. (2010). Hydrological modeling of Alberta using SWAT model. AWAG, Swiss Federal Institute of Aquatic Scienec and Technology, 83.

Abbaspour, K. C., Rouholahnejad, E., Vaghefi, S., Srinivasan, R., & Klöve, B. (2015). Modelling hydrology and water quality of the European Continent at a subbasin scale: calibration of a high-resolution large-scale SWAT model. J. Hydrol, 524, 733–752.

Abbaspour, K. C., Vaghefi, S. A., & Srinivasan, R. (2018). A guideline for successful calibration and uncertainty analysis for soil and water assessment: A review of papers from the 2016 International SWAT Conference. Multidisciplinary Digital Publishing Institute.

Abbaspour, K. C., Vaghefi, S. A., Yang, H., & Srinivasan, R. (2019). Global soil, landuse, evapotranspiration, historical and future weather databases for SWAT Applications. Scientific Data, 6(1), 1–11.

Alemayehu, T., Van Griensven, A., Woldegiorgis, B. T., & Bauwens, W. (2017). An improved SWAT vegetation growth module and its evaluation for four tropical ecosystems. Hydrology and Earth System Sciences, 21(9), 4449.

Arnold, J. G., Williams, J. R., & Maidment, D. R. (1995). Continuous-time water and sediment-routing model for large basins. Journal of Hydraulic Engineering, 121(2), 171–183.

Arnold, J. G., Srinivasan, R., Muttiah, R. S., & Williams, J. R. (1998). Large area hydrologic modeling and assessment part I: model development 1. JAWRA Journal of the American Water Resources Association, 34(1), 73–89.

Arnold, J. G., Kiniry, J. R., Srinivasan, R., Williams, J. R., Haney, E. B., & Neitsch, S. L. (2012). Input/Output Documentation Soil & Water Assessment Tool. Retrieved from https://swat.tamu.edu/media/69296/swat-io-documentation-2012.pdf

Arnold, J. G., Moriasi, D. N., Gassman, P. W., Abbaspour, K. C., White, M. J., Srinivasan, R., et al. (2012). SWAT: Model use, calibration, and validation. Transactions of the ASABE, 55(4), 1491–1508.

Arroyo Morales, L., Heidinger, H., & Araya Morales, E. J. (2010). Modelo Hidrológico SWAT como Herramienta para Procesos de Toma de Desición. San Jose: Proyecto Microriego Plantón-Pacayas.

Ayivi, F., & Jha, M. K. (2018). Estimation of water balance and water yield in the Reedy Fork-Buffalo Creek Watershed in North Carolina using SWAT. International Soil and Water Conservation Research, 6(3), 203–213.

Barquero-Ureña, A. (2015a). Modelación hidrológica en las cuencas San Jerónimo-Piedras, Río Blanco y Tenorio usando SWAT.

Barquero-Ureña, A. (2015b). Modelación hidrológica en las cuencas San Jerónimo-Piedras, Río Blanco y Tenorio usando SWAT [Hydrological modeling in the San Jerónimo-Piedras, White River, and Tenorio basins using SWAT]. Retrieved from http://www.kerwa.ucr.ac.cr/handle/10669/75480

Bayabil, H. K., & Dile, Y. T. (2020). Improving hydrologic simulations of a small watershed through soil data integration. Water (Switzerland), 12(10). https://doi.org/10.3390/w12102763

BCCR. (2017). Cuentas AGUA 2012-2015, 15. Retrieved from https://activos.bccr.fi.cr/sitios/bccr/cuentasambientales/DocCuentaAgua/Cuenta_agua_2012_2015.pdf

Benavides, F., & Veenstra, J. N. (2005). The impact of tropical deforestation on river chemical pollution. In Proceedings of the International Conference on Environmental Science and Technology (Vol. 1, pp. 173–178).

Brooks, K. N., Ffolliott, P. F., & Magner, J. A. (2013). Hydrology and the Management of Watersheds. John Wiley & Sons.

Calvo-Alvarado, J., McLennan, B., Sánchez-Azofeifa, A., & Garvin, T. (2009). Deforestation and forest restoration in Guanacaste, Costa Rica: Putting conservation policies in context. Forest Ecology and Management, 258(6), 931–940. https://doi.org/10.1016/j.foreco.2008.10.035

Calvo-Alvarado, J., Jiménez, V., Calvo-Obando, A., & Castillo, M. (2019). Current perspectives on forest recovery trends in Guanacaste, Costa Rica. International Forestry Review, 21(4), 425–431.

Carvajal-Vanegas, D. (2017). Dinámica hídrica bajo condiciones climáticas cambiantes en la subcuenca del Río Tempisquito, cuenca del Tempisque, Guanacaste, Costa Rica.

Castro-Magnani, M. (2018). Evaluating ecosystem services in Tropical Dry Forests, 127. Retrieved from https://era.library.ualberta.ca/items/eb06a5e3-73ba-4630-9b73-8070e6d58473/view/27178acf-2168-4f2d-b573-1bc9d5caab68/Castro-Magnani_Marissa_201804_MSc.pdf

Chen, J. (2020). Spatial Dynamic Modeling of Tropical Forest Change.

CIA-UCR. (2016). Digital Soil Map of Costa Rica. Retrieved from http://www.cia.ucr.ac.cr/?page_id=139

CIESIN. (2018). Gridded Population of the World, Version 4 (GPWv4): Population Count. New York. Retrieved from https://sedac.ciesin.columbia.edu/data/set/gpw-v4-population-count-rev11

Cooley, S. S., Williams, C. A., Fisher, J. B., Halverson, G. H., Perret, J., & Lee, C. M. (2019). Assessing regional drought impacts on vegetation and evapotranspiration: a case study in Guanacaste, Costa Rica. Ecological Applications, 29(2), e01834.

Correa-Ayram, C. A., Mendoza, M. E., Etter, A., & Pérez Salicrup, D. R. (2017). Anthropogenic impact on habitat connectivity: A multidimensional human footprint index evaluated in a highly biodiverse landscape of Mexico. Ecological Indicators, 72(January), 895–909. https://doi.org/10.1016/j.ecolind.2016.09.007

Damkjaer, S., & Taylor, R. (2017). The measurement of water scarcity: Defining a meaningful indicator. Ambio, 46(5), 513–531.

Dingman, S. L. (2015). Physical hydrology (Third). Waveland press.

Durham, R., Rivera-Araya, M. J., Madison, D., Quesada, L., Vanegas, N., & Cui, D. (2016). DEVELOP Technical Report. Costa Rica Water Resources. Monitoring Drought and Water Balance in the Guanacaste Province to Enhance Decision Making and Response Planning Costa Rica., (August). Retrieved from https://bit.ly/32rXN7K

ESA. (2015). Land Cover CCI-Product User Guide Version 2.0. Retrieved from http://maps.elie.ucl.ac.be/CCI/viewer/download/ESACCI-LC-Ph2-PUGv2_2.0.pdf

ESRI. (2016). Conditional Toolset. Retrieved from https://desktop.arcgis.com/en/arcmap/10.3/tools/spatial-analyst-toolbox/con-.htm

Essenfelder, A. H. (2018). SWAT Weather Database: A Quick Guide. https://doi.org/doi: 10.13140/RG.2.1.4329.1927

Etter, A., McAlpine, C. A., Seabrook, L., & Wilson, K. A. (2011). Incorporating temporality and biophysical vulnerability to quantify the human spatial footprint on ecosystems. Biological Conservation. https://doi.org/10.1016/j.biocon.2011.02.004

Faramarzi, M., Abbaspour, K. C., Schulin, R., & Yang, H. (2009). Modelling blue and green water resources availability in Iran. Hydrological Processes: An International Journal, 23(3), 486–501.

Faramarzi, M., Abbaspour, K. C., Vaghefi, S. A., Farzaneh, M. R., Zehnder, A. J. B., Srinivasan, R., & Yang, H. (2013). Modeling impacts of climate change on freshwater availability in Africa. Journal of Hydrology, 480, 85–101.

Faramarzi, M., Srinivasan, R., Iravani, M., Bladon, K. D., Abbaspour, K. C., Zehnder, A. J. B., & Goss, G. G. (2015). Setting up a hydrological model of Alberta: Data discrimination analyses prior to calibration. Environmental Modelling & Software, 74, 48–65.

Faramarzi, M., Abbaspour, K. C., Lu, W., Fennell, J., Zehnder, A. J. B., & Goss, G. G. (2017). Uncertainty based assessment of dynamic freshwater scarcity in semi-arid watersheds of Alberta, Canada. Journal of Hydrology: Regional Studies, 9, 48–68.

Fernandez-Palomino, C. A., Hattermann, F. F., Krysanova, V., Vega-Jácome, F., & Bronstert, A. (2020). Towards a more consistent eco-hydrological modelling through multi-objective calibration: a case study in the Andean Vilcanota River basin, Peru. Hydrological Sciences Journal, 1–16.

Filoso, S., Bezerra, M. O., Weiss, K. C. B., & Palmer, M. A. (2017). Impacts of forest restoration on water yield: A systematic review. PLoS ONE, 12(8), 1–26. https://doi.org/10.1371/journal.pone.0183210

Francesconi, W., Srinivasan, R., Pérez-Miñana, E., Willcock, S. P., & Quintero, M. (2016). Using the Soil and Water Assessment Tool (SWAT) to model ecosystem services: A systematic review. Journal of Hydrology, 535, 625–636. https://doi.org/10.1016/j.jhydrol.2016.01.034

Guzmán-Arias, I., & Calvo-Alvarado, J. C. (2013). Planning and development of Costa Rica water resources: current status and perspectives. Revista Tecnología En Marcha, 26(4), 52. https://doi.org/10.18845/tm.v26i4.1583

Hoyos, N., Correa-Metrio, A., Jepsen, S. M., Wemple, B., Valencia, S., Marsik, M., et al. (2019). Modeling streamflow response to persistent drought in a coastal tropical mountainous watershed, Sierra Nevada De Santa Marta, Colombia. Water, 11(1), 94.

IMN. (n.d.). ENSO. Retrieved April 14, 2021, from https://www.imn.ac.cr/en/54

Janzen, D. H., & Hallwachs, W. (2000). Costa Rica's Area de Conservación Guanacaste: a long march to survival through non-damaging biodevelopment. Biodiversity, 1(2), 7–20.

Johnston, R., & Smakhtin, V. (2014). Hydrological modeling of large river basins: how much is enough? Water Resources Management, 28(10), 2695–2730.

Khalid, K., Ali, M. F., Rahman, N. F. A., Mispan, M. R., Haron, S. H., Othman, Z., & Bachok, M. F. (2016). Sensitivity analysis in watershed model using SUFI-2 algorithm. Procedia Eng, 162, 441–447.

Krause, P., Boyle, D. P., & Bäse, F. (2005). Comparison of different efficiency criteria for hydrological model assessment.

Krysanova, V., & Arnold, J. G. (2008). Advances in ecohydrological modelling with SWAT—a review. Hydrological Sciences Journal, 53(5), 939–947.

Kuzdas, C. (2012). Unpacking water conflict in Unpacking water conflict in Guanacaste, Costa Rica.

Liu, W., Park, S., Bailey, R. T., Molina-Navarro, E., Andersen, H. E., Thodsen, H., et al. (2020). Quantifying the streamflow response to groundwater abstractions for irrigation or drinking water at catchment scale using SWAT and SWAT–MODFLOW. Environmental Sciences Europe, 32(1), 1–25.

Lopes, T. R., Folegatti, M. V., Duarte, S. N., Zolin, C. A., Junior, L. S. F., Moura, L. B., et al. (2020). Hydrological modeling for the Piracicaba River basin to support water management and ecosystem services. Journal of South American Earth Sciences, 103, 102752.

Lopes, T. R., Zolin, C. A., Mingoti, R., Vendrusculo, L. G., de Almeida, F. T., de Souza, A. P., et al. (2021). Hydrological regime, water availability and land use/land cover change impact on the water balance in a large agriculture basin in the Southern Brazilian Amazon. Journal of South American Earth Sciences, 108, 103224.

Luo, Y., Su, B., Yuan, J., Li, H., & Zhang, Q. (2011). GIS techniques for watershed delineation of SWAT model in plain polders. Procedia Environmental Sciences, 10(PART C), 2050–2057. https://doi.org/10.1016/j.proenv.2011.09.321

Martin-Ortega, J., Ferrier, R. C., & Gordon, I. J. (2015). Water ecosystem services: Moving forward. In S. K. J. Martin-Ortega, R. Ferrier, I. Gordon (Ed.), Water Ecosystem Services: A Global Perspective (pp. 170–173). Cambridge: Cambridge University Press. https://doi.org/10.1017/CBO9781316178904.021

Martin-Ortega, J., Jorda-Capdevila, D., Glenk, K., & Holstead, K. L. (2015). What defines ecosystem services-based approaches? In & S. K. J. Martin-Ortega, R. Ferrier, I. Gordon (Ed.), Water Ecosystem Services: A Global Perspective (pp. 3–14). Cambridge: Cambridge University Press. https://doi.org/10.1017/CBO9781316178904.003

Mateo-Sagasta, J., Zadeh, S. M., Turral, H., & Burke, J. (2017). Water pollution from agriculture: a global review. Executive summary. Rome, Italy: FAO Colombo, Sri Lanka: International Water Management ….

Mehan, S., Neupane, R. P., & Kumar, S. (2017). Coupling of SUFI 2 and SWAT for Improving the Simulation of Streamflow in an Agricultural Watershed of South Dakota. Hydrol. Curr. Res, 8(3).

Montecelos-Zamora, Y., Cavazos, T., Kretzschmar, T., Vivoni, E. R., Corzo, G., & Molina-Navarro, E. (2018). Hydrological modeling of climate change impacts in a tropical river basin: A case study of the Cauto river, Cuba. Water, 10(9), 1135.

Moriasi, D.N., Arnold, J. G., Van Liew, M. W., Bingner, R. L., Harmel, R. D., & Veith, T. L. (2007). Model evaluation guidelines for systematic quantification of accuracy in watershed simulations. Transactions of the ASABE, 50(3), 885–900.

Moriasi, Daniel N, Pai, N., Steiner, J. L., Gowda, P. H., Winchell, M., Rathjens, H., et al. (2019). SWAT-LUT: A desktop graphical user interface for updating land use in SWAT. JAWRA Journal of the American Water Resources Association, 55(5), 1102–1115.

Narasimhan, B., & Dhanesh, Y. (2012). SWAT user soil table template. Retrieved from shorturl.at/hmFRX

Neitsch, S. L., Arnold, J. G., Kiniry, J. R., & Williams, J. R. (2011). Soil & Water Assessment Tool Theoretical Documentation Version 2009. Texas Water Resources Institute, 1–647. https://doi.org/10.1016/j.scitotenv.2015.11.063

Oestreicher, J. (2008). Application of the Soil Water Assessment Tool in a Tropical Agricultural Catchment of the Panama Canal Watershed: Implications for its use in watershed management activities. McGill University.

de Oliveira Serrão, E. A., Silva, M. T., Ferreira, T. R., da Silva, V. de P. R., de Sousa, F. de S., de Lima, A. M. M., et al. (2020). Land use change scenarios and their effects on hydropower energy in the Amazon. Science of The Total Environment, 744, 140981.

Ortiz-Malavasi, E. (2014). Atlas de Costa Rica 2014. Retrieved from https://repositoriotec.tec.ac.cr/handle/2238/6749

Pachepsky, Y., & Rawls, W. J. (2004). Development of pedotransfer functions in soil hydrology. Elsevier.

Pagliero, L., Bouraoui, F., Willems, P., & Diels, J. (2014). Large-Scale Hydrological Simulations Using the Soil Water Assessment Tool, Protocol Development, and Application in the Danube Basin. Journal of Environmental Quality, 43(1), 145–154.

Peters, N. E., & Meybeck, M. (2000). Water quality degradation effects on freshwater availability: impacts of human activities. Water International, 25(2), 185–193.

Portillo-Quintero, C. A., & Sánchez-Azofeifa, G. A. (2010). Extent and conservation of tropical dry forests in the Americas. Biological Conservation, 143(1), 144–155.

Quintero, M., Wunder, S., & Estrada, R. D. (2009). For services rendered? Modeling hydrology and livelihoods in Andean payments for environmental services schemes. Forest Ecology and Management, 258(9), 1871–1880.

Ramos, J. H. (2016). Análisis Hidrológico de la Cuenca del río Sensunapán, como alternativa para el fortalecimiento de la Gestion de Riesgos y Reducción de la Vulnerabilidad, en el Departamento de Sonsonate, El Salvador [Hydrological Analysis of the Sensunapán River Basin, as. El Salvador University. Retrieved from http://ri.ues.edu.sv/id/eprint/10245/

Ray, D. K., Nair, U. S., Welch, R. M., & Lawton, R. O. (2002). Impact of Deforestation on Cloud Properties and Rainfall Over the Costa Rica-Nicaraguan region. In AGU Fall Meeting Abstracts (Vol. 2002, pp. B21B-0724).

Refsgaard, J. C., & Abbott, M. B. (1990). The role of distributed hydrological modelling in water resources management. In Distributed hydrological modelling (pp. 1–16). Springer.

Ritter, A., & Munoz-Carpena, R. (2013). Performance evaluation of hydrological models: Statistical significance for reducing subjectivity in goodness-of-fit assessments. Journal of Hydrology, 480, 33–45.

Rodríguez-Romero, A. J., Rico-Sánchez, A. E., Mendoza-Martínez, E., Gómez-Ruiz, A., Sedeño-Díaz, J. E., & López-López, E. (2018). Impact of changes of land use on water quality, from tropical forest to anthropogenic occupation: a multivariate approach. Water, 10(11), 1518.

Roth, V., & Lemann, T. (2016). Comparing CFSR and conventional weather data for discharge and soil loss modelling with SWAT in small catchments in the Ethiopian Highlands. Hydrology and Earth System Sciences, 20(2), 921–934.

Saxton, K. E., & Rawls, W. J. (2006). Soil water characteristic estimates by texture and organic matter for hydrologic solutions. Soil Science Society of America Journal, 70(5), 1569–1578.

Schilling, K. E., Jha, M. K., Zhang, Y., Gassman, P. W., & Wolter, C. F. (2008). Impact of land use and land cover change on the water balance of a large agricultural watershed: Historical effects and future directions. Water Resources Research, 44(7).

Schuol, J., Abbaspour, K. C., Yang, H., Srinivasan, R., & Zehnder, A. J. B. (2008). Modeling blue and green water availability in Africa. Water Resources Research, 44(7).

Shrestha, J. P., Pahlow, M., & Cochrane, T. A. (2020). Development of a SWAT hydropower operation routine and its application to assessing hydrological alterations in the mekong. Water (Switzerland), 12(8). https://doi.org/10.3390/W12082193

SINAC. (2010). Guanacaste Conservation Area (ACG). Retrieved from http://www.sinac.go.cr/EN-US/ac/acg/Pages/default.aspx

Stan, K., & Sanchez-Azofeifa, A. (2019). Deforestation and secondary growth in Costa Rica along the path of development. Regional Environmental Change, 19(2), 587–597.

Stan, K., Sanchez-Azofeifa, A., Calvo-Rodriguez, S., Castro-Magnani, M., Chen, J., Ludwig, R., & Zou, L. (2020). Climate change scenarios and projected impacts for forest productivity in Guanacaste Province (Costa Rica): lessons for tropical forest regions. Regional Environmental Change, 20(1), 1–13.

Stan, K. D., Sanchez-Azofeifa, A., Duran, S. M., Guzman, J. A., Hesketh, M., Portillo-Quintero, C., et al. (2021). Tropical Dry Forest resilience and Water Use Efficiency: an analysis of productivity under climate change. Environmental Research Letters. https://doi.org/https://doi.org/10.1088/1748-9326/abf6f3

SWAT. (2018). ArcSWAT. Retrieved from https://swat.tamu.edu/software/arcswat/

Tang, F. F., Xu, H. S., & Xu, Z. X. (2012). Model calibration and uncertainty analysis for runoff in the Chao River Basin using sequential uncertainty fitting. Procedia Environmental Sciences, 13, 1760–1770.

Tarigan, S., Wiegand, K., Sunarti, & Slamet, B. (2018). Minimum forest cover required for sustainable water flow regulation of a watershed: A case study in Jambi Province, Indonesia. Hydrology and Earth System Sciences, 22(1), 581–594. https://doi.org/10.5194/hess-22-581-2018

Ullrich, A., & Volk, M. (2009). Application of the Soil and Water Assessment Tool (SWAT) to predict the impact of alternative management practices on water quality and quantity. Agricultural Water Management, 96(8), 1207–1217.

UNESCO. (2019a). World Heritage List: Area de Conservación Guanacaste (Costa Rica).

UNESCO. (2019b). WWAP The United Nations World Water Development Report 2019. Leaving No One Behind. Retrieved from https://www.unwater.org/publications/world-water-development-report-2019/

Uribe, N., Corzo, G., Quintero, M., van Griensven, A., & Solomatine, D. (2018). Impact of conservation tillage on nitrogen and phosphorus runoff losses in a potato crop system in Fuquene watershed, Colombia. Agricultural Water Management, 209, 62–72.

Vapnik, V. (2013). The nature of statistical learning theory. Springer science & business media.

Wang, Y., Jiang, R., Xie, J., Zhao, Y., Yan, D., & Yang, S. (2019). Soil and water assessment tool (SWAT) model: A systemic review. Journal of Coastal Research, 93(SI), 22–30.

Wei, X., Garcia-Chevesich, P., Alejo, F., García, V., Martínez, G., Daneshvar, F., et al. (2021). Hydrologic Analysis of an Intensively Irrigated Area in Southern Peru Using a Crop-Field Scale Framework. Water, 13(3), 318.

Williams, J. R., Nicks, A. D., & Arnold, J. G. (1985). Simulator for water resources in rural basins. Journal of Hydraulic Engineering, 111(6), 970–986.

Zou, L., Cao, S., Zhao, A., & Sanchez-Azofeifa, A. (2020). Assessing the Temporal Response of Tropical Dry Forests to Meteorological Drought. Remote Sensing, 12(14), 2341.

CHAPTER 3: CONCLUSIONS AND FUTURE WORK

Alemayehu, T., Van Griensven, A., Woldegiorgis, B. T., & Bauwens, W. (2017). An improved SWAT vegetation growth module and its evaluation for four tropical ecosystems. Hydrology and Earth System Sciences, 21(9), 4449.

Brooks, K. N., Ffolliott, P. F., & Magner, J. A. (2013). Hydrology and the Management of Watersheds. John Wiley & Sons.

Calvo-Alvarado, J., Jiménez, V., Calvo-Obando, A., & Castillo, M. (2019). Current perspectives on forest recovery trends in Guanacaste, Costa Rica. International Forestry Review, 21(4), 425–431.

Chaudhary, S., McGregor, A., Houston, D., & Chettri, N. (2015). The evolution of ecosystem services: A time series and discourse-centered analysis. Environmental Science & Policy, 54, 25–34.

Filoso, S., Bezerra, M. O., Weiss, K. C. B., & Palmer, M. A. (2017). Impacts of forest restoration on water yield: A systematic review. PLoS ONE, 12(8), 1–26. https://doi.org/10.1371/journal.pone.0183210

Fisher, B., Turner, R. K., & Morling, P. (2009). Defining and classifying ecosystem services for decision making. Ecological Economics, 68(3), 643–653.

Gordon, I. J., Martin-ortega, J., & Ferrier, R. C. (2015). Introduction. In S. K. J. Martin-Ortega, R. Ferrier, I. Gordon (Ed.), Water Ecosystem Services: A Global Perspective (pp. 1–2).

Cambridge: Cambridge University Press. https://doi.org/10.1017/CBO9781316178904.002

Martin-Ortega, J., Jorda-Capdevila, D., Glenk, K., & Holstead, K. L. (2015). What defines ecosystem services-based approaches? In & S. K. J. Martin-Ortega, R. Ferrier, I. Gordon (Ed.), Water Ecosystem Services: A Global Perspective (pp. 3–14). Cambridge: Cambridge University Press. https://doi.org/10.1017/CBO9781316178904.003

Mengistu, A. G., van Rensburg, L. D., & Woyessa, Y. E. (2019). Techniques for calibration and validation of SWAT model in data scarce arid and semi-arid catchments in South Africa. Journal of Hydrology: Regional Studies, 25(July), 100621. https://doi.org/10.1016/j.ejrh.2019.100621

Morataya-Montenegro, R., & Bautista-Solís, P. (2020). Water Governance and Adaptation to Drought in Guanacaste, Costa Rica. In Integrated Water Resource Management (pp. 85–99). Springer.

Moriasi, D. N., Pai, N., Steiner, J. L., Gowda, P. H., Winchell, M., Rathjens, H., et al. (2019). SWAT-LUT: A desktop graphical user interface for updating land use in SWAT. JAWRA Journal of the American Water Resources Association, 55(5), 1102–1115.

Zhang, X., Izaurralde, R. C., Arnold, J. G., Williams, J. R., & Srinivasan, R. (2013). Modifying the soil and water assessment tool to simulate cropland carbon flux: model development and initial evaluation. Science of the Total Environment, 463, 810–822.

APPENDICES

Appendix 1. SWAT Input Data: Soil information. It comprises 12 soil suborders classified into four different hydrological soil groups (HYDGRP).

Suborder	SWAT Database Code	HYDGRP	2016	
			Area (km^2)	Area (%)
Aquents	AQUE	C	9.4	0.30%
Humults	HUMU	B	486.8	14.10%
Orthents	ORTH	C	1680.4	48.70%
Orthents / Ustepts	ORTH-USTEP	B	10.4	0.30%
Udands	UDAN	B	401.2	11.60%
Udepts	UDEP	A	69.3	2.00%
Urban	URBAN LAND	Not Defined	5.4	0.20%
Ustands	USTA	B	393.4	11.40%
Ustepts	USTEP	A	288.1	8.40%
Usterts	USTER	D	48	1.40%
Ustolls	USTO	B	5.1	0.10%
Ustolls / Ustepts	USTO-USTEP	B	51.1	1.50%
TOTAL			**3,448.50**	**100.00%**

Appendix 2. Effect of the DEM (Digital Elevation Model) over the generation of the stream. DEM of 90 m (left) greatly underestimates the number of streams and their spatial distribution. The DEM of 10 m improved the stream generation but produced an offset (centre). Through the use of the "Burn-in" option in ArcSWAT, the offset in streamflow generation is fixed (right).

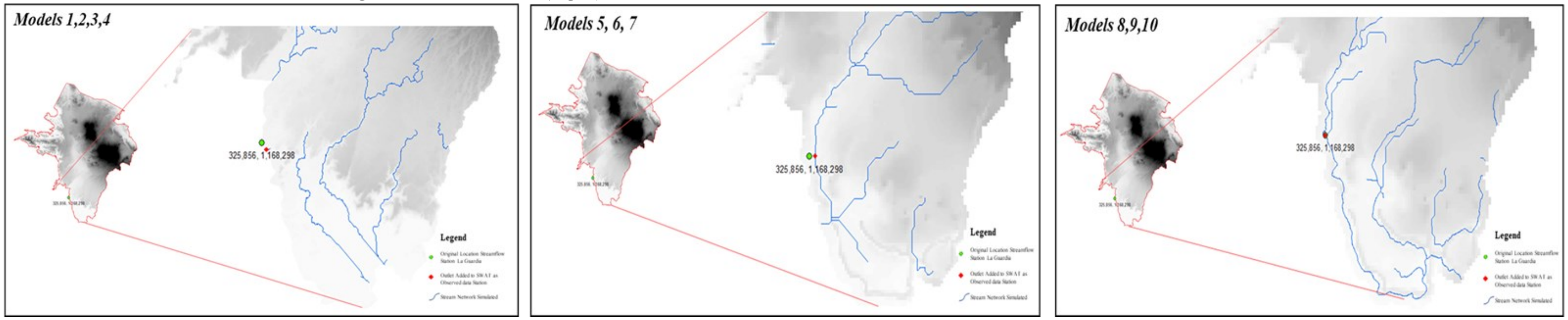

Appendix 3. SWAT Input Data: Land Use and Cover Information. 7 land cover classes of three different periods. The year 2015 was used for the calibrated model presented in this study, and the years 1979 and 1997 were used to evaluate the land use cover change (LUCC) impact in the water provision estimations.

Land Cover	**SWAT Database Code**	**1979**			**1997**			**2015**		
			Area (km^2)	**Area (%)**		**Area (km^2)**	**Area (%)**		**Area (km^2)**	**Area (%)**
Forest Deciduous	FRSD	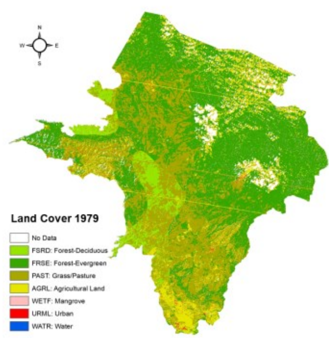	161.3	4.7%	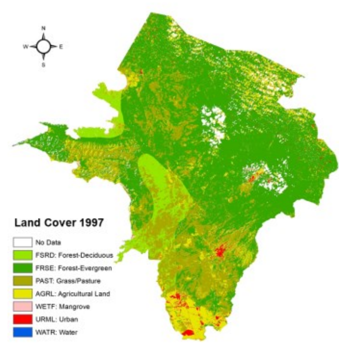	207.1	6.0%	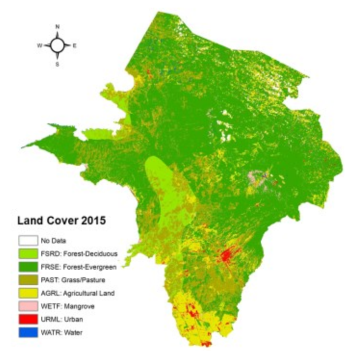	195.2	5.7%
Forest Evergreen	FRSE		1,593.8	46.2%		1,913.6	55.5%		2039.3	59.1%
Grass/Pasture	PAST		1,047.6	30.4%		716.7	20.8%		612.0	17.7%
Agricultural Land	AGRL		434.2	12.6%		415.0	12.0%		431.4	12.5%
Mangrove	WETF		57.0	1.7%		28.2	0.8%		41.4	1.2%
Urban	URML		17.7	0.5%		44.1	1.3%		46.7	1.4%
Water	WATR		1.7	0.0%		1.5	0.0%		9.8	0.3%
No Data ("Cloud")	Not Included		135.3	3.9%		122.5	3.6%		72.7	2.1%
TOTAL			**3,448.5**	**100.0%**		**3,448.5**	**3,448.5**		**3448.5**	**100.0%**

Appendix 4. Holdridge Life Zones in the ACG.

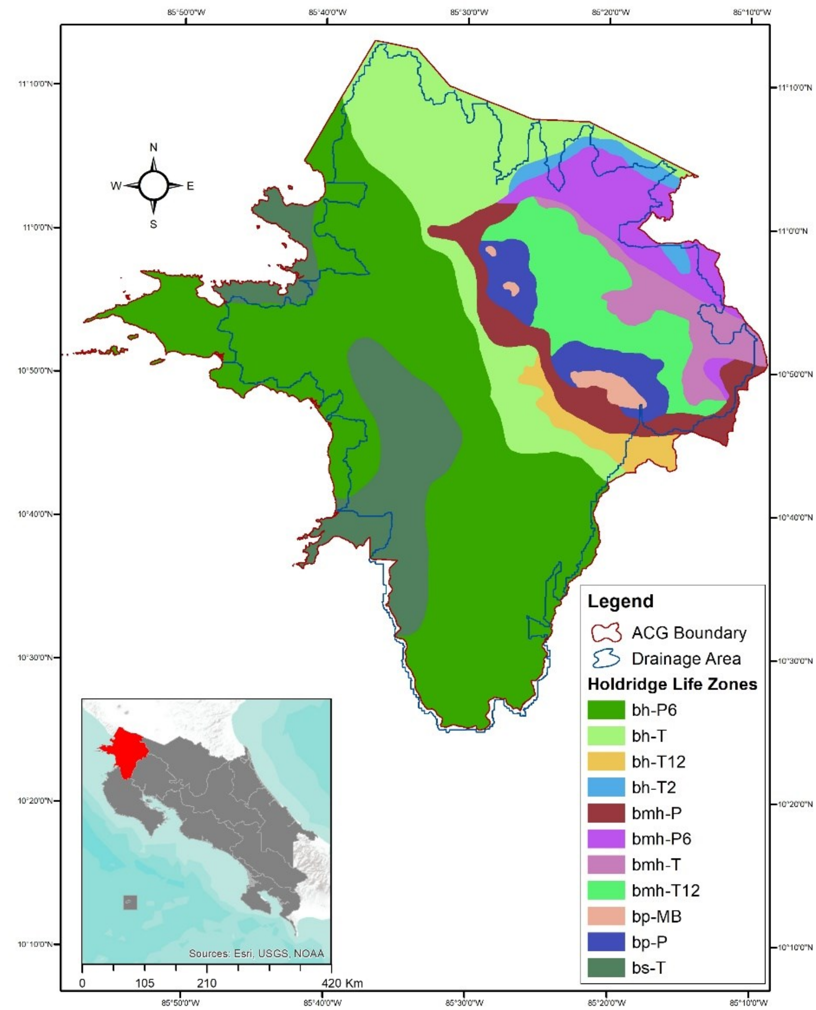

Appendix 5. Models created for the evaluation and selection of the more suitable input data for the construction of the SWAT model for the ACG. Model 9 is highlighted as it presented the best initial performance.

<table>
<tr><th rowspan="2">Name</th><th rowspan="2">Plot</th><th colspan="3">GeoSpatial Input</th><th rowspan="2">Time Series Input</th><th colspan="3">Initial Performance</th></tr>
<tr><th>Land Cover</th><th>Soil</th><th>DEM</th><th>r^2</th><th>NSE</th><th>br^2</th></tr>
<tr><td>Model 1</td><td>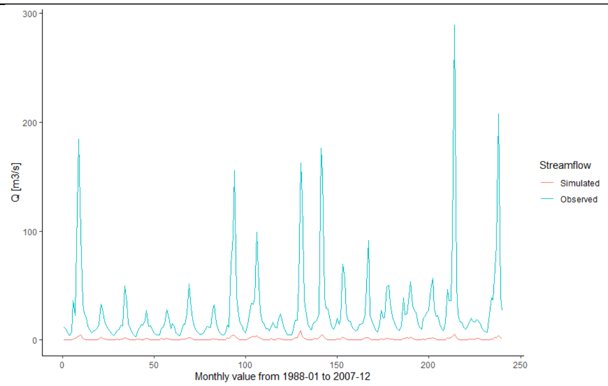
</td><td rowspan="2">2015: CEOS</td><td rowspan="2">2012: CIA-UCR</td><td rowspan="2">30 m: FONAFIFO</td><td>CSFR</td><td>0.65</td><td>-0.48</td><td>0.0178</td></tr>
<tr><td>Model 2</td><td>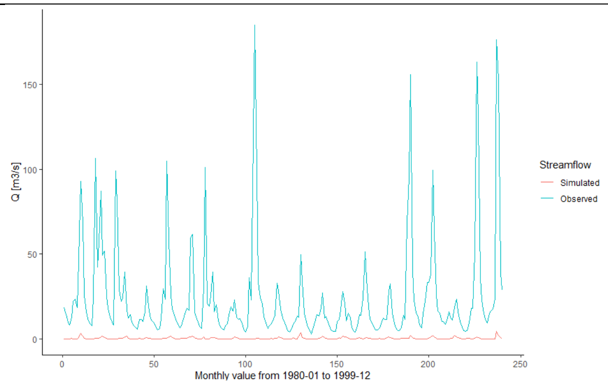
</td><td>IMN-CEOS</td><td>0.26</td><td>-0.61</td><td>0.0028</td></tr>
</table>

<table>
<tr><th rowspan="2">Name</th><th rowspan="2">Plot</th><th colspan="3">GeoSpatial Input</th><th rowspan="2">Time Series Input</th><th colspan="3">Initial Performance</th></tr>
<tr><th>Land Cover</th><th>Soil</th><th>DEM</th><th>r^2</th><th>NSE</th><th>br^2</th></tr>
<tr><td>Model 3</td><td>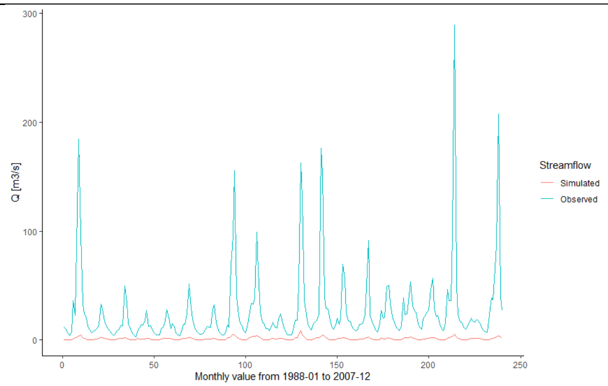
</td><td rowspan="2"></td><td rowspan="2">2007: FAO</td><td rowspan="2"></td><td>CSFR</td><td>0.61</td><td>-0.47</td><td>0.0167</td></tr>
<tr><td>Model 4</td><td>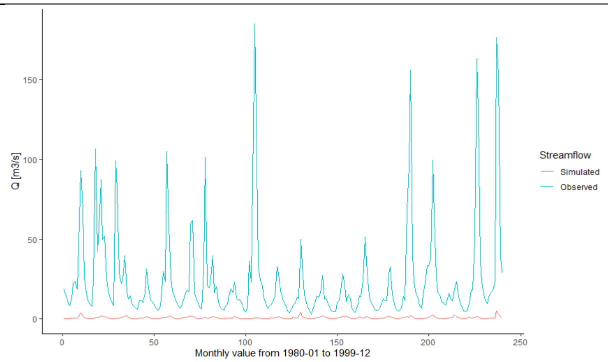
</td><td>IMN-CEOS</td><td>0.31</td><td>-0.6</td><td>0.004</td></tr>
</table>

<table>
<tr><th rowspan="2">Name</th><th rowspan="2">Plot</th><th colspan="3">GeoSpatial Input</th><th rowspan="2">Time Series Input</th><th colspan="3">Initial Performance</th></tr>
<tr><th>Land Cover</th><th>Soil</th><th>DEM</th><th>r^2</th><th>NSE</th><th>br^2</th></tr>
<tr><td>Model 5</td><td>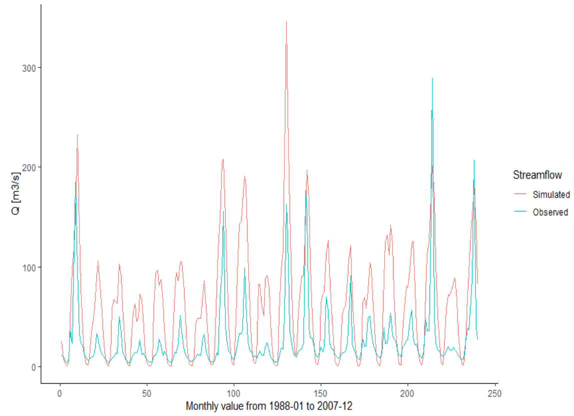
</td><td rowspan="2"></td><td rowspan="2">2016: CIA-UCR</td><td rowspan="2">10 m: Costa Rica Atlas</td><td>CSFR</td><td>0.53</td><td>-1.32</td><td>0.4572</td></tr>
<tr><td>Model 6</td><td>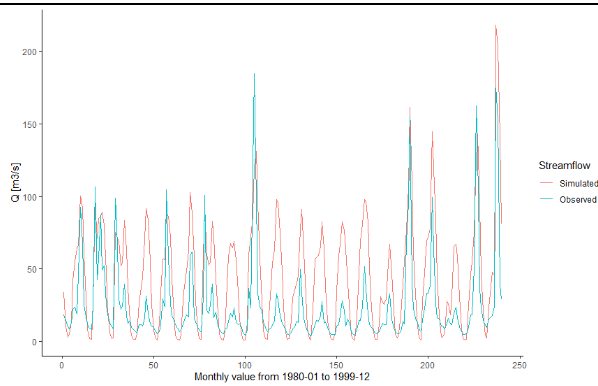
</td><td>IMN-CEOS</td><td>0.62</td><td>-0.01</td><td>0.6179</td></tr>
</table>

<table>
<tr><th rowspan="2">Name</th><th rowspan="2">Plot</th><th colspan="3">GeoSpatial Input</th><th rowspan="2">Time Series Input</th><th colspan="3">Initial Performance</th></tr>
<tr><th>Land Cover</th><th>Soil</th><th>DEM</th><th>r^2</th><th>NSE</th><th>br^2</th></tr>
<tr><td>Model 7</td><td>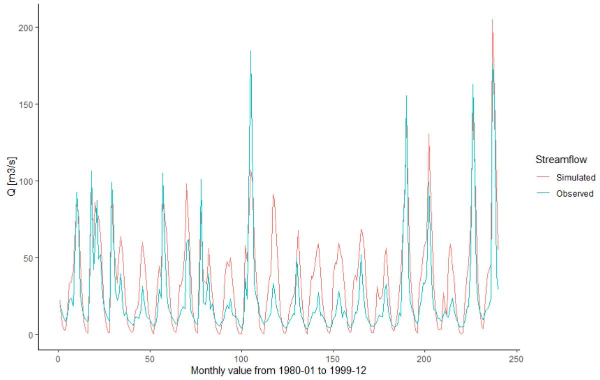
</td><td>1979:
(Chen, 2020)</td><td rowspan="2"></td><td rowspan="2"></td><td rowspan="2">IMN-CEOS</td><td>0.74</td><td>0.58</td><td>0.6759</td></tr>
<tr><td>Model 8</td><td>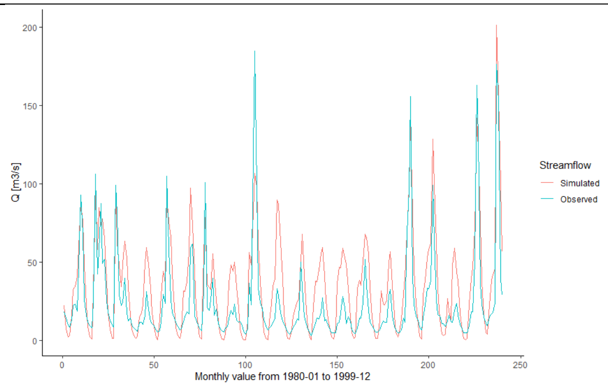
</td><td>1997
(Chen, 2020)</td><td>0.74</td><td>0.58</td><td>0.6663</td></tr>
</table>

Name	Plot	GeoSpatial Input			Time Series Input	Initial Performance		
		Land Cover	Soil	DEM		r^2	NSE	br^2
Model 9	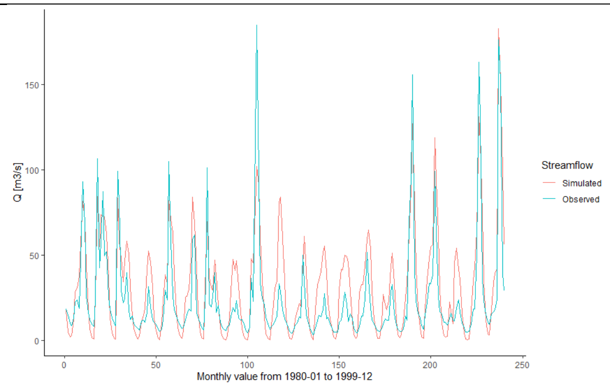	**2015 (Chen, 2020)**				**0.74**	**0.58**	**0.6666**
Model 10	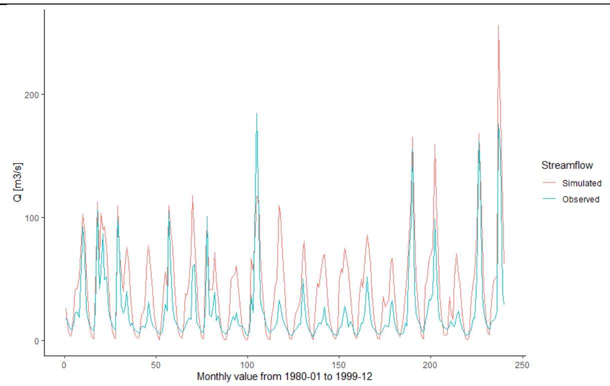	1992: ESA				0.73	0.22	0.6806